Reinforcement, Punishment and Risk in the Basolateral Amygdala

Inauguraldissertation

Zur Erlangung der Würde eines Doktors der Philosophie vorgelegt der Philosophisch-Naturwissenschaftlichen Fakultät der Universität Basel

Von

Alejandro Tsai Cabal

aus Kolumbien

Basel, 2021

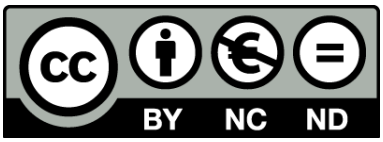

Genehmigt von der Philosophisch-Naturwissenschaftlichen Fakultät

auf Antrag von

Prof. Dr. Andreas Lüthi
(Fakultätsverantwortlicher)

Prof. Dr. Christian Lüscher
(Korreferent)

PD. Dr. Georg Keller
(Dissertationsleiter)

Basel, den 2. März 2021

Prof. Dr. Marcel Mayor
(Dekan)

Acknowledgements

I would like to thank Andreas Lüthi for the opportunity to pursue an exciting, challenging and educating scientific adventure in an exceptional environment with extraordinary colleagues. I am also very grateful to the other members of my thesis committee, Christian Lüscher and Georg Keller, for their helpful advice on my project.

A big thanks to all the current and past members of the Lüthi lab for their help and support, and for making life at the FMI a pleasure. A special thanks to Julien Courtin and Yael Bitterman, for their mentoring and collaboration.

To the FMI and Novartis, thanks for providing a world-class institute with all the conditions to help science thrive. Special thanks to my colleagues in the Imaging Facility, Animal Facility and IT team for their outstanding commitment to support. To the Neuroscience community at the FMI and the University of Basel, thanks for all the stimulating seminars, courses, talks, symposia, journal clubs, and scientific interactions.

To the football squad, thanks for the team spirit and the beer times.

To my old and new friends, thanks for the precious moments.

To Anja, my parents, my brother and to my whole family: thanks for the love and the unconditional support.

Merci vielmal!

Table of Contents

I SYNOPSIS **10**

II ABBREVIATIONS **14**

III PREFACE **16**

1. INTRODUCTION **19**

1.1 Beginnings 19

1.2 Amygdala and Fear learning 20

1.3 BLA and reward 25

1.4 Reward and Punishment in the BLA 31

1.5 BLA anatomy 32

1.6 Imaging cellular activity in freely moving animals 36

1.7 Instrumental conditioning 40

2. AIM OF THE THESIS **44**

3. METHODS **47**

3.1 Animals 47

3.2 Food restriction 47

3.3 Instrumental training 47

3.4 Surgery 51

3.5 Tissue clearing and implant localization 52

3.6 Analysis and statistics 53

4. RESULTS **56**

4.1 Establishment of a behavioral paradigm 56

4.1.1 Small reward is rewarding but not enough to induce a switch in the risk period *57*

4.1.2 A large alternative reward will cause mice to switch during the risk period *59*

4.1.3 Omission of the reward has no effect on instrumental behavior *61*

4.2 Behavioral changes upon the introduction of risk of punishment 62

4.2.1 Unpredictable air puff punishment disrupts instrumental behavior *62*

4.2.2 Risk of punishment disrupts the regular instrumental sequence *64*

4.2.3 Risk induced no changes in locomotion but in time spent in zones *65*
4.2.4 Speed and onset of escape do not change with puffs, but direction rapidly adapts *66*
4.3 PHYSIOLOGICAL CHANGES UPON THE INTRODUCTION OF RISK OF PUNISHMENT 68
4.3.1 Number of imaged neurons per mouse varied by imaging lens size *68*
4.3.2 Anatomical identification of cells *69*
4.3.3 Functional classification of cell ensembles *71*
4.3.4 Instrumental actions, reinforcer and punisher ensembles dynamics *76*
4.3.5 Air puff ensemble rapidly adapts to punishment *77*
4.3.6 Instrumental actions and reinforcer ensembles during risk *78*
5. DISCUSSION **87**
5.1 DECREASE IN INSTRUMENTAL PERFORMANCE REFLECTS RISK TAKING BEHAVIOR 87
5.2 MICE RAPIDLY LEARN TO LOCALIZE THE SOURCE OF THE AIR PUFF PUNISHMENT 88
5.3 DISTINCT ENSEMBLES AND CHANGES UPON RISK ONSET 88
5.4 RAPIDLY ADAPTING PUNISHER ENSEMBLE SUGGESTS RAPID LEARNING 91
5.5 IMPLICATIONS AND LIMITATIONS 92
BIBLIOGRAPHY **95**

I Synopsis

The ability to learn behaviors that lead to reward is as fundamental for survival as is the ability to react to punishment and adapt behavior accordingly. At the neuronal level, changes that affect the circuits that support the latter ability are thought to underlie many maladaptive behaviors, such as addiction. The basolateral amygdala (BLA) has been proposed to play a central role within such circuits, given its importance in aversive stimuli-driven associative learning and in encoding values of specific reinforcers in instrumental learning. Research in the field of valence encoding in the BLA has uncovered the existence of positive and negative valence cell groups, which *learn* to respond to cues that predict appetitive or aversive outcomes, respectively. These studies have shown that valence cells can update the value of a cue when it changes from predicting one valence to predicting the other, and that the BLA is indeed needed to orchestrate the appropriate adaptive behavior. However, it is not known whether there exist BLA valence cells that learn to respond to actions with appetitive or aversive outcomes, nor if these cells update the value of an action whose outcome changes from being a reward to being a punishment. Because integrating new information on the outcome of actions is of paramount importance to adaptive behavior, an investigation on this matter at the cellular level is fundamental to enhance our understanding of maladaptive behaviors. Yet, the study of changes in the value of learned actions differs from that of changes in the value of learned cues in that cues can be presented to the study subjects regardless of their state, while actions need to be executed by the subjects themselves. To address this methodological challenge, we successfully established a behavioral paradigm where we suddenly introduce a probabilistic risk of punishment to a previously only-rewarded action. We use a head-mounted calcium imaging microscope to present the first account on action-encoding BLA projection-neurons in freely moving animals. Our main findings indicate that:

- Largely non-overlapping BLA ensembles encode primary and secondary reinforced instrumental actions.
- The instrumental action reinforcer and punisher are also encoded by largely non-overlapping BLA ensembles.
- Punisher encoding BLA ensembles are anatomically clustered, have a response magnitude several times larger than action- and reinforcer- encoding ensembles, and rapidly adapt their response magnitude and timing (Fig. I A, B).
- A larger fraction of BLA cells is recruited to the punisher ensemble than to the instrumental actions' ensembles.
- Instrumental action BLA ensembles do not reflect the change in action-outcome contingency when a probabilistic risk of punishment, instead of reward, is introduced (Fig. I B). We did not find other cells that significantly responded to the instrumental actions during risk.
- A fraction of BLA action-encoding cells is also responsive to the punisher (Fig. I A), but they do not exhibit changes in activity during the risk period.

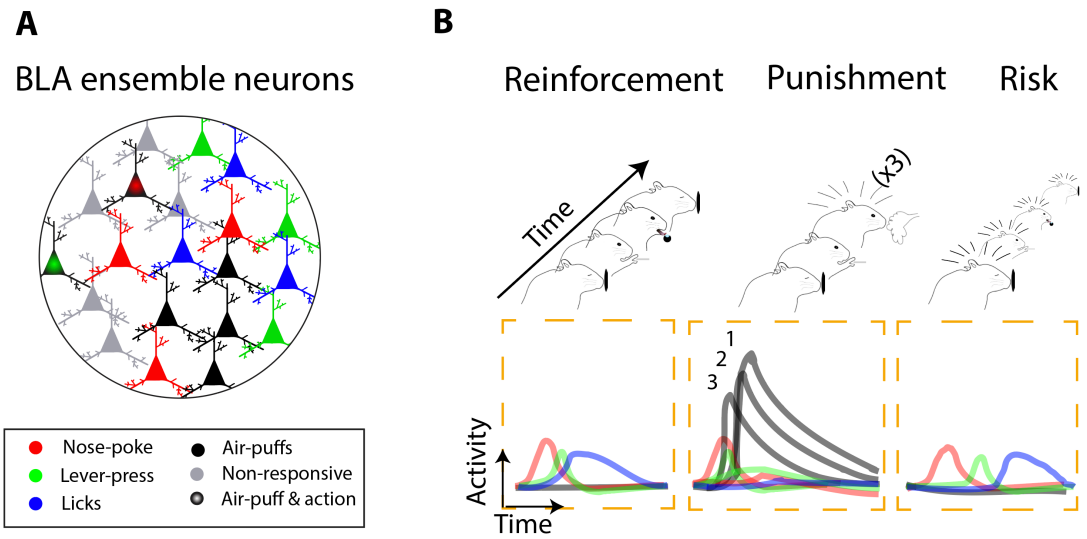

Figure I. Summary of main findings. (**A**) Identified BLA primary (lever-press) and secondary (nose-poke) actions, reinforcer (licks), and punisher (air-puff) ensembles. A fraction of mixed (air-puff and action) responsive cells is also represented. (**B**) Top: nose-poke, lever-press, licks and air puff. Bottom: BLA ensemble activity during the reinforcement (safe), punishment and risk time periods in the experimental task.

Our findings suggest that BLA action ensembles do not integrate new information on potential risks of punishment, but that this information is represented prominently by a separate BLA ensemble instead. While this implies the punishment-driven learning is not taking place at the individual 'action cell' level in the BLA, the existence of action, reinforcer and punisher ensembles certainly suggests that the BLA is ideally suited to play a key role in circuits mediating risk-taking and, by extension, adaptive behavior. Moreover, our findings imply that adaptive behavior may be impaired by deficits in the circuits controlling the learning about a potential risk of punishment, rather than by failure to integrate punishment information into the circuits that mediate reward-driven learning.

II Abbreviations

AAV	Adeno associated virus
BA	Basal amygdala
BLA	Basolateral amygdala
CEA	Central amygdala
CS	Conditioned stimulus
GECI	Genetically encoded calcium indicator
GRIN	Gradient-index
IL	Infralimbic
LA	Lateral amygdala
LK	Lick
LP	Lever press
Miniscope	Miniature microscope
mPFC	Media prefrontal cortex
NAc	Nucleus accumbens
NP	Nose-poke
PIT	Pavlovian to instrumental transfer
PL	Prelimbic
sPIT	Specific PIT (see PIT)
US	Unconditioned stimulus

III Preface

Learning and remembering actions that help us procure specific rewards is as important to survive as it is to refrain ourselves from these actions when there is a risk of punishment instead of reward. For example, learning to find and approach open fields provides an advantage to predators and hunters over preys. However, the proper reaction to a lightning crashing nearby in an open field is to withdraw from the field. Failing to adapt behavior in both cases leads to a decreased chance of survival. In fact, many maladaptive behaviors such as addiction and compulsive behaviors are thought to be driven by changes in the circuits that modulate punishment behavior (Diagnostic, 2013; Hu et al., 2019; Lesscher & Vanderschuren, 2012; L. J. Vanderschuren & Ahmed, 2013). The ability to associate a harmless stimulus (such as the flash of a lightning) with its potentially dangerous outcome has been shown to critically rely on the basolateral amygdala (BLA), a deep brain nucleus that lies at the heart of a distributed network of forebrain regions orchestrating fear learning (Tovote, Fadok, & Luthi, 2015). In addition, the BLA also supports reward-seeking behaviors, presumably by providing and updating the neural representations of the specific rewards that are predicted by conditioned cues (Balleine & Killcross, 2006). Other lines of research (Paton, Belova, Morrison, & Salzman, 2006) have shown the existence of BLA valence-specific ensembles that update the value of cues: positive valence cells start responding to cues that previously predicted an aversive stimulus if they now predict an appetitive one, and the opposite is true for negative valence cells. Therefore, given its role in updating the value of cues, we hypothesized that the BLA is important for updating the representation of instrumental actions. In this sense, the ability to adapt behavior when actions that previously lead to reward-only become associated with a risk of punishment should also depend on the BLA. Indeed, in rats optogenetic inactivation of the BLA during the delivery of a foot-shock punishment reduces the suppression of a previously reinforced instrumental action that becomes associated to a risk of punishment (Orsini et al., 2017). However, it is unclear whether this is the effect of disrupting the activity BLA cells that

update the value of an action or BLA cells that integrate the punishment information to drive learning otherwise. In fact, it is not known if instrumental actions leading to rewards are represented at the cellular level in the BLA. Given these important gaps in our knowledge of the function of the BLA, we decided to investigate the role of the BLA in representing instrumental actions and in updating their representation based on changes in their outcomes. To do so, we had to overcome methodological challenges in order to be able to establish an appropriate behavioral paradigm to study actions whose outcome change from reward to punishment in a probabilistic fashion. Additionally, we took advantage of the recent technological development of miniature calcium imaging microscopes and viral vectors tools. As a result, we provide the first ever dataset of BLA activity at the cellular resolution during safe and risky instrumental actions. More specifically, we found that largely distinct BLA ensembles encode instrumental actions, but that their representations are not updated when the outcome of the action is undermined with a risk of punishment, while the behavior does change dramatically. Instead, we found that a separate ensemble prominently encodes the punisher. Thus, our results suggest that, in regards to the BLA, the deficits underlying maladaptive behavior are not related to problems in updating the representation of the actions at the cellular level, but rather to problems in encoding the information of the punishment and/or relaying this information to other circuits for learning. Further research will be needed to elucidate the mechanism by which punishment and reward information integrate in the brain. Nonetheless, our research adds to the body of evidence suggesting the BLA is a key structure within the circuits that allow this integration to take place.

1. Introduction

The relevance of the findings hereby presented is better understood within the context of the historical development of the body of research that has shed light on amygdala, and in particular, BLA function. Therefore, the following sections focus on briefly and by no means exhaustively summarizing the timeline and relevance of experiments that have revealed the role of the BLA in conditioned fear, appetitive instrumental conditioning, and punishment. By the end of this section, it should become clear that a description at cellular level of the punishment-induced changes in BLA representations provides valuable insights for future research aiming to understand adaptive and by extension maladaptive behavior.

1.1 Beginnings

When Heinrich Klüver had his colleague Paul Bucy remove Aurora's temporal lobes, he did so with the intention to later test whether mescaline could exert its hallucinogenic effects on a brain without these (H. Klüver & Bucy, 1937; Nahm & Pribram, 1998). Aurora had been given to Klüver, known for his monkey-handling skills, because its previous owner found her too vicious to use her in experiments. The experiment showed that that temporal lobes were not necessary for mescaline to elicit behaviors similar to those in patients suffering a temporal-lobe epileptic attack, such as lip smacking. More interestingly, however, was the finding that Aurora had become tame. Experiments on more Rhesus monkeys revealed a wider spectrum of behavioral changes. These had, nonetheless, been described 50 years before by Sanger Brown and Edward Schäfer (Brown & Schäfer, 1888), but overlooked because the scientist were focused on finding the brain areas responsible for vision and audition. The bilateral anterior temporal lobectomy caused increased oral exploration of objects, hypersexuality, and more strikingly, the inability to react accordingly to objects that called for orthogonally different behaviors, such as a (fake) snake and food (Heinrich Klüver & Bucy, 1939). The

observed deficits in appropriate escape and approach behaviors spurred half-century of research that sought to narrow down the areas responsible for fear and reward related behaviors, respectively. In 1956 Lawrence Weiskrantz showed that lesions restricted to the amygdala made it difficult for monkeys to recognize the reinforcing properties of both positive (food) and negative (electric shocks) stimuli (Weiskrantz, 1956). The wave of research that followed Weiskrantz study, however, would be fostered by the use of Pavlovian fear conditioning as a standard simple behavior to study the association between neutral stimuli (light or auditory cues) and their conditioned reinforcing properties (contingent air puffs or foot shocks). Therefore, the field advanced in a disproportionate fashion towards elucidating the role of the amygdala within the aversive realm of adaptive behavior, and it was not until the early 2000s that the role of the amygdala within the appetitive realm began to catch up (A. Beyeler & Dabrowska, 2020).

1.2 Amygdala and Fear learning

Beyond hallucinations, (ictal) fear has long been a well-documented symptom of patients with temporal lobe epilepsies (Jackson & Stewart, 1899; MacLean, 1986). In 1954, William Feindel and Wilder Penfield showed that electric stimulation of the amygdala in such patients evoked fearful emotions (Feindel & Penfield, 1954). These findings, in addition to evidence from animal studies pointing in the same direction (Jose M. R. Delgado, Roberts, & Miller, 1954; José M. R. Delgado, Rosvold, & Looney, 1956; MacLean & Delgado, 1953), inspired the field to undertake research determined to isolate the role of the amygdala in fear behaviors. For that purpose, rodents, specially rats, became popular as an animal model and respective behavioral tasks (Fig. 1.1) (Miller, 1948) to study fear induced learning and changes in behavior were developed – by then Charles Darwin's idea of the biological study of emotions in animals (Darwin, 1872) had gained momentum. In particular, chambers equipped with a metallic grid floor through which an electric shock could be delivered became widely used in

conjunction with neutral (non-aversive nor appetitive) light (D. C. Blanchard & Blanchard, 1972) or auditory cue (Henke, 1983). In such experiments, the presentation of the cue would be followed by a brief mild foot-shock. This Pavlovian fear conditioning was used to address questions relating to both the expression and acquisition of fear behaviors. In this sense, it came forward as a model to study the memory and learning underlying the behavioral changes that the animals display towards a previously neutral cue (the conditioned stimulus, CS) that becomes a predictor of a punishment (the unconditioned stimulus, US). Rodents' defensive repertoire against the aversive CS include avoidance of CS-related context (when this is possible) and freezing, a state of immobility that is accompanied by physiological changes such as increased blood pressure (LeDoux, Cicchetti, Xagoraris, & Romanski, 1990), increased muscle tone (M. S. Fanselow, 1994), parasympathetically induced bradycardia and pupil dilation (Applegate, Kapp, Underwood, & McNall, 1983). Importantly, learning and remembering new threats in the environment and being able to deploy the appropriate defensive behavior increases chances of survival. The selection mechanism for either freezing or avoidance strategies (passive avoidance or flight) has been proposed to depend on threat imminence: the ratio between the intensity of the threat and the distance to it (D. C. Blanchard & Blanchard, 1988; Michael S. Fanselow & Lester, 1988), with lower ratios evoking freezing and higher ones flight.

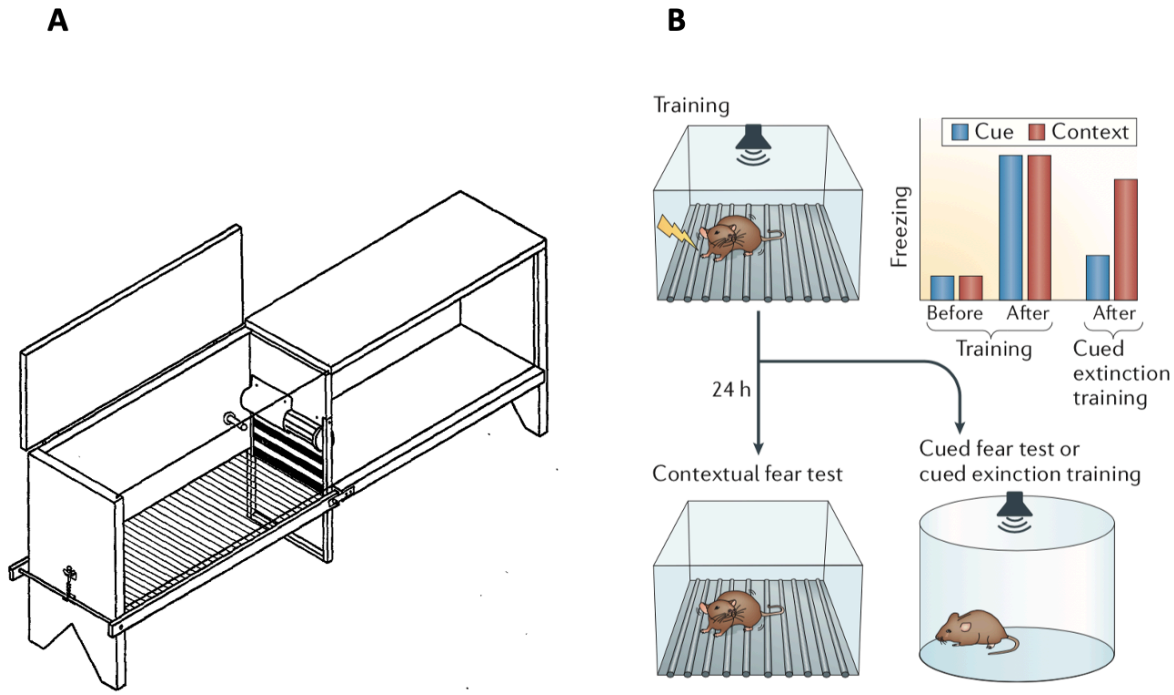

Figure 1.1. An overview of fear conditioning setups. (**A**) Miller box (Miller, 1948) displays a shock-grid and a door with black stripes that animals can open by using the rotary wheel or side-wall bar. (**B**) Contemporary fear conditioning and extinction contexts (Tovote et al., 2015). Learning about the tone cue is inferred from freezing levels (inset).

Early studies on avoidance strategies of rats with radiofrequency or electrolytic lesions to the amygdala (King, 1958; Robinson, 1963; Horvath, 1963; Ursin, 1965; Pellegrino, 1968) revealed deficits in the aversive CS driven learning: lesioned animals displayed normal fear and motor reactions to the onset of the electric shock, but failed to acquire the appropriate escape responses to the CS in anticipation of the shock (Gaston & Freed, 1969). However, it became clear that under these circumstances it could not be necessarily inferred that because the rats failed to execute an escape they also failed to acquire an emotional response to the CS (Gaston & Freed, 1969), given that both the fear response and the instrumental avoidance response overlapped in time. In paradigms that did not involve instrumental learning it was shown that

amygdalectomized rats did not discriminate between a context where they had received foot-shocks and one where they had not (Gaston & Freed, 1969). Around the same time, freezing behavior was being pushed forward as an index of fear (R. J. Blanchard & Blanchard, 1969; R. J. Blanchard, Dielman, & Blanchard, 1968), and it was shown that rats with amygdala lesions freeze less when exposed to a sedated cat or to a shock prod after learning it delivers shocks (D. C. Blanchard & Blanchard, 1972). The amygdala was therefore linked to freezing behavior elicited by both conditioned (the prod) and unconditioned (the cat) stimuli. In 1983 it was shown that amygdala cells that respond when the rat is forcibly restrained, also become responsive to the initially neutral white noise that was present when the restraining procedure took place (Henke, 1983). Building up on these findings, as well as on anatomical (Johnston, 1923; Meynert, 1868) and electrophysiological (Gloor, 1955) characterization of the amygdala, many future studies focused on studying subdivisions of the amygdala within the context of auditory Pavlovian fear conditioning. Non-selective aspiration or radiofrequency lesions of the amygdala fell out of favor because of the extended damage to projection fibers passing near and through (Baxter & Murray, 2002) and, instead, more specific fiber-sparing excitotoxins (e.g. NMDA) and stereotactic electrolytic lesions as well as substance-mediated reversible inhibition (GABA agonists, e.g. muscimol) were used (Baxter & Murray, 2002). These studies broadly defined the roles of the two principal subnuclei of the amygdala in aversive conditioning. On the one hand, basolateral amygdala (BLA), which profusely receives thalamic and cortical input on its lateral unit (lateral amygdala, LA), was identified as an important relay of sensory information: damage to the BLA interferes with Pavlovian fear conditioning (Campeau & Davis, 1995; LeDoux et al., 1990). Its basal unit (the basal amygdala, BA), was also found to play an important role in contextual fear conditioning: the expression of fear responses in contexts where a punishment has been delivered (JJ Kim & Fanselow, 1992). On the other hand, the central amygdala came forward as the interface with motor systems: damage to this nucleus disrupts expression of conditioned fear responses (Kapp, Frysinger, Gallagher, & Haselton, 1979) and damage to the areas the CEA projects to selectively disrupted the

expression of individual components of the conditioned fear behavior (LeDoux, Iwata, Cicchetti, & Reis, 1988), such as blood pressure (damage to the lateral hypothalamus) and freezing (damage to the periaqueductal gray, PAG).

In the last couple of decades, Neuroscience has seen a remarkable rise in technologies: genetic (Kuhn, Schwenk, Aguet, & Rajewsky, 1995), pharmacogenetic (Armbruster & Roth, 2005), optogenetic (Boyden, Zhang, Bamberg, Nagel, & Deisseroth, 2005) and viral (Wall, Wickersham, Cetin, De La Parra, & Callaway, 2010) tools have allowed for unprecedented interrogation of specific subpopulations into the cellular and molecular levels. As initially most tools became available for mice, this helped to propel them as the most used animal model in Systems Neuroscience (Ellenbroek & Youn, 2016). Modern system-level studies have taken previous findings a step forward: for example, it has been established that the way the LA gates fear learning is by a control element consisting of interneuron subtypes that gate the acquisition of conditioned fear responses by disinhibition (Krabbe et al., 2019; Wolff et al., 2014): a motif that has also been shown to be a control element in the auditory cortex circuits for fear learning (Letzkus et al., 2011). In regards to the previously mentioned role of the BA in contextual fear learning, it has been shown that there is a specific hippocampal circuit that projects to the BA and is required for contextual fear memory retrieval (Xu et al., 2016). Finally, in contrast to what was originally thought, it has been shown that the CEA is not only an output nucleus for the expression of conditioned fear responses, but is also involved in the learning and consolidation of Pavlovian fear conditioning (Wilensky, Schafe, Kristensen, & LeDoux, 2006). More specifically, its lateral (CEl) and medial (CEm) subdivisions were found to have differential contributions in conditioned fear acquisition and expression (Ciocchi et al., 2010): CEl, required for acquisition, has cells that are excited (CEl^{ON}) and inhibited (CEl^{OFF}) by the CS, and CEl^{ON} are inhibited by CEl^{OFF} cells, which also form an inhibitory connection with CEm cells, required for expression. Moreover, genetic markers have been found for CEl^{OFF} cells (Haubensak et al., 2010) as well as for cells that control conditioned freezing (cells expressing somatostatin, SOM)

or flight (cell expressing corticotropin-releasing factor, CRF), which have been shown to form a competitive inhibitory circuit for the selection of these mutually exclusive active and passive fear responses (Fadok et al., 2017). Furthermore, a long-range inhibitory pathway from the CEA to the ventrolateral PAG that gates freezing has been identified (Tovote et al., 2016). Finally, at the molecular level, it has been shown that the infusion of glutamate (i.e., NMDAR, AMPAR) receptors antagonists into the BLA can impair the acquisition, expression and extinction of conditioned fear, and the infusion of NMDAR agonist into the BLA can facilitate extinction (Zimmerman & Maren, 2010).

In summary, vast progress has been made in identifying the control elements of the amygdala circuitry mediating conditioned fear, an essential learning and memory mechanism that allows an organism to adapt its behavior in ways that are critical for survival. In particular, the BLA has come forward as a key structure of the neural network that orchestrates the learning of new threats in the environment by receiving sensory information and driving defensive behaviors via downstream circuits. However, as will be described in the next section, when it comes to the learning and memory of rewards instead of punishments, the role of the BLA is less clear.

1.3 BLA and reward

Early studies (Schwartzbaum, 1960; Weiskrantz, 1956) described pronounced changes in appetitive behaviors induced by amygdala lesions. However, the overwhelming increase in publications on the role of the amygdala in aversive learning, driven in part by the wide adoption of fear conditioning paradigms in the 1990s, was not matched by an increase in publications referring to the role of the amygdala in appetitive learning (Wassum & Izquierdo, 2015). Relatively recently, nonetheless, the role of the amygdala in reward learning has been revisited (Baxter & Murray, 2002; Murray, 2007; Wassum & Izquierdo, 2015). In particular, the BLA has been implicated in encoding the representation of a specific predicted reward (Balleine, Killcross, & Dickinson, 2003;

Balleine & Killcross, 2006). Evidence in support of this role comes from experiments on instrumental outcome devaluation (Balleine et al., 2003) and revaluation (Wassum, Cely, Balleine, & Maidment, 2011; Wassum, Ostlund, Maidment, & Balleine, 2009), outcome-specific reinstatement (Ostlund & Balleine, 2008; Ostlund & Balline, 2007), (Cador, Robbins, & Everitt, 1989), conditioned cue-induced reinstatement (Fuchs, Weber, Rice, & Neisewander, 2002; Meil & See, 1997), CS-potentiated feeding (Holland & Petrovich, 2005; Holland, Petrovich, & Gallagher, 2002) and specific Pavlovian-instrumental transfer (Corbit & Balleine, 2005).

In instrumental outcome devaluation by sensory-specific satiety rats that have been trained to press levers to gain food rewards are given free access to one of two different rewards and subsequently placed in a context with two levers, each of which yields a one of the two rewards. BLA lesions attenuate the devaluation effect, by which control subjects work more for the reward they have not been given access to previously (Balleine et al., 2003). Interestingly, rats with BLA lesions also exhibit a decreased sensitivity to action-outcome degradation and impaired ability to discriminate between rewarded and unrewarded actions by using reward-specific properties (Balleine et al., 2003). Conversely, in instrumental outcome revaluation rats are made hungry, a manipulation that increases the incentive value of food as a reward outcome. Behaviorally, this translates to an increase in reward-seeking behavior, which can be read out of lever presses (Wassum et al., 2011; Wassum et al., 2009). Infusion of μ-opioid receptor antagonists into the BLA blocks this increase, suggesting that shifts in endogenous opioid transmission in the BLA mediate the encoding of incentive value. Importantly, consummatory licking behavior is unchanged, indicating that this BLA μ-opioid receptor-dependent mechanism is important for the encoding the incentive value changes rather than changes in the hedonic value (Wassum & Izquierdo, 2015). Evidence from outcome-specific reinstatement, where the delivery of a reward selectively motivates the execution of the response it was trained with instead of an alternative response that was paired with a different reward, indicates that both pre-

and post-training BLA lesions abolish this outcome-specific motivated behavior, suggesting that the BLA may play an important role in the memory and/or expression of specific reward representations (Ostlund & Balleine, 2008; Ostlund & Balline, 2007). On the other hand, in conditioned reinforcement, animals learn perform a novel action to gain exposure not to a reward but to a conditioned reinforcer cue (e.g., a tone or a light) that has been previously used to signal reward delivery in a different context. BLA lesioned rats exhibit a significant selective reduction in responding to a lever that has provides the conditioned reinforcer, compared to control animals (Cador et al., 1989). In conditioned cue-induced reinstatement, a behavior that models addiction relapse, rats learn to self-administer an intravenous cocaine solution by pressing a lever. The lever pressing causes a sound and a light cue to go off. Subsequently, the animals undergo an extensive extinction of this response and afterwards the ability of the cue (sound and light) to reinstate the extinguished action is evaluated. Bilateral NMDA BLA lesions abolish the ability of the cue to reinstate responding (Fuchs et al., 2002; Meil & See, 1997). Moreover, studies on CS-potentiated feeding, where sated rats are presented with food pellets and the number of pellets they consumed in the presence of an auditory CS that was previously paired with food (CS+) is compared to that consumed in the presence of a CS that has never been paired with food (CS-), show that BLA sham rats eat more pellets during the CS+ period, whereas rats with bilateral BLA lesions fail to exhibit this CS-potentiated feeding (Holland & Petrovich, 2005; Holland et al., 2002). Finally, in sPIT, animals are trained in a Pavlovian task to associate two different neutral cues to the delivery of a specific food reward each. Separately, animals are trained in an instrumental task to execute two different actions, each of which yields one of the two rewards that were also used during the Pavlovian task. Although the Pavlovian cues and the instrumental actions are never paired, presenting one of the cues will selectively invigorate the performance of the action that earn the same specific reward associated with the cue (Colwill & Motzkin, 1994; Colwill & Rescorla, 1988; Holmes, Marchand, & Coutureau, 2010; Kruse, Overmier, Konz, & Rokke, 1983). BLA lesion and inactivation abolishes this effect, by presumably disrupting the ability of the

animals to retrieve the Pavlovian-Instrumental shared outcome representation (Fig. 1.2) (Corbit & Balleine, 2005).

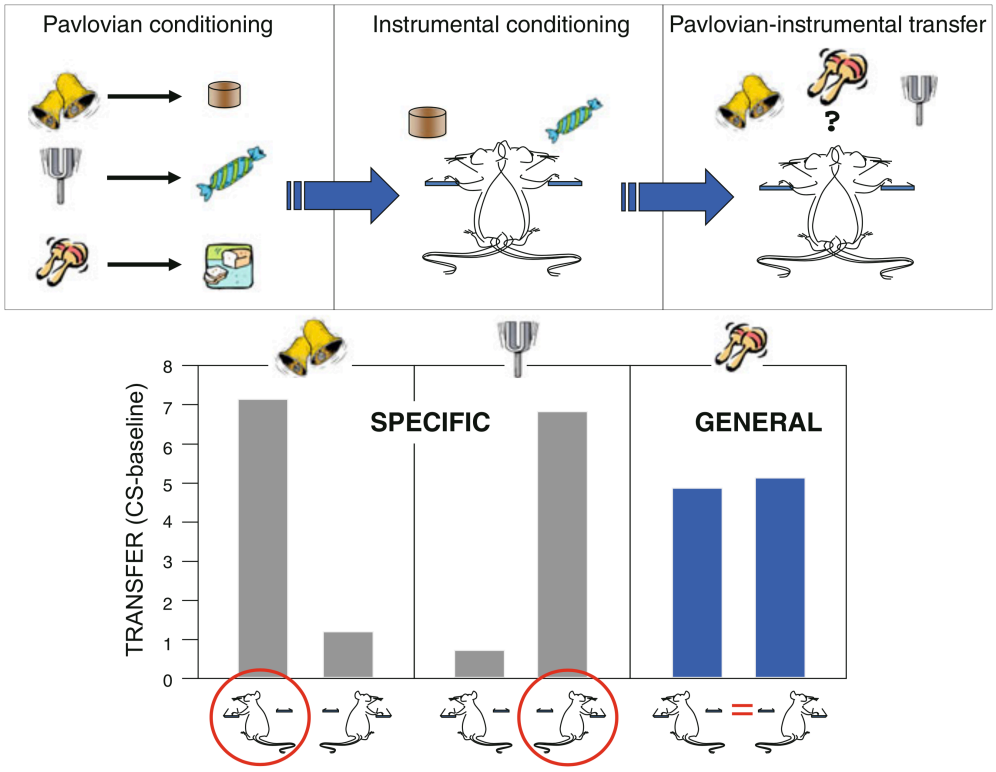

Figure 1.2 Specific and general Pavlovian-instrumental transfer (PIT) (Corbit & Balleine, 2005). Animals learn to associate three cues to three different rewards, and two actions to two of those rewards separately (top panel). Presentation of each Pavlovian cue in the instrumental context motivates those actions (lever pressings) that lead to the same reward as the cue, even though no reward is present during testing. When none of the available actions leads to the same rewards as the Pavlovian cue, the cue motivates behavior unselectively (general PIT). BLA lesions impair the reward-specific motivational effect of Pavlovian cues on instrumental action.

In summary, there is an extensive body of evidence implicating the necessity of the BLA for the encoding and expression of outcome specific reward representations in both Pavlovian stimulus-outcome (S-O) and instrumental response-outcome (R-O) associative learning. Admittedly, large part of this evidence comes from lesion and inactivation manipulations whose specificity is not up to modern neuroscience standards, but

nonetheless the consistency in the findings across different studies speaks in favor of the proposed role for the BLA.

In addition to the findings from the loss of function experiments discussed above, evidence from neural recordings in animal models also supports the role of the amygdala in the encoding and expression of outcome specific reward representations. An important feature of outcome specificity is the valence associated to the outcome: appetitive outcomes (i.e., rewards) have a positive valence and aversive outcomes (i.e., punishments) have a negative valence. Rodents and monkeys studies have shown that BLA cells respond to CSs associated to positive and negative valence (A. Beyeler et al., 2016; Fuster & Uyeda, 1971; Shabel & Janak, 2009). Moreover, some BLA neurons track the valence of the CS (Paton et al., 2006): if a neutral image is paired with juice reward positive valence cells start to respond more to the image, but if the image is subsequently paired with an air puff punishment positive valence cells decrease their response and instead negative valence cells start to respond more to that image. The anatomical organization of valence cells in the BLA is still open to debate, with some studies suggesting valence cells are intermingled (Belova, Paton, Morrison, & Salzman, 2007; A. Beyeler et al., 2016; Burgos-Robles et al., 2017; Morrison, Saez, Lau, & Salzman, 2011; Namburi et al., 2015; Paton et al., 2006) and a other studies suggesting they are segregated and organized along an anterior-posterior gradient that can be also defined by genetic markers (J. Kim, Pignatelli, Xu, Itohara, & Tonegawa, 2016; J. Kim, Zhang, Muralidhar, LeBlanc, & Tonegawa, 2017). In the latter studies, the proposed genetic markers are Rspo2, which is enriched in anterior BLA magnocellular neurons, and Ppp1r1b, which is enriched in the posterior BLA parvocellular neurons (J. Kim et al., 2016). Whereas optogenetic stimulation of Rspo2+ cells elicits a defensive response in naïve mice, optogenetic stimulation of Ppp1r1b+ cells promotes an appetitive response (J. Kim et al., 2016). The connectivity of these BLA subpopulations to the CeA has also been characterized (J. Kim et al., 2017). Nonetheless, it has to be noted that these studies examined BLA responses to stimuli with innate valence, whereas studies where

valence cells appear to be intermingled assessed the neural response to conditioned stimuli (with acquired valence). Hence, both observations are not necessarily inconsistent with one another, but suggest that BLA topography for innate aversive or appetitive stimuli may be different than that for stimuli with conditioned valence.

While little is known about genetically defined valence-specific subpopulations and their anatomical organization in the BLA, a growing body of evidence indicates that projection targets mediate conditioned valence-specific behaviors. For example, whereas optogenetic activation of BLA cells that project to the nucleus accumbens (BLA-NAc) supports positive reinforcement (Britt et al., 2012; Namburi et al., 2015; Stuber et al., 2011), optogenetic activation of BLA cells that project to the central amygdala (BLA-CeA) drives real-time place aversion (Namburi et al., 2015). Moreover, as reveal by pharmacological disconnection of the BLA and the NAc, the BLA-NAc pathway is critical for cocaine seeking (Di Ciano & Everitt, 2004).

Furthermore, BLA-NAc projectors are preferentially excited by a positive cue and BLA-CeA ones are excited by a negative one (A. Beyeler et al., 2016). In terms of plastic changes, it has been shown that synaptic inputs on BLA-NAc projections are potentiated after reward learning and depressed after fear conditioning, while inputs on BLA cells that project to the medial central amygdala (CeM) undergo opposing synaptic changes (Namburi et al., 2015). From the observed activity profiles, however, inference of valence coding from projection-defined populations is only possible at the population level, due to a high heterogeneity of single-neuron activity within these populations (A. Beyeler et al., 2016).

In conclusion, the existence of BLA cells that respond to conditioned positive or negative valence and the behaviors induced by their activity suggests that their modulation could play an important role in the system that allows for a flexible associative S-O and R-O

learning. Such flexibility would serve the encoding and expression of outcome specificity for both stimuli and responses, therefore supporting adaptive behavior.

1.4 Reward and Punishment in the BLA

Deficits in adaptive behavior induced by BLA lesions manifest in tasks that require the comparison of two alternative outcomes for the same stimulus or response. A particular case is that of reversal learning, where the contingency for two different stimuli is reversed: the reward predictive stimulus becomes predictive of punishment (or no reward) and vice versa (Churchwell, Morris, Heurtelou, & Kesner, 2009; Paton et al., 2006; Schoenbaum, Chiba, & Gallagher, 1999; Schoenbaum, Setlow, Nugent, Saddoris, & Gallagher, 2003). As mentioned earlier, many BLA neurons adapt to this contingency shift and start responding according to the novel stimulus-outcome pairing. Because the new contingencies become stronger as a function of reward history and learning based on the strength of these contingencies must occur to update previous contingencies (Rescorla & Solomon, 1967), these results suggest that plastic changes occur in the BLA at the onset of reversal. Besides reversal, introduction of a risk of explicit punishment also violates the expectations from a cue or action based on recent reward history. In the case of an instrumental action, such aversive reinforcement suppresses the execution of the action. This suppression is supported by learning about environmental cues that predict the punishment (CSs) and also by learning about behavioral antecedents that lead to the punishment (the instrumental action itself). For example, optogenetic inactivation of BLA during punishment makes rats less prone to suppress their choice behavior towards the risky choice (Orsini et al., 2017), resulting in a more risk-taking preference profile. A similar phenotype is observed when the risk is a longer time out (Zeeb & Winstanley, 2011), although in experiments with risk of implicit punishment (such as omission of rewards) BLA lesions make rats risk averse (Ghods-Sharifi, St Onge, & Floresco, 2009; Tremblay et al., 2014). The different effects observed on risk taking profiles may be due to the nature of the punishment (Wassum & Izquierdo,

2015), the lesion location within the BLA (Jean-Richard-Dit-Bressel & McNally, 2015) or a the timing of disruption of BLA function within the specific task (Orsini et al., 2017).

In sum, the evidence described above indicates that the BLA plays a critical role in integrating reward and punishment outcomes into the representation of the instrumental action itself. This is in agreement with and comes as an extension of the evidence implicating the BLA role in outcome-specific representation of instrumental actions, and with the valence-specific responses of BLA subpopulations to conditioned stimuli. However, what happens at the cellular level when the behavior calls to incorporate punishment information to suppress an ongoing instrumental sequence is both unknown and at the very heart of the understanding of maladaptive behaviors. Certainly, it is tempting to examine the cellular activity projection-target defined subpopulation, such as BLA-NAc and BLA-CeA discussed above. Indeed, projection-defined BLA functionality has been described before (Burgos-Robles et al., 2017; Senn et al., 2014). For example, 'fear-on' and 'fear-off' neurons (Cyril 2008), which modulate their firing in opposing ways during fear expression and extinction, differentially project to the prelimbic (PL) and infralimbic (IL) subdivisions of the medial prefrontal cortex (mPFC) in mice (Senn et al., 2014). However, state of the art deep brain calcium imaging technology makes it possible to examine general population activity in the BLA without having to compromise the data by restricting the analysis to subpopulations defined in the literature. This is the approach and analysis we support in this study, where we aim to a provide a description at cellular level of the punishment-induced changes in BLA representations of instrumental actions.

1.5 BLA anatomy

The BLA was first described an al almond-shaped structure deep within the temporal lobe by Karl Friedrich Burdach (Burdach, 1819). Historically, based on macro-anatomical features, it is frequently divided into the lateral amygdala (LA) and the basal amygdala

(BA) (Fig 1.3). In humans the LA consist of around 5.48 million neurons and the BA of 5.02 million (García-Amado & Prensa, 2012; Rubinow et al., 2016), while in mice the numbers are orders of magnitude smaller with the LA containing 62,000 neurons and the BA 131,000 (Erö, Gewaltig, Keller, & Markram, 2018). Around 60% of the BLA cells in mice are neurons, whereas in humans this number goes down to between 20 and 35%. However, although there are also differences, there are strong similarities across mammalian species in the organization of the amygdala (Janak & Tye, 2015; Pitkänen, 2000).

Golgi staining in rats were the first to show that up to 95% of the BLA neurons are glutamate-releasing pyramidal cells and the remaining 5% are smaller ovoid interneurons that release gamma amino-butyric acid (GABA) (Alexander J. McDonald, 1982). In mice, the proportions are 91% and 9% respectively, while in monkeys GABAergic cells can reach up to 25%, bringing down the proportion of pyramidal cells to 75%. In all cases both types of neurons appear randomly distributed.

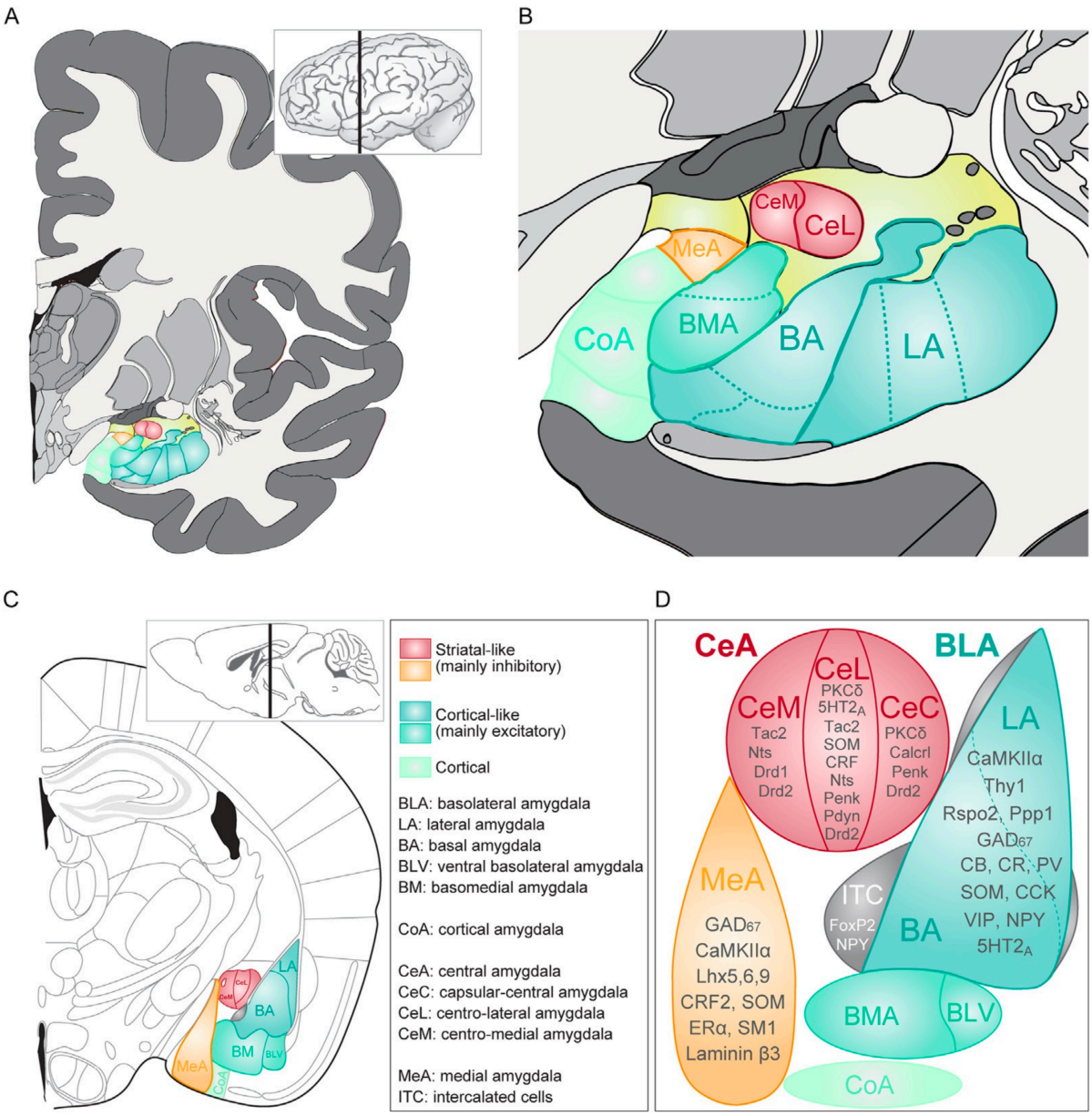

Figure 1.3. Human and mouse anatomy of the BLA. (**A**) Location of the amygdala in the human brain. (**B**) Detailed human amygdala. (**C**) Location of the amygdala in the mouse brain. (**D**) Detailed mouse amygdala and candidate marker genes for subpopulations (A. Beyeler & Dabrowska, 2020).

Pyramidal cells are also called projection cells, because their axons project out of the BLA, with several collateral that arborize within the BLA (Alexander J. McDonald, 1982). In contrast, inhibitory interneurons have dense local arborizations and can be classified as bipolar, multipolar, bitufted and chandelier according to their dendritic branching

pattern (A. Beyeler & Dabrowska, 2020). Although some of them do have long-range inhibitory projections, most synapse locally (A. Beyeler & Dabrowska, 2020). BLA pyramidal cells fire broad action potentials (half-width 1.2 ms) that are followed by a lasting after-hyperpolarization (AHP, 1-5s) and can adapt to different firing frequencies. Conversely, BLA interneurons fire short-duration action potentials (half-width of 0.7ms) and have a rather consistent firing frequency (A. Beyeler & Dabrowska, 2020; Faber & Sah, 2002; Rainnie, Asprodini, & Shinnick-Gallagher, 1993; Sah, Faber, Armentia, & Power, 2003). In the BA, the number of large magnocellular projection neurons decreases along the anterio-posterior direction, while the one of smaller parvocellular projection neurons does so in the opposite direction, with both gradients meeting at the intermediate zone (Anna Beyeler et al., 2018; Price, Russchen, & Amaral, 1987; Savander, Go, Ledoux, & Pitkänen, 1995). As in the cortex, projection neurons express the calcium/calmodulin-dependent protein kinase II (CaMKII) in their cell body, dendrites and spines, and initial segment of the axon terminals (A. J. McDonald, Muller, & Mascagni, 2002). To date, no genetic markers have been identified for neurons that undergo plastic changes during appetitive or aversive associative learning (stimulus/action responsive cells), nor for projection specific BLA populations (A. Beyeler & Dabrowska, 2020). Therefore, the use of CaMKII-promoter genetic constructs serves as an entry point to selectively target BLA pyramidal neurons. In addition, like all excitable cells (Tsien, Lipscombe, Madison, Bley, & Fox, 1988), CaMKII neurons have voltage-gated calcium channels (VGCCs) and exhibit transient increases of intracellular calcium ions concentration ([Ca2+]) during action potential firing and neurotransmitter receptor activation (Hagiwara , Chichibu , & Naka 1964), making it possible to use a calcium imaging approach to study their activity. In the following section we discuss the calcium imaging approach used in the present study.

1.6 Imaging cellular activity in freely moving animals

The pioneering studies that sowed the ideas of the technology implemented in modern miniature calcium imaging microscopes were published almost two decades ago. On the one hand, in 2001 a study describing a miniaturized two-photon microscope that rats could wear as a hat was published (Helmchen, Fee, Tank, & Denk, 2001). It involved conventional tabletop optical instruments that could not be readily used on multiple animals and it was far from living up to the promise of cellular resolution imaging in freely moving animals due to major limitations, such as low resolution, small field of view and motion-induced artifacts (Flusberg et al., 2008). However, the idea was embraced by several groups and soon major improvements followed. In particular, the approach taken by Mark Schnitzer's group at Stanford University proved to be successful: gradient index (GRIN) lenses to reduce the components necessary to manipulate light (Barretto, Messerschmidt, & Schnitzer, 2009), epifluorescence microscopy to increase field of view and avoid two-photon microscopy scanners-induced motion artifacts (Flusberg et al., 2008), and miniaturization and integration of optic and electrical components into a light-weight microscope (Ghosh et al., 2011).

Gradient index materials (Gale, 1907) have a refractive index that varies regularly as a function of a certain dimension. This makes it possible to converge or diverge light in a predictable manner. GRIN lenses are glass cylinders where the refractive index decreases as a function of the radial distance in a way that makes light travel in a sinusoidal path through the lens. Taking advantage of this feature and optimizing optical resolution (Barretto et al., 2009) was an important step in reducing the number of components, size, weight and points of failure of modern miniature microscopes. Additionally, it was important to prioritize the higher acquisition rates and broader fields of view of epifluorescence microscopy versus the deeper penetration and higher resolution of a two-photon system which would have required a scanning mechanism, probably prone to more motion artifacts (Flusberg et al., 2008).

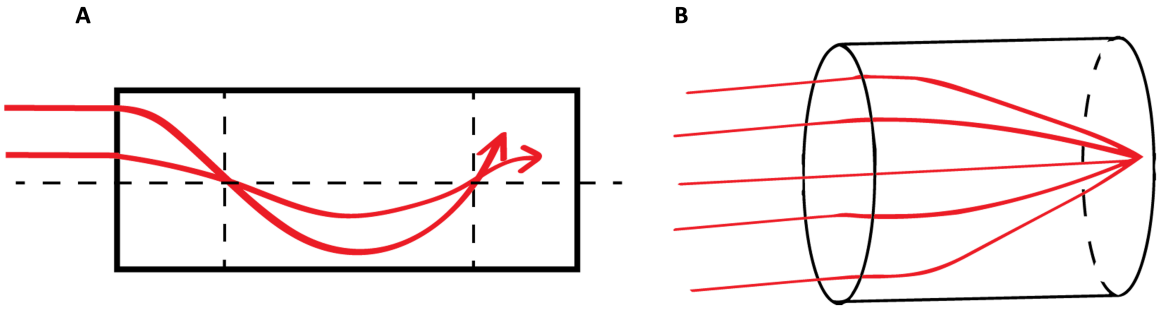

Figure 1.4 Light path through a GRIN lens. (**A**) Side view of a GRIN lens and light (red), showing center (horizontal dashed line) and points where the light converges (vertical dashed lines). Despite being flat, the diffraction gradient makes the light travel in a sinusoidal path. (**B**) GRIN lenses properties allow to converge or diverge light within the same lens.

Finally, instead of conducting signal light back into a remote image acquisition device using optical fiber, a miniature complementary metal–oxide–semiconductor (CMOS) camera and a LED light source were integrated into the head-mounted microscope, allowing to replace the finite-bending-radius fiber for electrical lines and thus increasing mechanical flexibility and portability for the animal (Ghosh et al., 2011).

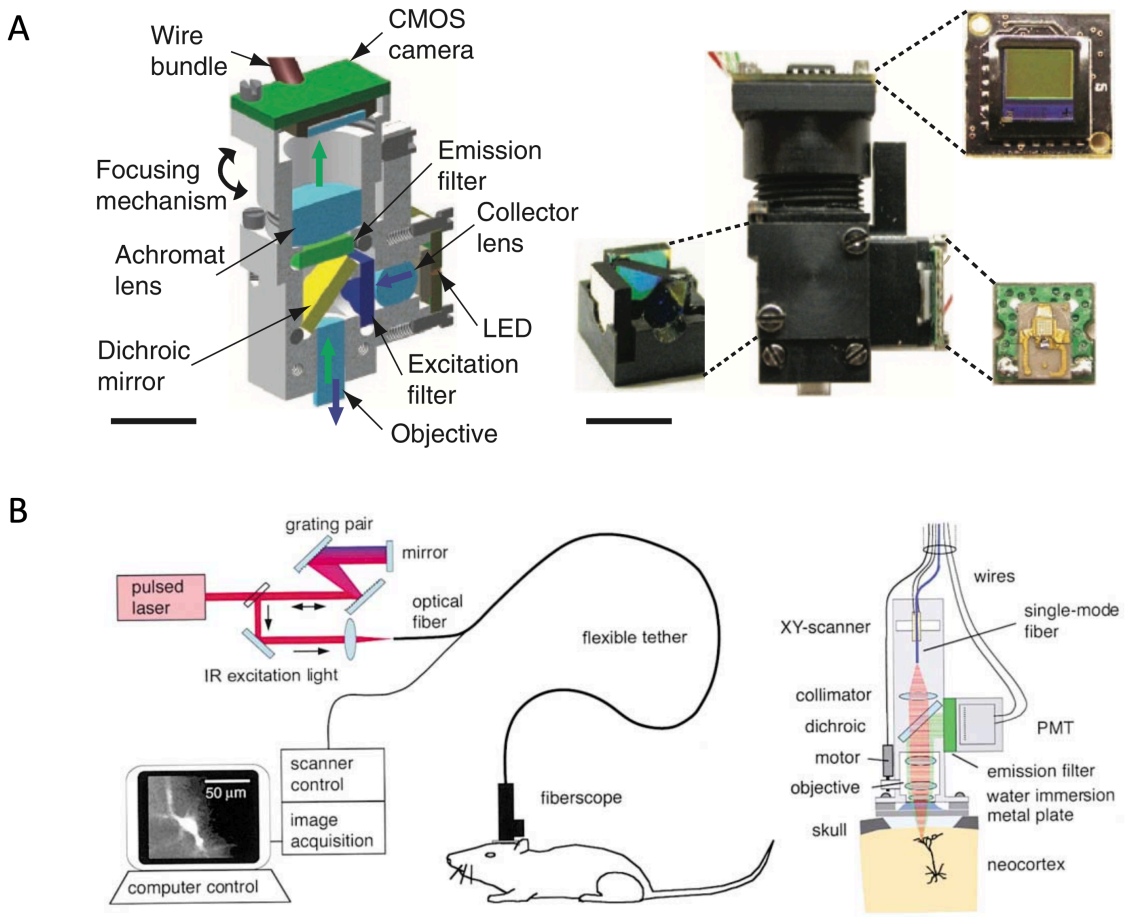

Figure 1.5 Modern and early miniature microscopes. (**A**) Miniaturized-integrated microscope (Ghosh et al., 2011). (**B**) First proposed head-mounted miniature microscope setup (Helmchen et al., 2001).

On the other hand, parallel developments on genetically encoded calcium indicators (GECIs) and viral vectors as gene delivery tools allowed for the maturation of complementary technology employed in modern 'miniscope' imaging experiments. As opposed to small-molecule calcium sensitive dyes, which are often highly phototoxic, GECIs enable long term, repeated non-invasive imaging of specific cells (Lin & Schnitzer, 2016). In particular, the single-wavelength sensor GCaMP family has become widely used in in vivo experiments (Tian et al., 2009). Although it was introduced in 2001 (Nakai, Ohkura, & Imoto, 2001), current ultra-sensitive versions, such as the GCaMP6 family, have improved the original version by achieving low-baseline fluorescence and high

signal-to-noise ratios (SNRs) (Chen et al., 2013). Three different versions with varying kinetics are available: slow (s), medium (m) and fast (f). GCaMPs consist of a circularly permuted green fluorescent protein (cpGFP), the calcium-binding protein calmodulin (CaM) and CaM-interacting M13 peptide. Upon the binding of a calcium ion, they undergo conformational changes that cause increase chromophore brightness. Although calcium transients do reflect underlying electrical cell activity (Chen et al., 2013), they have complex spatiotemporal dynamics and inferring the type electrical event (e.g. spiking activity vs. subthreshold events) becomes challenging for fast-spiking cells. Genetically encoded voltage indicators (GEVIs) could overcome this limitation, but the long-concerted effort to develop them has yet to see a GEVI that meet all performance requirements (Lin & Schnitzer, 2016), as most of them suffer from insufficient SNRs. Alternatively, 'next generation' GECIs capable of resolving fast spike trains have been developed (Inoue et al., 2019). The ability of traditional GECIs to detect neuronal inhibition has also been contested, and for that matter inverse-type calcium indicators, whose fluorescence increases as intracellular calcium concentration decreases, have been developed (Hara-Kuge et al., 2018). However, experimental evidence indicates that GECIs can detect inhibitory events (Betley et al., 2015; Forli et al., 2018; Otis et al., 2017; Wei et al., 2020) although there is no consensus on their interpretation in terms of the underlying electrical phenomena (Ali & Kwan, 2019).

In order to introduce GECIs into the appropriate target cells, viral vectors that can carry the specific genetic constructs have to be used. Because of their ability to infect postmitotic cells and their low toxicity (Akli et al., 1993; Kaplitt et al., 1994), adeno-associated viruses (AAVs) are frequently used for this purpose. These small (20 nm) defective (viral gene expression has been eliminated) viruses are non-pathogenic, well tolerated over long periods of time and spread efficiently within brain tissues (Campos, Walker, & Mollard, 2020). They exist in different serotypes, meaning that their exterior capsid is made of different proteins that makes them have more or less affinity to different cell types. Different serotypes, including optimized hybrid serotypes (Choi,

McCarty, & Samulski, 2005; Hildinger et al., 2001), and different promoters used in the genetic constructs account for most of the wide range of gene expression rates, which goes from few days to several weeks.

In conclusion, diverse technological advances have been put together in creative ways to meet the methodological needs of scientific brain research. Calcium imaging through miniature microscopes allows for an unprecedented examination of cellular activity in a freely-moving animal. The latter is an essential requirement to study the cellular correlates of behavior, given that alternative head-fixation approaches limit the behavioral repertoire and are incompatible with most rodent behavioral assays (Ghosh et al., 2011; Helmchen et al., 2001). In the following section we briefly discuss the principles of instrumental conditioning in mice.

1.7 Instrumental conditioning

Edward Lee Thorndike first described instrumental learning in hungry cats that were locked in a box from which they could only escape by learning to operate latches (Thorndike & Woodworth, 1901). Successful escape responses were rewarded with food. Based on his findings, Thorndike formulated the *law of effect*: "responses that produce a satisfying effect in a particular situation become more likely to occur again in that situation, and responses that produce a discomforting effect become less likely to occur again in that situation". Burrhus Frederic Skinner would further formalize and refine the formulation of the basic principles of modern instrumental (also known as operant) conditioning in his book *The Behavior of Organisms: An Experimental Analysis* (Skinner, 1938). Differently from the classical conditioning where animals learn to associate neutral stimuli to rewards or punishments (Pavlov, 1927), associative learning in instrumental conditioning occurs between a behavior and a reinforcement or a punishment. Reinforcers increase the chance that the behavior is repeated in the future, while punishment decrease it. Both reinforcement and punishment can be achieved by

adding (positive) or removing (negative) stimuli. For example, positive reinforcement consists on adding an appetitive stimulus following the correct instrumental response, while negative reinforcement is the removal of a punishment following the appropriate aversive stimulus cancelling (escape) or avoiding (active avoidance) response. Conversely, positive punishment consists on adding an aversive stimulus following the instrumental action whereas negative punishment consists on the removal of an appetitive stimulus following that action. It should be noted that punished behavior is not forgotten but repressed, as indicated by the fact that punished behavior readily returns if the source of punishment is removed (Miltenberger, 2008). An alternative way to suppress a certain instrumental response is by extinction, where the contingency and/or contiguity between the previously reinforced action and the reward is degraded or eliminated (Davis & Platt, 1983; Thomas, 1981). Interestingly, different reinforcement schedules have different response rates (the rate at which behavior repeats) and extinction rates (how soon the behavior stops). For example, continuous (1 response: 1 reward) reinforcement has a slow response rate and fast extinction rate, whereas in variable ratio reinforcement (unpredictable number of responses: 1 reward) the response rate is fast and extinction is slow (Miltenberger, 2008). Notably, the latter has been proposed to model human gambling (Haw, 2008).

Practically, in experimental setups for rodents, ultrasensitive levers and nose-poking devices are used to study instrumental learning. Food restricted mice readily learn to nose-poke and lever press in return for a food reward delivered through a spout (liquid) or a food port (solid). Frequently, mild electric shocks or air-puffs are used as punishments, although other punishments such as quinine delivery (bitterness) and lithium chloride injections (malaise) have also been used (L. J. M. J. Vanderschuren, Minnaard, Smeets, & Lesscher, 2017). In self-paced tasks, the reinforced action may become available only upon execution of a secondary initiation action (Cardinal & Howes, 2005; Orsini, Trotta, Bizon, & Setlow, 2015; St Onge & Floresco, 2009). For example, levers may retract after being pressed and only be extended again upon a

nose-poke. In the absence environmental cues, this design ensures the completion of a task cycle and prevents the unintended degradation of the contingency between the primary reinforced action and reward delivery.

All in all, the procedures to train mice in instrumental tasks are well described in the literature, as are the conditioning principles that should guide the fundamental task design to ensure the desired associative learning. In this study we combined the use of rewards and punishments to interrogate changes in response representations at the cellular level in the BLA.

2. Aim of the thesis

This thesis aims to investigate the existence and behavior of BLA ensembles that encode instrumental actions in freely moving mice. In particular, we want to address the following question: are there BLA cells that learn about actions and update their value? This has been shown to be the case for cues, but there is no evidence supporting the same is true for actions. Therefore, through stereotactic, viral and miniaturized imaging tools we assess the activity of a large number of BLA cells per mouse, and a refined behavioral paradigm allows us to do so while the mice perform an instrumental action whose rewarding outcome is suddenly undermined by a risk of punishment. Our own preliminary data revealed that indeed there are BLA neurons that selectively respond to actions that have been reinforced through instrumental training. Thus, we delve on investigating the integration of the information regarding the risk of punishment to the representation of the learned actions, as this questions itself bears high construct validity to maladaptive behaviors: how do BLA ensembles that encode reinforced actions respond when the outcome of the action has a risk of punishment instead of a reward? Based on the current body of evidence, especially on that of the literature on BLA valence cells, we hypothesized that positive valence cells would encode the instrumental action while its outcome is a reward, and that this representation should significantly change when the risk of punishment is introduced. Conversely, a separate ensemble of negative valence cells should start responding when the risk of punishment is introduced (Fig 2.1). Our work represents the first reported attempt ever addressing this research question at the cellular level in freely-moving animals.

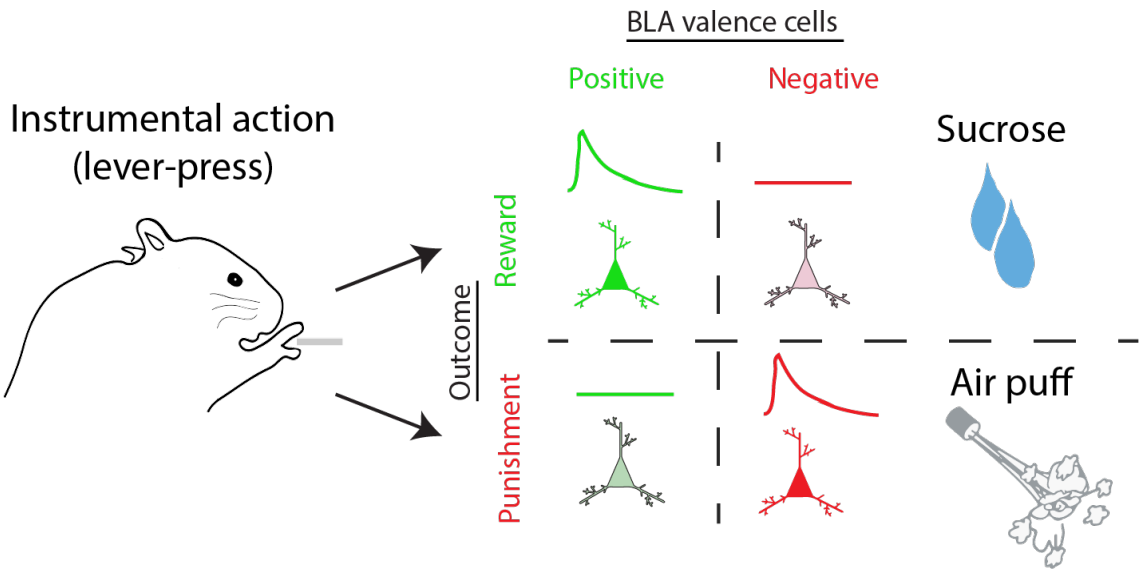

Figure 2.1 Working hypothesis. We expect positive valence BLA cells to encode an instrumental action if the outcome of this action is a reward, and negative valence BLA cells to do so if the outcome is a punishment. This implies that positive valence cells do not encode actions that result in punishment, and vice versa for negative valence cells.

3. Methods

3.1 Animals

Male C57BL6/J mice (Envigo RMS B.V., Inc., Venray, The Netherlands) 2 months old were housed in groups of five under a 12 h light/dark cycle and provided with food and water ad libitum, wood bedding, cotton nesting, and a clear red polycarbonate igloo. During the first week animals were left to habituate to the new environment and the experimenter, who handled them daily 10 minutes per cage. Afterwards mice were housed individually, each with an igloo, bedding and nesting material, in preparation for behavioral experiments, surgery and/or food restriction. All animal procedures were performed in accordance with institutional guidelines and were approved by the Veterinary Department of the Canton of Basel-Stadt, Switzerland.

3.2 Food restriction

One week before instrumental shaping and training, animals were put into a food restriction schedule to maintain them at 85% of their baseline body weight. Every mouse was given between 2 and 3 grams of food pellets according to their body weight fluctuations. To allow for habituation to the rewards used during instrumental training, one day before the start of the training mice were given free access to 0.5 ml of 10%-sucrose diluted condensed milk solution and 0.5 ml of 2% sucrose solution through 1 ml syringes placed on the grid cover of the cage.

3.3 Instrumental training

The behavioral arena consisted of a 25 cm wide x 25 cm long x 40 cm tall transparent acrylic box placed over a white PVC floor. One of the walls was equipped with two custom made spouts, two levers and one nose-poke (ENV-312-2M and ENV-314W, Med Associates, Fairfax, VT, USA). The nose-poke was placed between the two levers, and the spouts were placed besides each lever on the distal side relative to the nose-poke.

The pressing of each lever was associated to a liquid reward delivered into the respective adjacent spout via a syringe pump (PHM-107, Med Associates).

When needed, a plastic divider was used to split the arena into smaller areas to adjust it to the specific needs of each training schedule (Fig. 3.1). To compensate for side biases, when the arena was divided mice were trained in either sub-compartment one day and in the other one the following day.

Figure 3.1 Different arena configurations used during training. Dashed lines represent walls.

For the lever pressing training (Fig. 3.2A), both levers and their spouts were isolated by placing two dividers on each side of the nose-poke. On the first training session levers were baited with a food paste that was allowed to dry on top of the lever itself. After 2 minutes the lever would automatically extend. Upon a lever press, 12.5 µl of 7.5% sucrose solution or 10%-sucrose diluted condensed milk solution was delivered through the spout. Five seconds after the first lick, the lever would extend again.

For nose-poke training (Fig. 2.2B) a divider was placed on either side of the nose-poke in order to exclude one of the lever-spout sets. On the first training session, the nose-poke hole was baited. Upon nose-poking, the nose-poke sensor would deactivate and the lever would extend and the same rules as in lever pressing training would apply,

except that instead of an automatic lever extension the nose-poke sensor would become active again when the rewarded spout was licked.

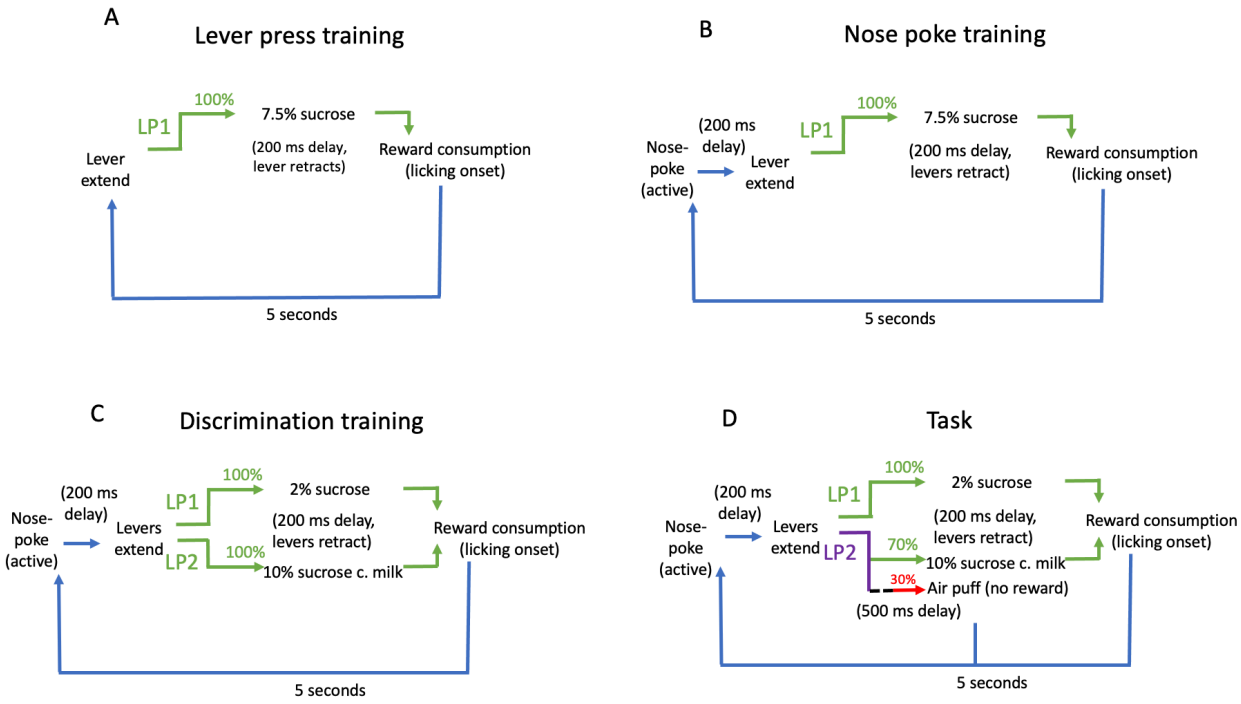

Figure 3.2 Rules of different training schedules (A-C) and task (D).

For discrimination training (Fig. 3.2C), no divider was used. One lever was paired with the large reward and the other with a small reward, and the pairings were alternated between days. Both spouts delivered the same reward volume (12.5 µl). The difference in reward magnitudes between levers was set so that mice would establish an exclusive preference for the large-reward-associated lever. To that end, enabling a clear discrimination between the large and small rewards was critical to our paradigm. Based on literature values, a 10% sucrose concentration solution of condensed milk was chosen as the large reward and a 2% sucrose solution as small one.

To familiarize mice with the lever-reward rules on a given session, an initial forced exploratory period was introduced where only one lever was extended upon nose-poking. Mice had to press the extended lever and lick at least once the rewarded spout.

Each lever extended five times on a 1-to-1 alternating schedule that ended always on the small reward lever side. Once the forced-choice task was completed, nose-poking extended both levers and mice were free to choose either, as choosing one lever would make both levers retract. Mice were trained for two days for lever pressing and nose-poking, and until they reached the performing criteria of 100 trials for the discrimination training. Training was done once per day and each session, as well as the task, was 100 trials or 60 minutes long, whichever came first. Mice that successfully completed discrimination training were tested on the task (Fig. 3.3) which followed the same rules except that after 40 lever presses (cumulative sum of all lever presses) a risk of 30% of air-puff punishment was introduced on the lever that delivered the milk solution, and if a punishment was delivered the nose-poke sensor would become active again without the need for licking any spout (Fig. 3.2D).

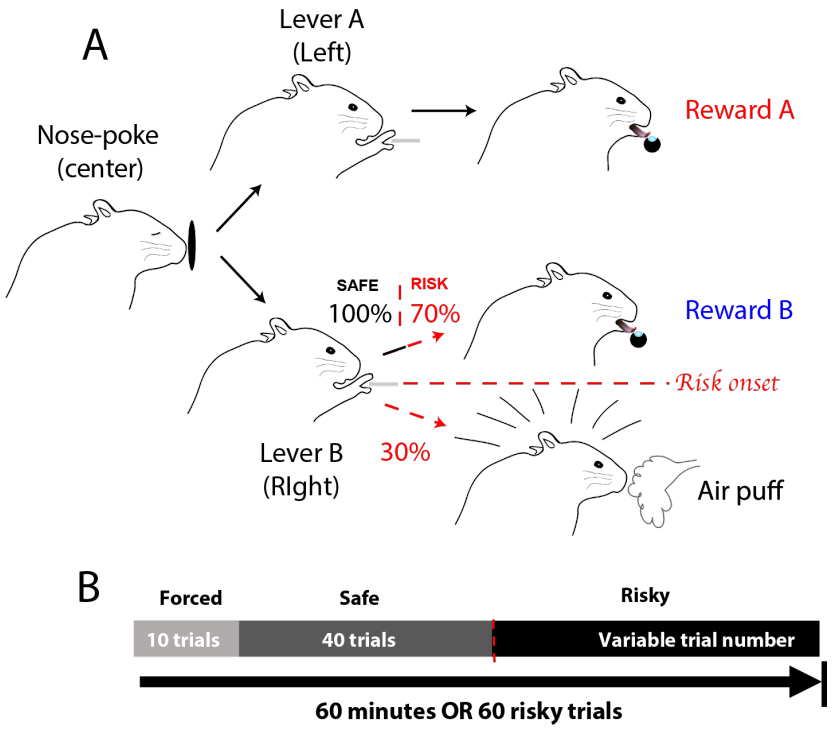

Figure 3.3 Instrumental task. (**A**) Sketch of the task. (**B**) Time course and periods of the task.

3.4 Surgery

General analgesia was induced with buprenorphine (Temgesic 0.3 mg/ml, Indivior Schweiz AG) 2 µL/g body weight injected subcutaneously 30 minutes before surgery and every 4-6 hours following surgery if needed. Anesthesia was induced with 4% and maintained with 2-3% isoflurane (Attane, Provet AG, Switzerland) in 95 volume % oxygen (Oxymat 3, Weinmann Geräte für Medizin GmbH + Co. KG, Germany). After induction local analgesia was applied by injecting a mixture of 2.86 mg/mL lidocaine (Boehringer Ingelheim, Germany) and 0.86 mg/mL ropivacaine (Naropin 2mg/ml, AstraZeneca, UK) subcutaneously under the scalp. Hair on the head between the ears was removed using a veterinary hair clipper (ISIS Aesculap, Buchbach, Germany). Mice were then placed in a stereotactic frame (Model 1900 Stereotaxic Alignment System, David Kopf Instruments, Tujunga, CA, USA). Eye gel drops (Viscotears, Bausch + Lomb, Laval, Quebec, Canada) were applied to both eyes and body temperature was maintained at 36.5 °C using a feedback-controlled heating pad (FHC, Bowdoin, ME, USA). An incision was made to expose the top surface of the skull and a precision dental drill was used to carefully drill a 1.2 mm-diameter hole in the skull above the left BLA at -1.2 mm anterioposterior and -3 mm mediolateral coordinates from bregma. The exposed dura was carefully removed with precision tweezers, and a calibrated microcapillary pipette (5 µl tube, Sigma- Aldrich Inc., St. Louis, MO, USA) was lowered 4.8 mm deep. A preloaded volume of 180 nl of AAV2/5-CaMK2-GCaMP6f.WPRE.SV40 virus batch C51250 (Penn Vector Core, University of Pennsylvania, Philadelphia, PA, USA) was slowly injected using an air pressure injection system (Picospritzer III, Parker, Hollis, NH). After allowing some time for diffusion of the virus, the pipette was retracted and a needle was used to make a track to later position a GRIN lens (1.0 mm diameter, 9.0 mm length, Inscopix Inc., Palo Alto, CA, USA) just over the injection site. All elements penetrating the brain were moved slowly at a µm/s scale using a micro positioner (David Kopf Instruments, Tujunga, CA, USA). The GRIN lens was fixed to the skull using UV-curated glue (Loctite 4305, Loctite, Düsseldorf, Germany) and dental cement (Paladur, Heraeus Gmbh, Hannau, Germany). A titanium head bar was placed with one end inside the

dental cement and the other end protruding to allow for future microscope de/mounting. During the next two days mice received a daily subcutaneous 10uL/g-body weight injection of meloxicam (0.5 mg/ml Metacam, Boehringer Ingelheim Pharma GmBh + Co. KG, Germany) to extensively address any possible remaining pain sensation. Mice were allowed to recover for two weeks, during which the exposed end of the lens was covered with silicone rubber (Mold Start 15, Smooth-On Inc., Macungie, PA, USA) for protection. After recovery, viral expression levels were checked weekly using a miniature microscope (NVista 2.0, Inscopix Inc, Palo Alto, CA, USA). When fluorescence levels where sufficient for imaging, mice were head fixed, placed on a custom running and briefly anesthetized. A baseplate was then fixed on the dental cement using dental flowable composite (Vertise Flow, Kerr, Bioggio, Switzerland) in a position where the microscope could capture an optimal imaging plane. Mice were allowed to recover for one day, and thereafter handled regularly with the microscope mounted on their heads to allow them to habituate.

3.5 Tissue clearing and implant localization

Mice were terminally anesthetized using an intraperitoneal 2 µg/g-body weight injection of urethane and perfused with ice-cold phosphate-buffered saline (PBS) followed by 4% paraformaldehyde (PFA) in PBS. Brains were extracted and further fixed overnight at 4°C. Brains that had been implanted with a 1mm GRIN lens were embedded in 3% agarose and cut into horizontal sections using a Leica precision vibratome (Leica Microsystems, Heerbrugg, Switzerland). Care was taken to extract a 2mm thick section containing the imaging plane, which was stained using a far-red nuclear staining (RedDot 2, 200X in DMSO, Biotium Inc., Fremont, CA) and cleared using CUBIC (Susaki et al., 2014). A confocal microscope (LSM700, Carl Zeiss AG, Oberkochen, Germany) was used to take a z-stack of the implantation site using 40x oil-immersion objective, and to image the whole horizontal section using a 10x water objective. These imaging data were used to identify the imaging plane as seen in the field of view (FOV) of the calcium imaging recordings and to put it into an anatomical context using a brain atlas (Franklin & Paxinos,

2008). Brains that had been implanted with a 600 µm GRIN lens were sliced into 80 µm thick coronal sections, stained with the nuclear staining DAPI, mounted on slides and imaged using a slide scanner (Axio Scan.Z1, Carl Zeiss AG, Oberkochen, Germany). The imaging plane was identified by superimposing images of the slides to a brain atlas.

3.6 Analysis and statistics

All statistical analyses and visualizations were based on custom MATLAB (MathWorks, Natick, Massachusetts, USA) scripts and Prism software (GraphPad, San Diego, CA, USA). Behavior was analyzed using the data acquired through the CinePlex and OmniPlex software (Plexon Inc, Dallas, TX, USA). Calcium imaging data were motion-corrected using a custom code based on efficient subpixel image registration (Guizar-Sicairos, Thurman, & Fienup, 2008). Individual cells were identified, aligned and selected using custom scripts based on constrained nonnegative matrix factorization for microendoscopic data (CNMFE) (Zhou et al., 2018). Based on anatomical classification (see §3.5), only BLA cells were selected and their calcium activity was detrended and z-scored within the same session. To determine the statistical significance of a calcium response to a behavioral event, the magnitude of the response in a time window of 7 seconds around the event (2 seconds before and 5 seconds after) was compared to a distribution of 1000 randomly sampled time windows of the same size using a t-test for a significance threshold of $p<0.01$. Based on this criterion cells were classified as nose-poke (only those nose-pokes leading to lever extensions), lever-press, or lick (first lick after a reward) cells accordingly for the behavioral events before the first air puff punishment, and as air puff cells for punishment events. Significance of the overlaps among the defined groups of cells was evaluated using Chi-square test for a significance level of $p<0.05$. For other analyses, only cells overlapping between the air puff group and the other groups were included in the other group, respectively, and excluded from the air puff group, while all other overlapping cells were excluded.

In all graphs the stars (*) indicate the level of significance for Wilcoxon matched-pairs signed rank tests, with 1 star denoting $p<5x10^{-2}$ and $1<n\leq4$ stars signifying $p<1x10^{-n}$.

4. Results

Below we report the results starting from the behavioral observations, followed by the results from the imaging procedures, anatomical and functional cell classification, and the physiological characterization of the reinforcement, punishment and risk periods of the task. Results from experiments done to establish the behavioral paradigm, such as the exploration of different punishments and rewards, are omitted if they do not directly contribute towards clarifying our research question.

4.1 Establishment of a behavioral paradigm

An important methodological challenge we had to overcome was establishing a paradigm that would allow us to:

- Give the animals a choice between two actions with two different rewarding outcomes. For this reason, we used two different levers coupled to the delivery of two different outcomes. Moreover, to avoid any spatial bias, we used a central nose-poke (located exactly at the middle of the two levers) to activate (extend) both levers at the same time.
- Reliably predict the preference between both actions across mice. Therefore, we refined the magnitude of the small reward such that all mice would develop an exclusive preference for the large reward.
- Suddenly and unpredictably introduce a risk of punishment to the preferred action.
- Deliver only-reward and only-punishment outcomes upon the introduction of risk, as opposed to punished but also rewarded actions.
- Use a mild punishment intensity to avoid completely discouraging risk taking and to keep behavioral reactions to the punishment within the time constrains for the imaging method (e.g., avoid prolonged freezing bouts).

To that end, below we compiled the most relevant results supporting the suitability of our task to asses safe and risk behavior within one experimental session in freely moving mice.

4.1.1 Small reward is rewarding but not enough to induce a switch in the risk period

One important part of establishing our behavioral paradigm was to ensure that mice could discriminate between the two different rewards paired to each of the actions. Therefore, we fixed the value of the big reward (as described in §3.3), but we explored different magnitudes of sucrose concentration as a small reward (Fig. 4.1A). Within a session, the small and large reward location did not change, so we alternated their location across different sessions to evaluate discrimination. We found that a small reward of 2% sucrose was optimal to enhance reward discrimination.

Subsequently, we evaluated the rewarding nature of the 2% small reward compared to water. These control experiments revealed that the discriminability between small and high reward choices was impaired when using a small reward larger than 2% sucrose (Fig. 4.1A), and that 2% sucrose was low enough to reliably induce an exclusive preference for the large reward (10%-sucrose diluted condensed milk Fig. 4.1A) while still retaining rewarding properties compared to water (Fig. 4.1B).

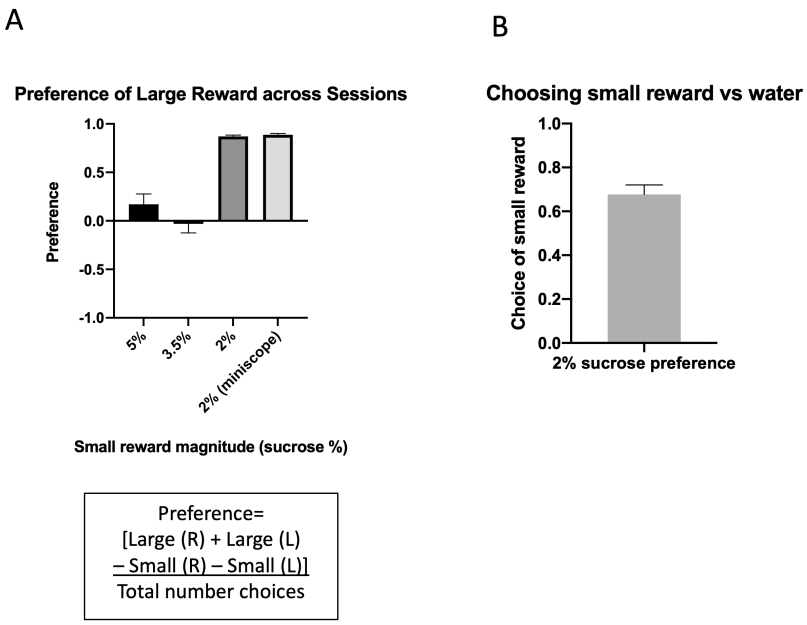

Figure 4.1 Small reward values and discriminability. (**A**) Mice prefer exclusively the large reward lever regardless of whether it is located on the left or right side (in a given experimental session) if the small reward is 2% sucrose, but not 3.5% or 5% (N= 10 mice with miniscope, 16 mice with no miniscope). (**B**) 2% sucrose is nonetheless rewarding compared to water (N= 16 mice)

4.1.2 A large alternative reward will cause mice to switch during the risk period

To evaluate the animals' ability to switch from the punished to the unpunished choice, we ran the task using two equally rewarding choices. It was established that using an alternative reward equal to the large reward produces a switch from performing the instrumental sequence on the side that becomes risky to performing it on the side that remains safe, for both animals with and without a miniscope (Fig. 4.2, 4.3). Because air puff delivery was limited to the right side of the arena, some mice had to be placed multiple times in the arena until they selected the right side by chance.

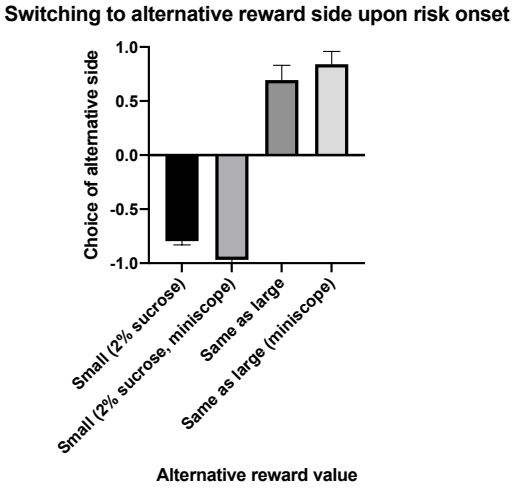

Figure 4.2 Switching choices. Normalized choice of alternative reward vs. large-but-risky reward for mice with and without a miniscope (N=4 and 16 mice, respectively).

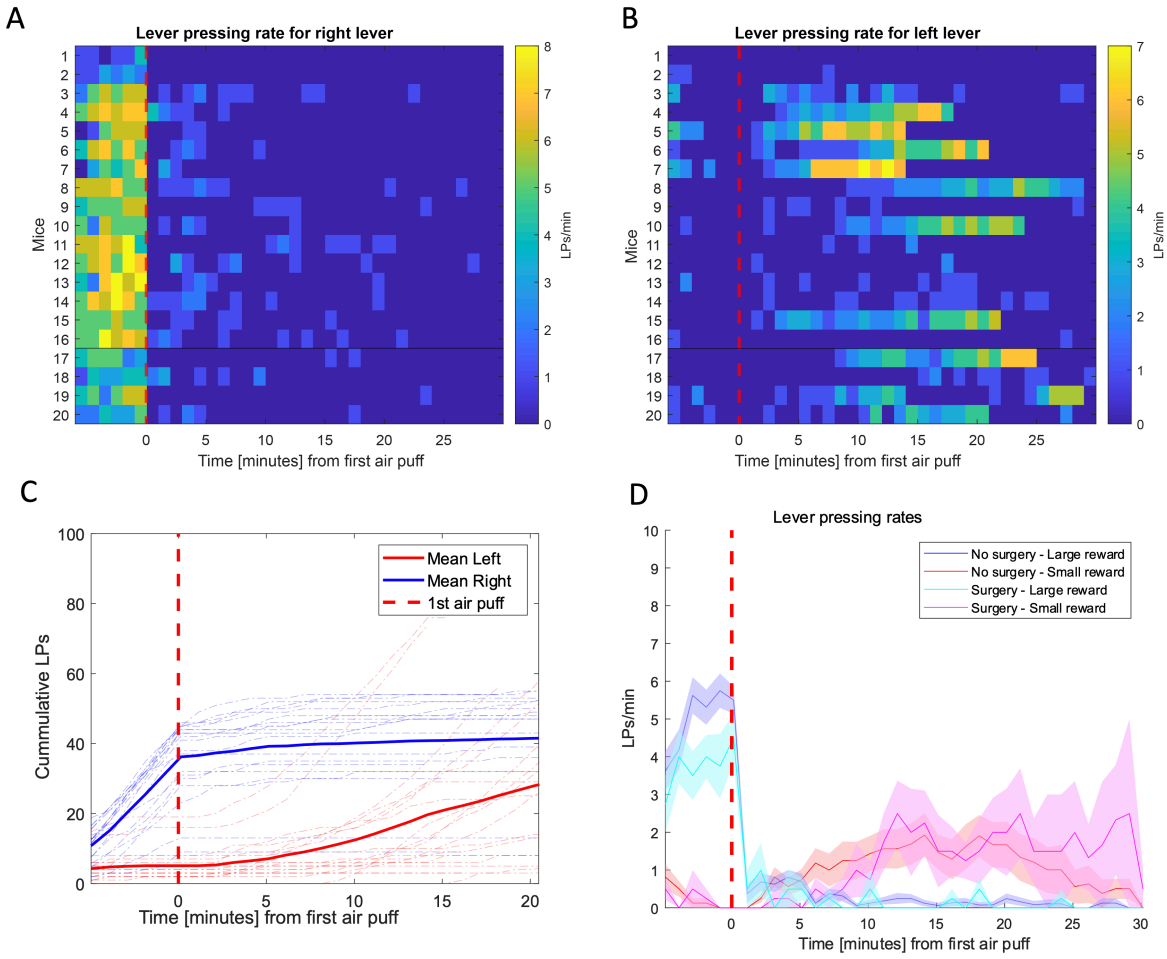

Figure 4.3 Switching strategy. Lever pressing (LP) rate of mice without (1-16) and with (17-20) a miniscope around the time of the first air puff (red dotted line) for the right (**A**) and left (**B**) levers. (**C**) Cumulative LP rate for both large (right) and small (left) levers around the first air puff (N=20 mice). (**D**) LP rates for mice with and without miniscope (surgery) around the first air puff (N= 4, 16 mice respectively).

4.1.3 Omission of the reward has no effect on instrumental behavior

Because delivering punishment-only trials during risk implied omitting the delivery of the reward, we assessed whether the omission itself, without an air puff punishment, would have a punishing effect. A control experiment, using only omissions with the same risk schedule as air puff punishments in the task, revealed that omissions alone have no effect on instrumental performance (Fig. 4.4).

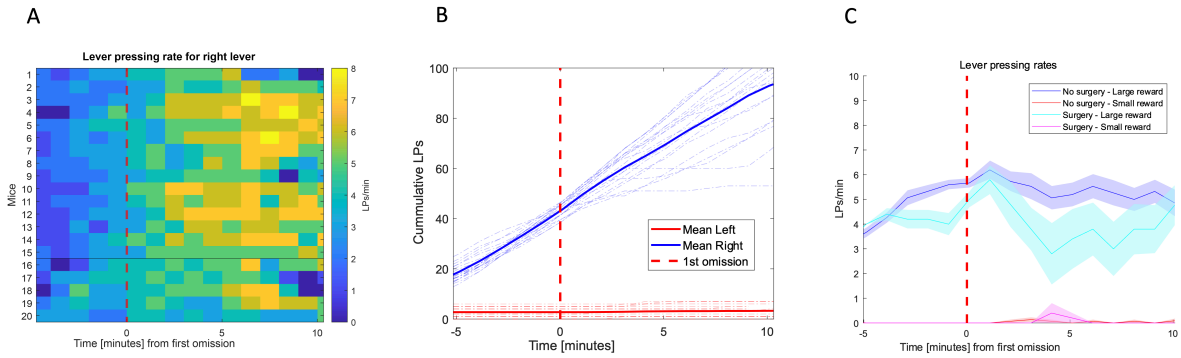

Figure 4.4 The effect of omission of reward. (**A**) Lever pressing (LP) rate of mice without (1-16) and with (17-20) a miniscope around the time of the first omission (red dotted line) for the right lever. (**B**) Cumulative LP rate for both large (right) and small (left) levers around the first air puff (N=20 mice). (**C**) LP rates for mice with and without miniscope (surgery) around the first air puff (N= 4, 16 mice respectively).

Having ensured that we controlled the variables for reward discrimination, small reward magnitude, switching ability, and omission effect, we concluded that our experimental setup was suitable to address the question of instrumental actions representations during both safe and risky situations. Below we summarize our main results.

4.2 Behavioral changes upon the introduction of risk of punishment

In this section we summarize the main experimental results with regards to the changes we observed in behavior upon introducing a risk of punishment to the preferred instrumental action.

4.2.1 Unpredictable air puff punishment disrupts instrumental behavior

First, we examined the changes induced by the punishment and risk of punishment on the behavioral strategy level. All mice, with and without a miniscope (surgery), exhibited a pronounced and prolonged decrease in performance of the instrumental behavior required for the task after the delivery of the first air puff punishment (Fig. 4.5). Although this decrease concerned the instrumental sequence required to obtain the large-but-risky reward through the right-side lever of the behavioral arena (Fig. 4.5A), there was no compensatory increase in performance of the small-but-safe reward on the left-side hand of the arena (Fig 4.5B, C). The decrease in lever-pressing (LP) rate, which is taken as a measure of performance for the whole instrumental sequence (nose-poke, lever-press, licking), was significantly different before and after the delivery of the first air puff punishment (the start of the risk period of the task) for mice with and without a miniscope (Fig 4.5D), although there was a significant difference between these two cohorts of mice in terms of peak (maximum) and average LP rate before and after the first air puff (Fig. 4.6A, B).

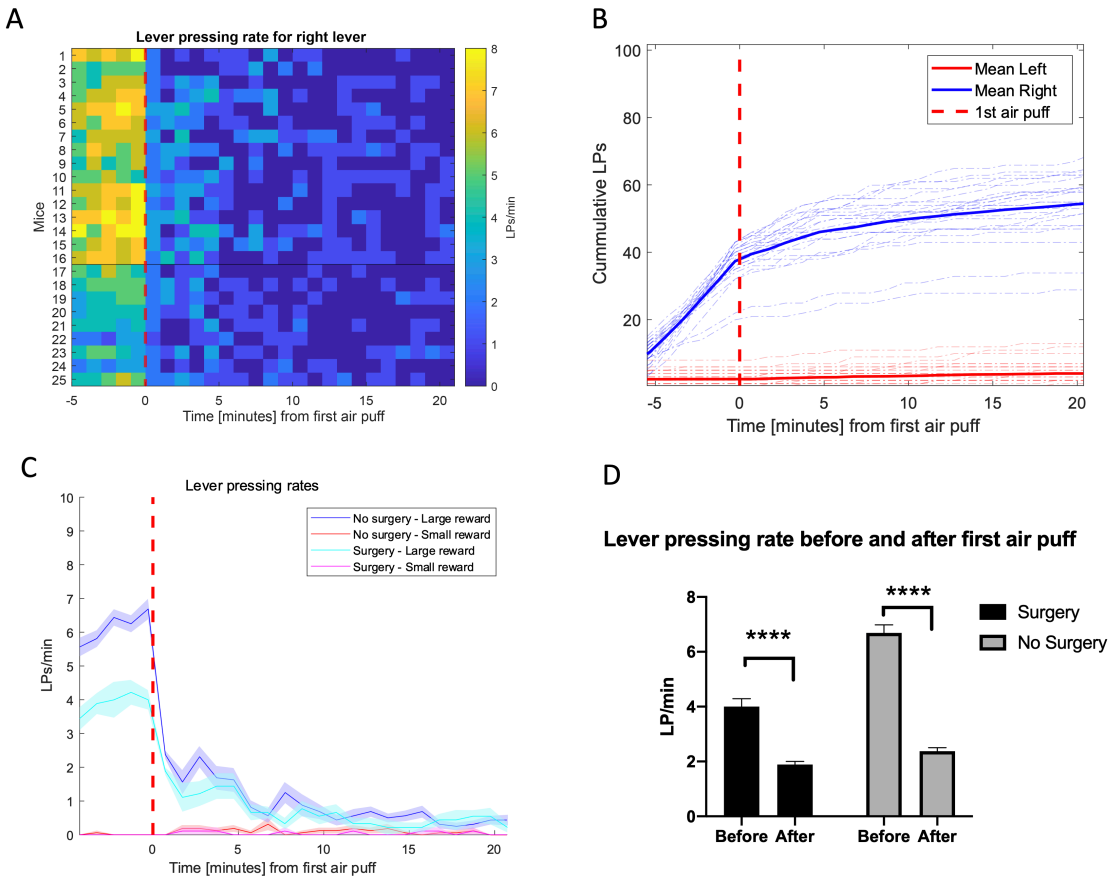

Figure 4.5 Punishment and risk of punishment significantly decreased instrumental performance without causing a switch in preference. (**A**) Lever pressing (LP) rate of mice without (1-16) and with (17-25) a miniscope around the time of the first air puff (red dotted line). (**B**) Cumulative LP rate for both large (right) and small (left) levers around the first air puff (N=25 mice). (**C**) LP rates for mice with and without miniscope (surgery) around the first air puff (N= 9, 16 mice respectively). (**D**) Quantification of LP rates before and after the first air puff in a 120 s time window for mice with and without miniscope.

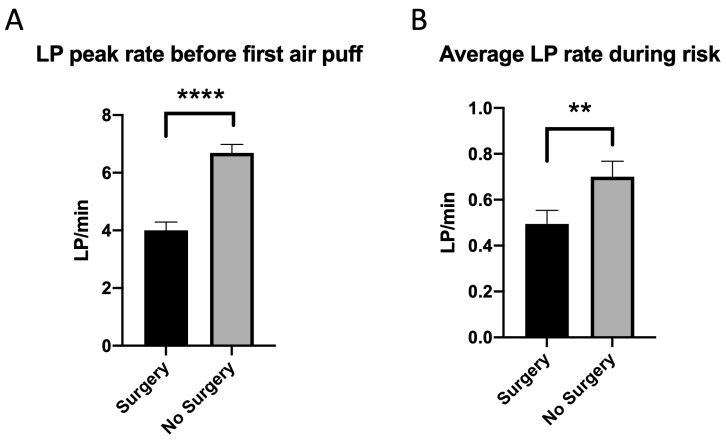

Figure 4.6 Mice without a miniscope had a higher performance in the task during both safe and risk periods. (**A**) LP rate peak (maxima) before the first air puff (safe period) for mice with and without miniscope surgery (N= 9, 16 mice respectively). (**B**) Average LP rate before and after the first air puff for mice with and without surgery.

4.2.2 Risk of punishment disrupts the regular instrumental sequence

Next, we looked into changes induced by the risk of punishment in the structure of the instrumental sequence performed by the animals. All mice exhibited a stable instrumental behavior with regular latencies between the different actions in the task sequence (Fig. 4.7A). Upon the first air puff punishment, the latencies between all actions significantly increased (Fig. 4.7B). The probability of a lever-press (Fig. 4.7C, D) or a lick (Fig. 4.7C, E) occurring 5 seconds after a nose-poke also significantly decreased.

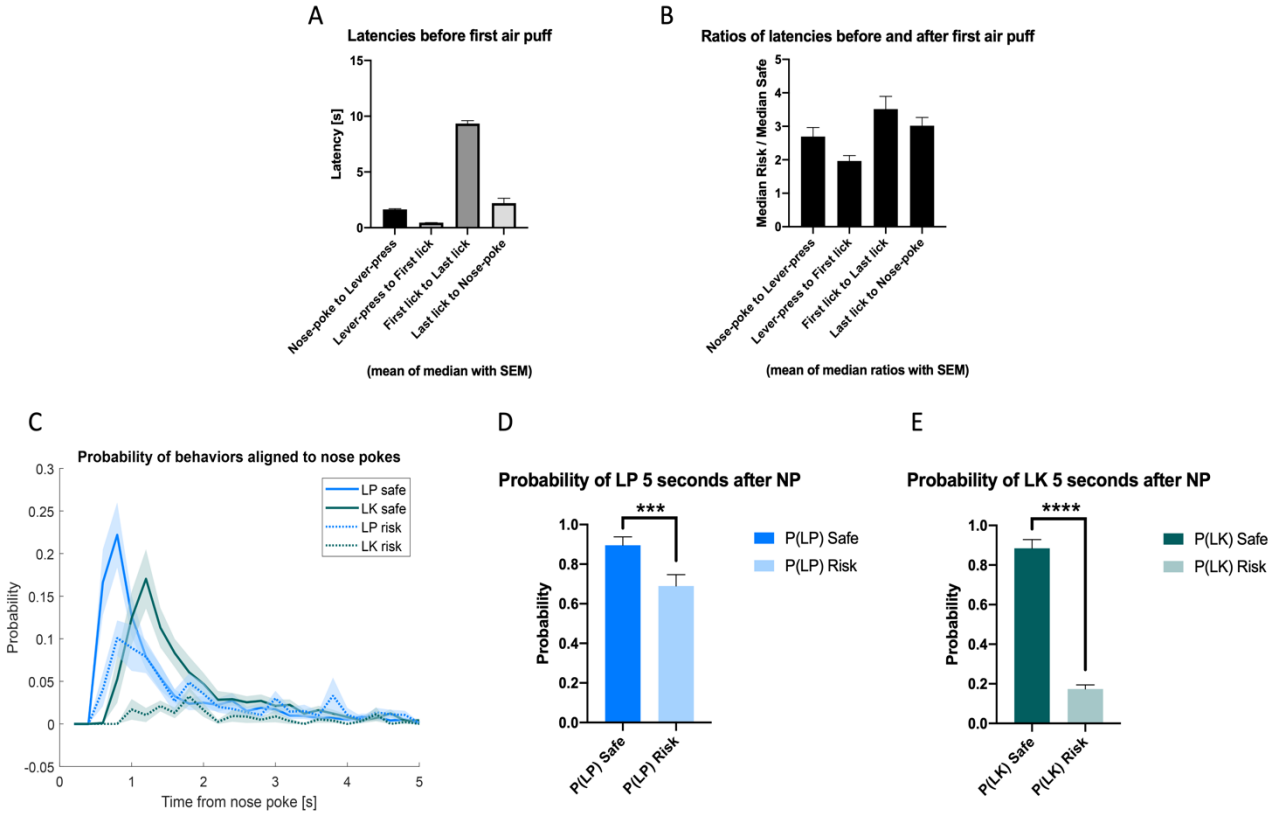

Figure 4.7 Behavioral latencies and probabilities. (**A**) Latencies between sequence actions before the first air puff (safe). (**B**) Ratio of latencies between sequence actions after (risk) and before (safe) the first air puff. Note that 'last lick' is defined as the last lick before a nose-poke, not as the last lick of a licking bout. (**C**) Probability density of behaviors after a nose poke during safe and risk periods (LP: lever press, LK: first lick on rewarded spout). (**D**) Probability of lever-pressing (LP) within a window of 5 s after a nose-poke during safe and risk periods. (**E**) Probability of licking (LK) the rewarded spout within a window of 5 s after a nose-poke during safe and risk periods.

4.2.3 Risk induced no changes in locomotion but in time spent in zones

Although the performance and rate of execution of the instrumental task dropped significantly for all mice (§4.2.1, 4.2.2) during the risk period of the task, the average speed (Fig. 4.8A) and the distanced covered (Fig. 4.8B) remained unchanged compared to the safe period of the task for both mice with and without miniscope (surgery). During the risk period, mice without a miniscope spent more time in the small reward zone (Fig. 4.8D) and both cohorts of mice spent less time in the large reward zone (4.8E).

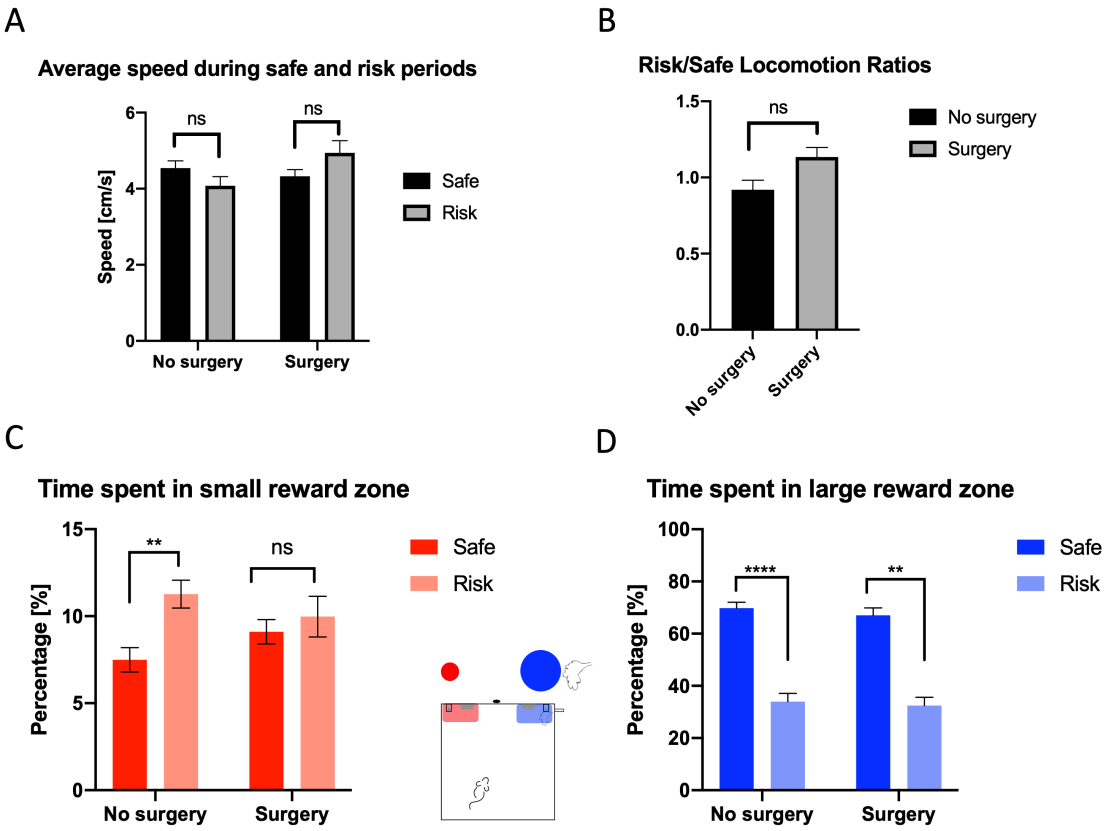

Figure 4.8 Speed, locomotion and time in reward zones. (**A**) Average speed during safe and risk periods for mice with (N=9 mice) and without (N=16 mice) a miniscope (surgery). (**B**) Ratio of distance covered during the risk and safe periods of the task. (**C**) Time spent in the small reward zone. (**D**) Time spent in the large reward zone.

4.2.4 Speed and onset of escape do not change with puffs, but direction rapidly adapts

Mice rapidly ran away every time they received an air puff. The number of punishments received by each mouse was variable but all mice received at least three punishments. Therefore, we used this first three air puff punishments in our analysis across mice. We did not observe any significant changes in escape speed or onset for the first three air puff punishments (Fig. 4.9A, D, E). On average, mice ended their escape more aligned to the diagonal of the arena on the second and third air puff than on the first one (Fig. 4.9B, C).

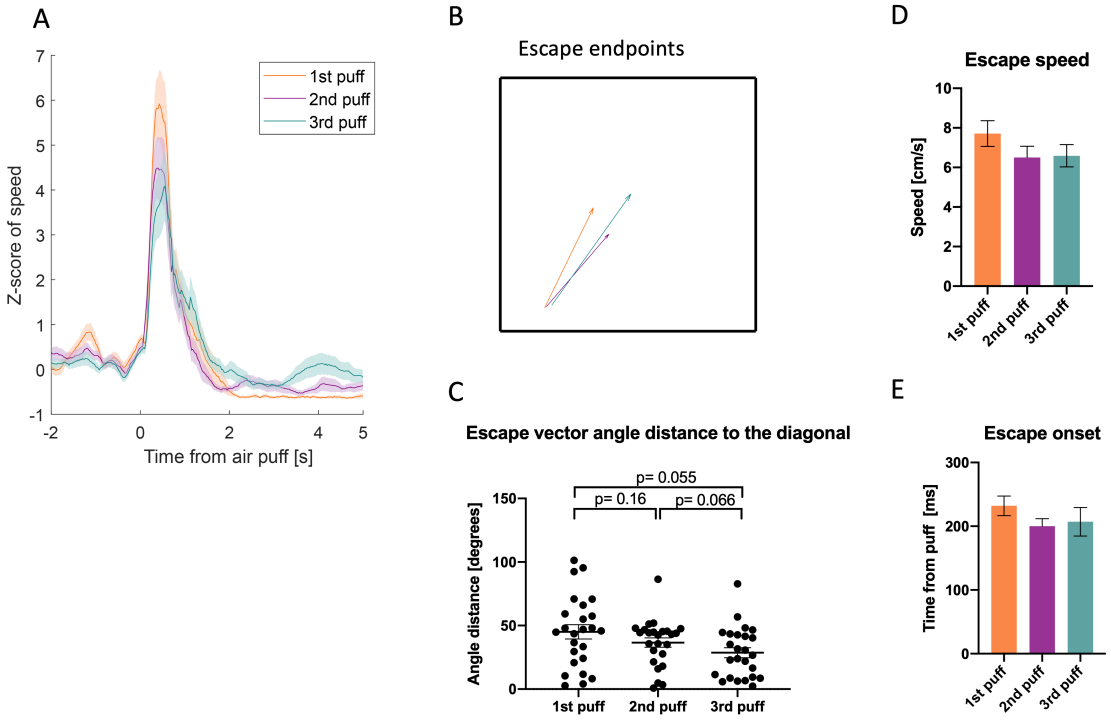

Figure 4.9 Escape strategy. (**A**) Statistically normalized (z-scored) escape speed across mice (N =25) for the first 3 air puff punishments. (**B**) Escape vector showing the average change in position across mice from the air puff delivery (t=0) to 2 seconds afterwards for the first 3 air puffs. (**C**) Escape vector angle distance to the diagonal (45°) of the arena. (**D**) Maximum escape speed across mice for the first 3 air puffs. (**E**) Onset of escape bout across mice for the first 3 air puffs (maximum of the speed derivative between t= 0 and 2 seconds).

4.3 Physiological changes upon the introduction of risk of punishment

In this section we present the main experimental results regarding the changes in physiology we observed in the BLA after the introduction of the risk of punishment. However, before diving into the main results, we briefly discuss results related to the experimental methods described in section 3 as they complement and will help the reader understand better our data. Namely, we present data in relation to the different sizes of GRIN lenses used, and to how we identified and selected BLA cells based on their anatomical location.

4.3.1 Number of imaged neurons per mouse varied by imaging lens size

Imaging with a 1 mm GRIN lens allowed for a larger field of view than imaging with a 600 µm GRIN lens and therefore more cells could be extracted from the imaging files for further analysis (Fig 4.10B). However, to account for putative non-BLA cells these cells had to be anatomically characterized as described in section 4.6.

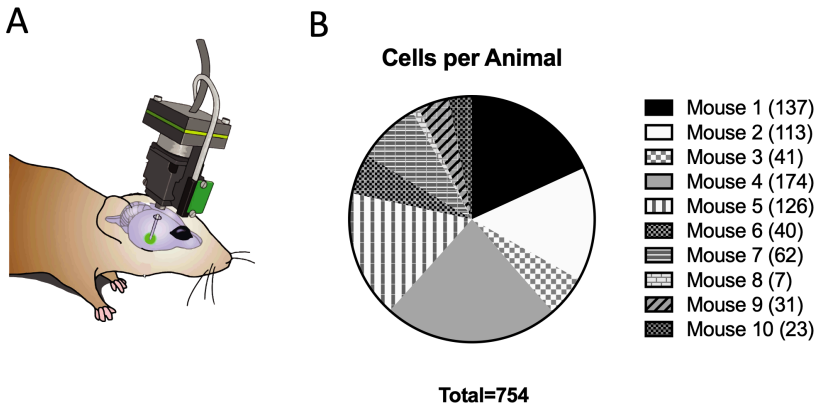

Figure 4.10 Miniscope setup and imaged cells per mouse. (**A**) Schematic representation of virus injection site inside the brain (green), GRIN lens implant, and head-mounted miniature microscope ('miniscope'). (**B**) Number of cells per mouse. Mice 1-5 had a 1 mm GRIN lens implanted and mice 6-10 had a 600 µm GRIN lens implanted.

4.3.2 Anatomical identification of cells

Because the maximum horizontal section of the murine BLA covers an area of around 1 mm^2 (Franklin & Paxinos, 2008), we considered the probability of unintentionally imaging cells from neighboring structures with the 1 mm diameter GRIN lens. Therefore, in this case we anatomically identified BLA cells before including them in our analysis. To that end, for mice with a 1 mm GRIN lens (mice 1-5), confocal imaging of the cleared and stained tissue (§3.5) allowed to identify anatomical landmarks that could be also found the miniscope imaging data, thus it was possible to identify the miniscope imaging plane in the confocal data. Moreover, it was possible to match anatomical features in the imaging plane found in the confocal data to those detailed in a brain atlas, thereby allowing for the anatomical identification of the structures to which the imaged cells most probably belong to (Fig 4.11A-C). The majority of identified cells belonged to the basal (BA) and lateral (LA) amygdala, which together form the basolateral (BLA) amygdala. Only these cells were selected for further analysis.

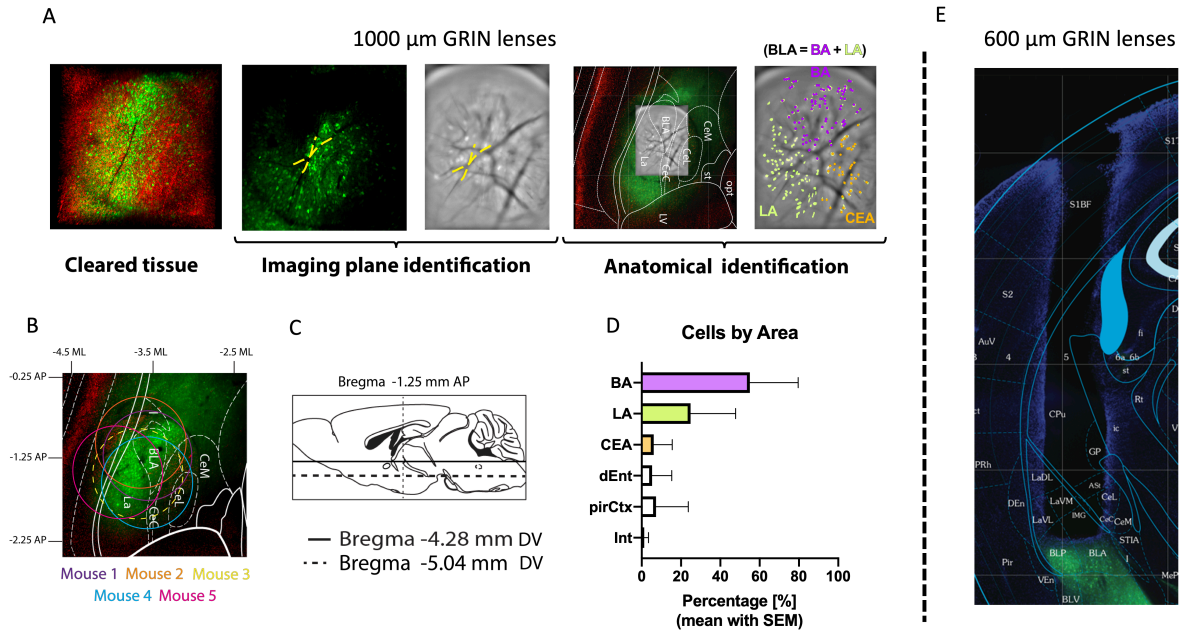

Figure 4.11 Anatomical identification of imaged cells. (**A**) Example cleared tissue, imaging plane identification and anatomical identification (mouse 4). (**B**) Estimated location of the implantation site for mice with 1 mm GRIN lens (mice 1-5). (**C**) Estimated dorsoventral coordinates (solid line: mice 1,

2, 4, 5; dashed line: mouse 3). (**D**) Number of cells per identified anatomical structure (mice 1-5). (E) Example coronal slice with implantation site for a mouse with 600 µm GRIN lens (mouse 6).

For mice with 600 µm lens the GRIN lens all imaged cells were estimated to belong to the BLA (Fig. 4.11E). On average, these mice had a more medial and ventral implantation site (Table 4.1).

Mouse	AP	ML	DV
6	-1.55	-2.9	-4.1
7	-1.31	-2.6	-4.7
8	-1.67	-2.7	-4.6
9	-1.43	-2.7	-4.5
10	-1.07	-2.6	-4.3

Table 4.1. Imaging plane coordinates for mice with 600µm GRIN lenses. AP: anterioposterior, ML: mediolateral, DV: dorsoventral.

4.3.3 Functional classification of cell ensembles

To analyze the calcium recordings in a meaningful way, we first looked at the cellular activity in relation to behavioral events. We found that large groups of cells were encoding these behavioral events (Fig. 4.12) and therefore proceeded to classify cells in functional ensembles as previously described (§3.6).

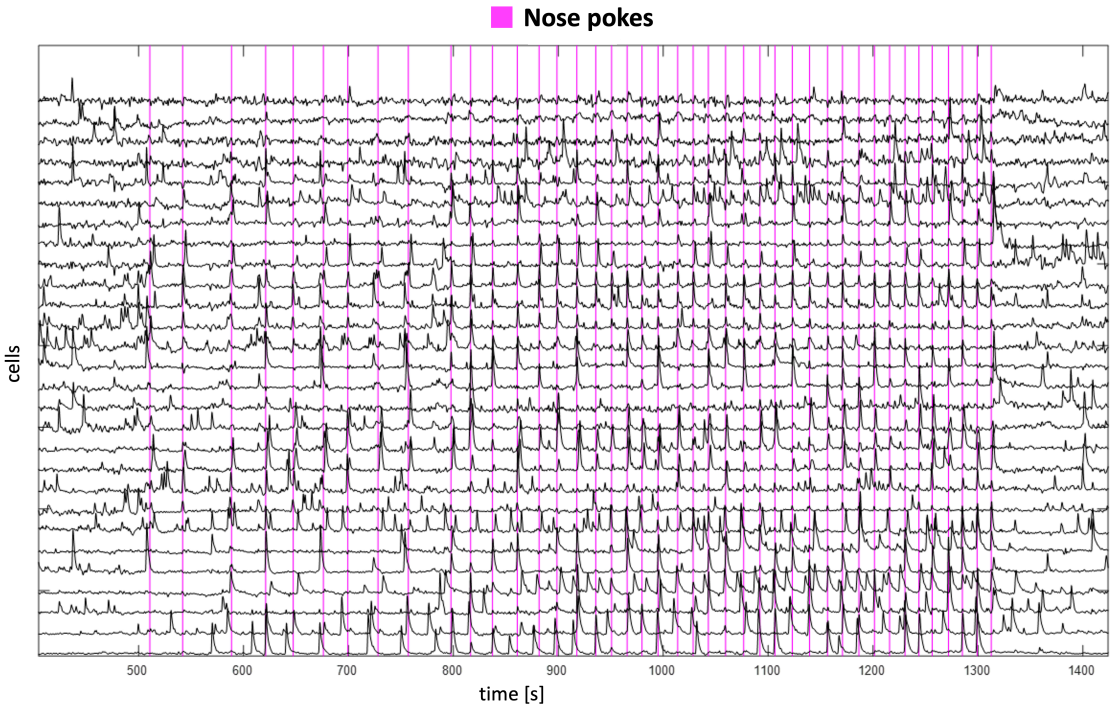

Figure 4.12 Example raw traces of BLA cells locked to nose-pokes during the safe period of the task. Cells locked to lever-presses, licks and air puffs were also analyzed and classified to the appropriate ensemble.

As a result, we found cells with activity patterns significantly and selectively locked to each of the instrumental actions, the reinforcer, and the punisher (Fig. 4.13, .4.14). We called these 'nose-poke', 'lever press', 'licks', and 'air puff ensembles', respectively.

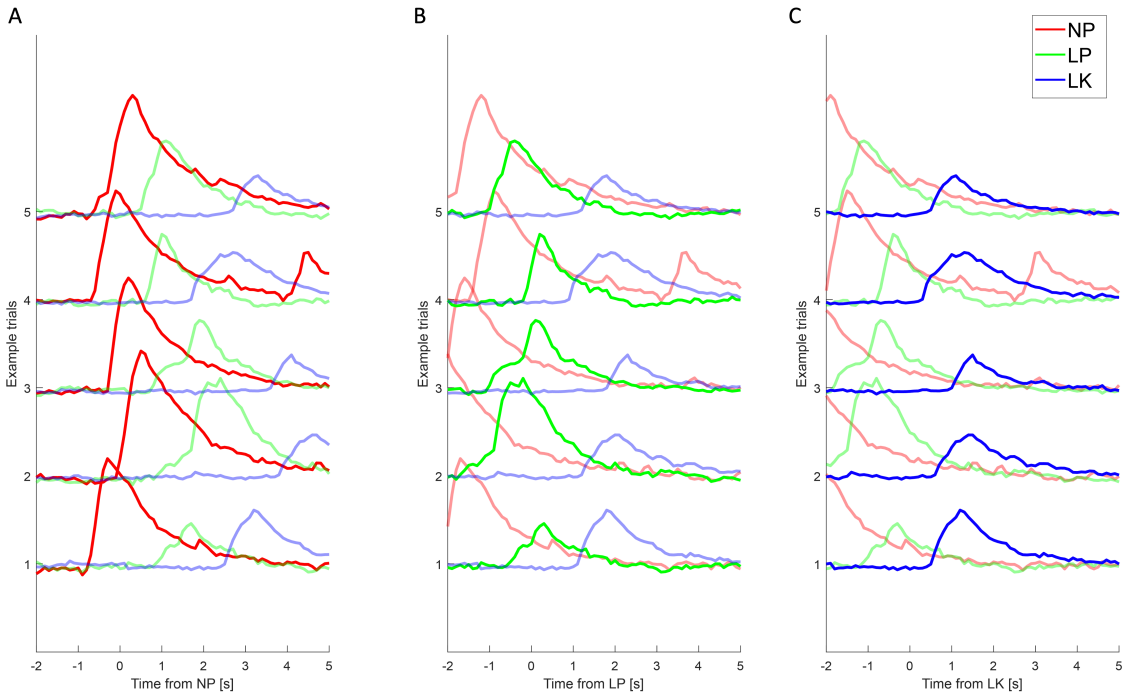

Figure 4.13 Example cells from each task-related ensemble. Example cell for each of nose-poke, lever-press and licks cell groups, shown across five example trials aligned to nose-poke (**A**), lever-press (**B**) and licks (**C**) onset.

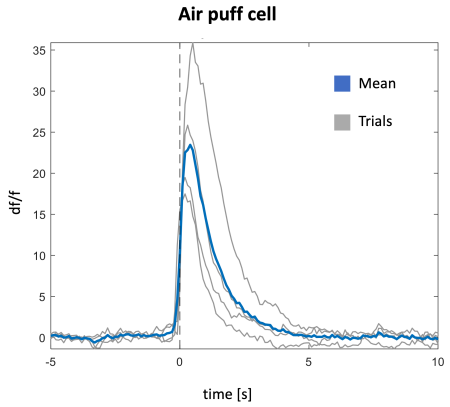

Figure 4.14 Example air puff ensemble cell. Mean activity across trials is shown in blue and individual trials are shown in gray.

The selection process involved examining pairwise correlation and distance to assess the degree of functional connectivity among cells and also to verify no significant number of duplicate cells was included. On a first level analysis, we examined the overlap between these groups of cells, their distribution across mice and their anatomical distribution.

4.3.3.1 Overlaps between functional ensembles

We found that ensembles representing contiguous events in the instrumental sequence are more likely to overlap (Fig. 4.15A), however none of these overlaps was higher than expected by chance (4.15B). In fact, for the nose-poke and licks ensembles we found the overlap to be less than expected by chance. Interestingly, some of the nose-poke, lever press and licks cells were also responsive to the air puff punishment (Fig. 4.15A). The proportion of the BLA population (on a mouse-by-mouse basis) for the actions ensembles was lower than for the reinforcer and punisher ensembles (Fig. 4.15C).

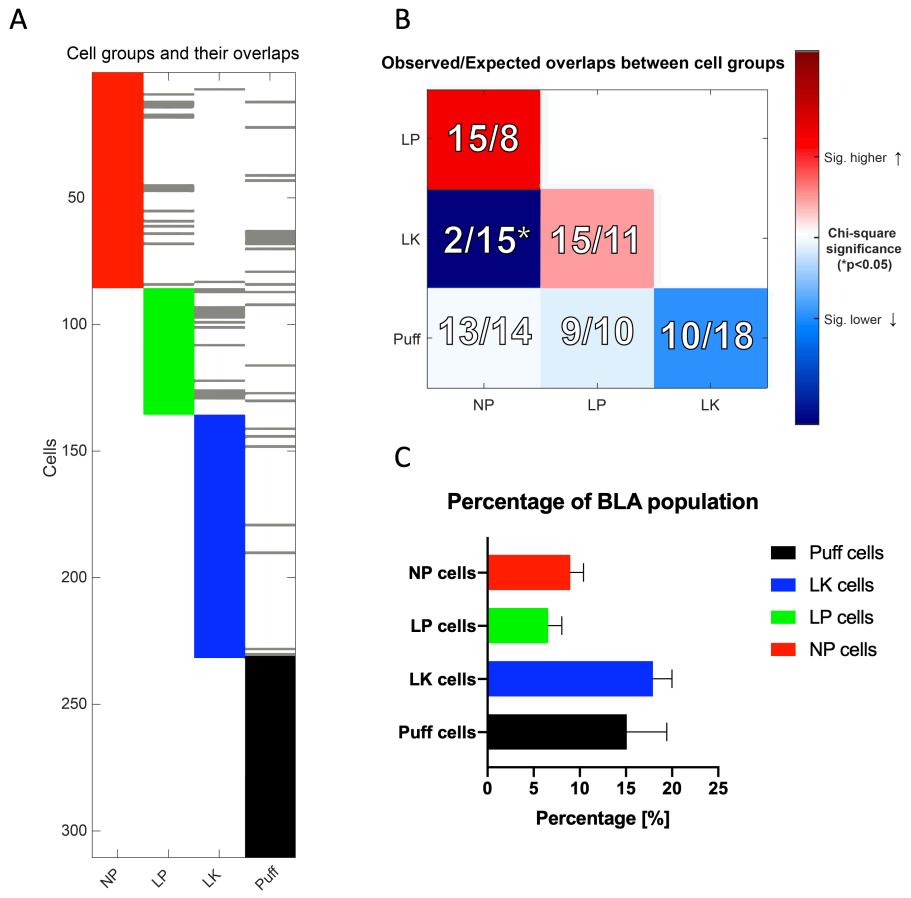

Figure 4.15 Functional classification of imaged cells and overlaps. (**A**) Cells with significant responses to nose-pokes (NP), lever-presses (LP), licks (LK), and air puffs (Puff). (**B**) Observed and expected overlaps between cell groups, and significance of the overlap. (**C**) Percentage of all cells classified in a group across animals (N=10 mice).

4.3.3.2 Distribution across mice of functional ensembles

We then examined the distribution of the ensembles across all imaged animals. Most imaged sections across mice exhibited cells from all functionally classified BLA ensembles (Fig. 4.16).

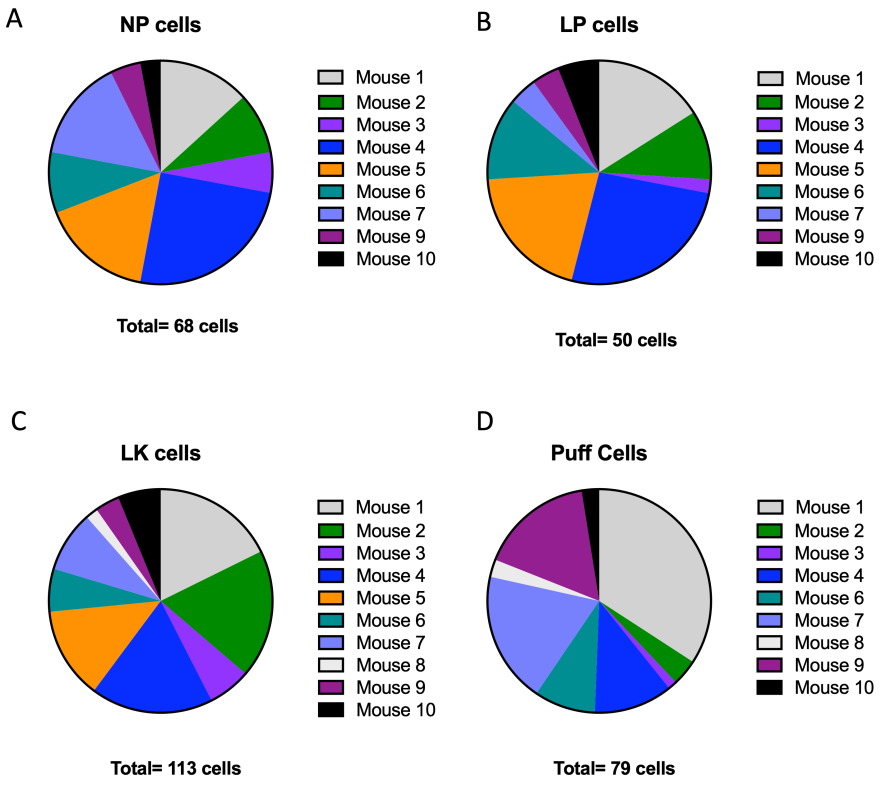

Figure 4.16 Functionally classified cells per mouse. Share of nose-poke (**A**), lever-press (**B**), lick (**C**) and puff (**D**) cells coming from each mouse.

4.3.3.3 Anatomical distribution of functional ensembles

To assess whether functionally classified cells were anatomically clustered or scattered along the horizontal plane, we performed pairwise distance analyses. For that purpose, the estimated centroid of each cell was plotted and the distance between and within classified cells groups analyzed (Fig. 4.17). Cells from the 1 mm GRIN lens mice cohort and those form the 600 µm GRIN lens mice cohort (before and after -3.2 mm in the medio lateral coordinate, respectively) were analyzed separately. In both cases and overall, air-puff cells were found to be anatomically more likely to be clustered than chance along the horizontal plane (Fig. 4.17C).

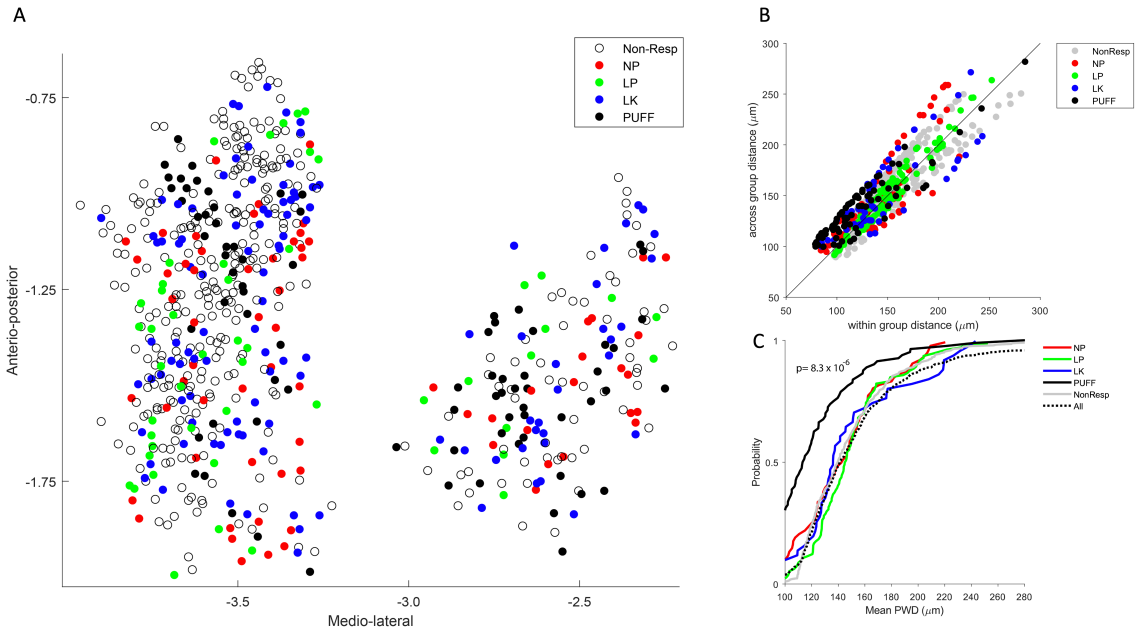

Figure 4.17 Anatomical distribution of functionally BLA ensembles. (**A**) Anatomical location of cells in mice with a 1 mm GRIN lens (left cluster) and mice with a 600 µm GRIN lens (right cluster). Cells appear clustered in two groups because the lenses were implanted on different coordinates for both groups of mice, as previously described (§4.6). (**B**) Across and within cell groups pairwise distance. (**C**) Probability of mean pairwise distances for each cell group. The p value is from two- sample Kolmogorov-Smirnov test and shows puff cells are significantly more likely than chance to be closer together (spatially clustered).

4.3.4 Instrumental actions, reinforcer and punisher ensembles dynamics

Having analyzed the properties of the BLA ensembles we defined, our next level of analysis consisted in characterizing the dynamics of their responses at the ensemble level, for which we took two reference points: the nose-poke, as the start of the instrumental sequence required in the task, and the air-puff punishment, as an important time point after which we expected to see changes in the responses of the instrumental action groups. On the one hand, we found that nose-poke, lever-press and licks ensembles responded consistently and highly-specifically to each behavioral event (Fig. 4.18A). On the other hand, air puff cells did not respond significantly to the other behaviors (Fig. 4.18A, C). Conversely, none of the cell groups related to the instrumental task responded significantly to the punishment (Fig. 4.18B, D). As previously noted, a few cells were responsive to both the air puff punishment and another behavior (Fig. 4.18D).

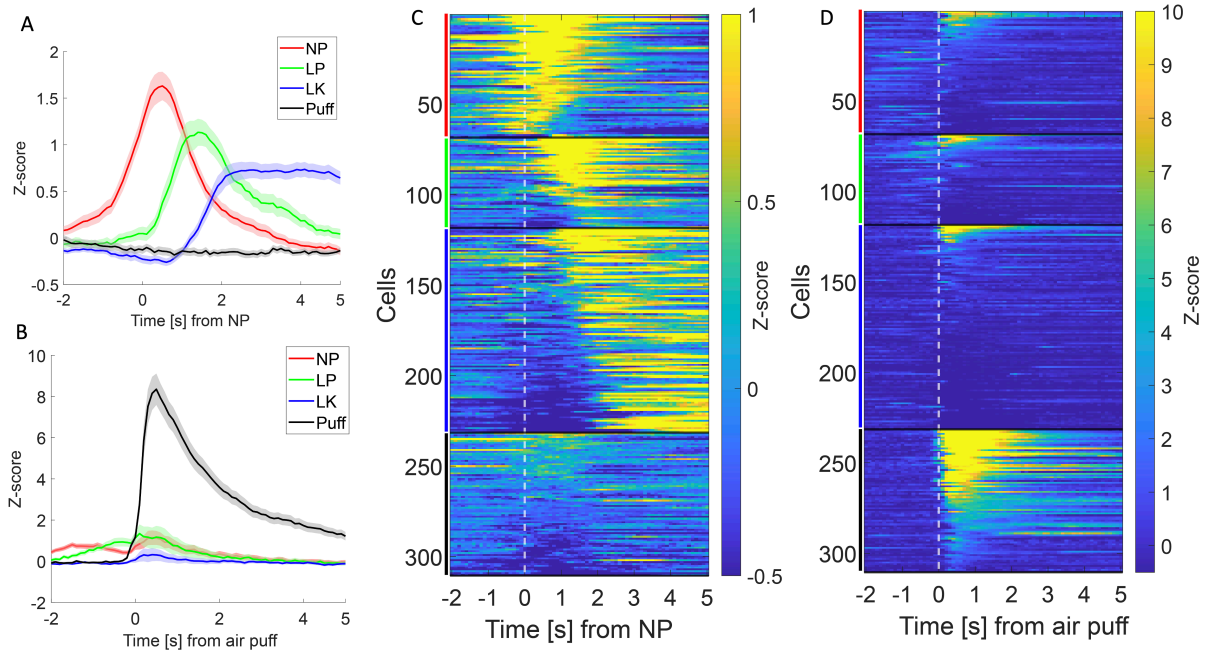

Figure 4.18 BLA ensembles during instrumental sequence and punishment. Functionally classified cell groups and their mean (**A**) and individual cell (**C**) activity across trials around nose-poke time (shades represent the standard error of the mean). Cell groups and their mean (**B**) and individual cell (**D**) activity across trials around air puff punishment time.

4.3.5 Air puff ensemble rapidly adapts to punishment

To assess the evolution of the air puff ensemble response to punishments with experience, we examined its response on a trial-by-trial basis. Because all mice received at least three air puff punishments, we decided to analyze the air puff ensemble response for these three first punishments. We discovered that air puff cells rapidly decreased the magnitude of their response to the air puff punishment (Fig. 4.19A, B, C) and started to respond before the actual delivery of the air puff punishment (Fig. 4.19A, B, D, E).

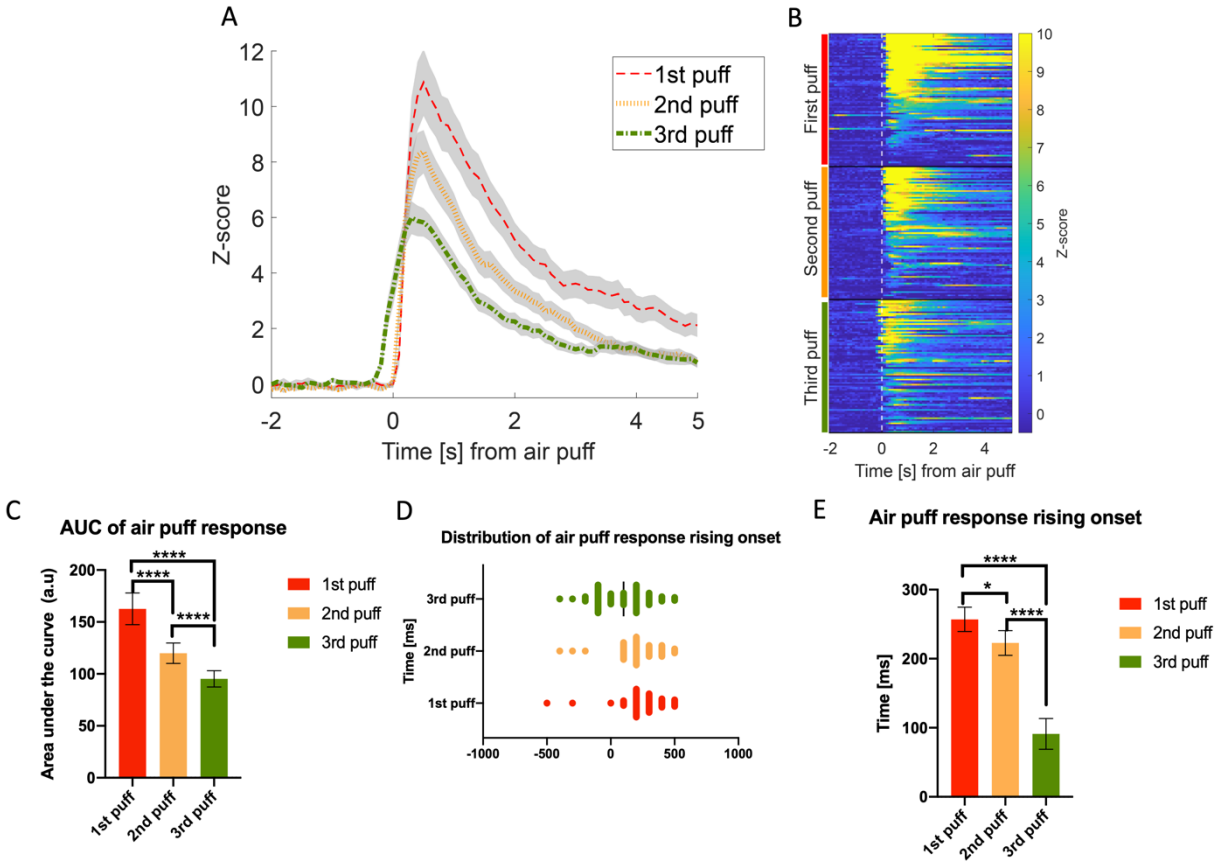

Figure 4.19 BLA punishment ensemble activity across trials. (**A**) Air puff cells mean activity for the first three air puff punishments (standard error of the mean shaded). (**B**) Individual air puff cells activity for the first three air puffs. (**C**) Mean area under the curve (AUC) with SEM for the first three air puffs. (**D**) Distribution of the response rising onset (maximum of the first derivative of the response in a 1 s window around the air puff). (**E**) Mean of the response rising onset with SEM.

One possibility was that the early response of punishment ensemble in relation to the actual delivery of the air puff reflected a prediction signal originating from the lever-press preceding the punishment (or reward). Therefore, we looked at the punishment ensemble activity across safe and risk instrumental and reinforcer trials (Fig. 4.20). We did not find a significant change in activity in the punishment ensemble across safe and risk instrumental or reinforcer trials.

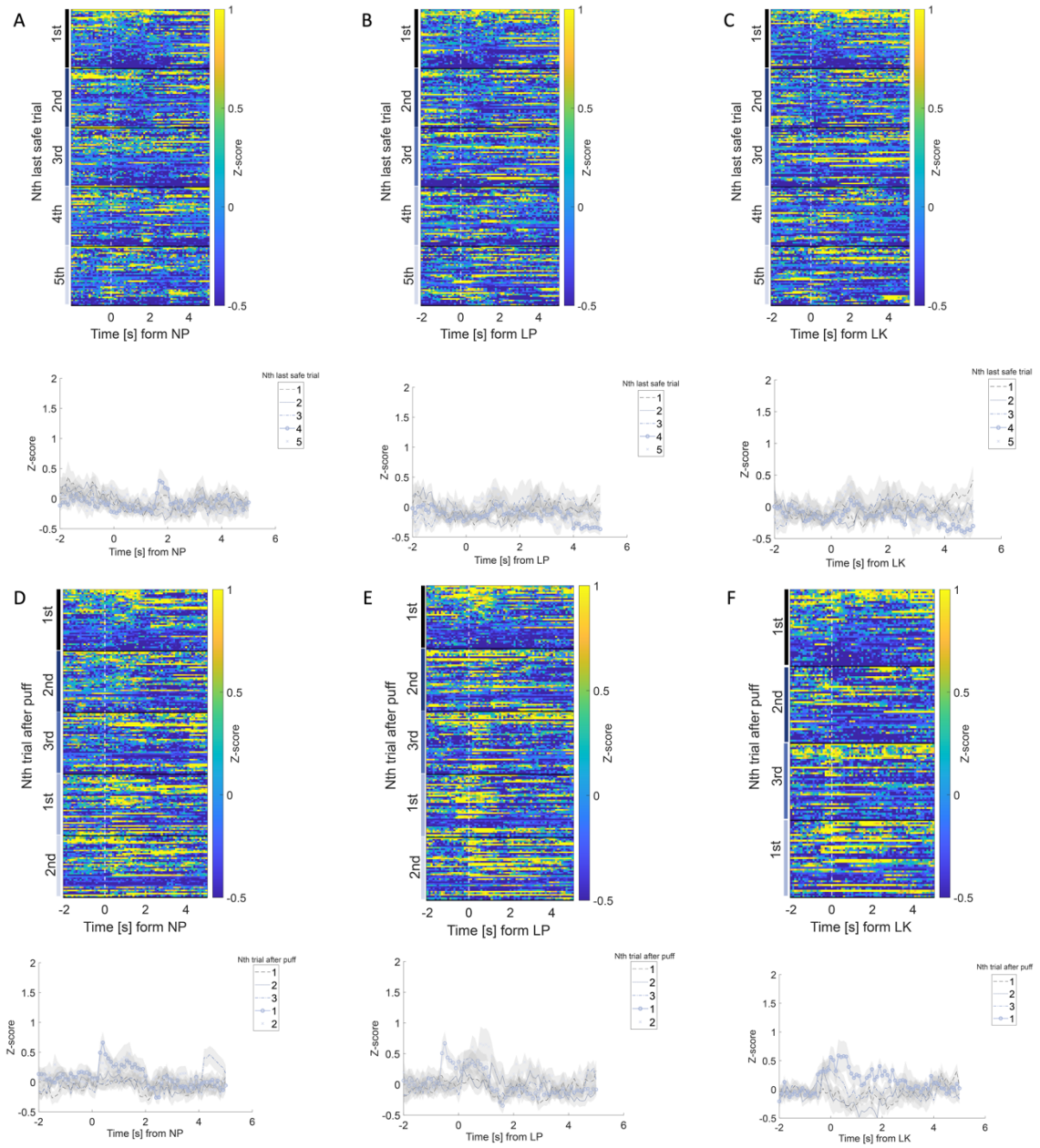

Figure 4.20 BLA punishment ensemble activity across safe and risk instrumental and reinforcer trials. Air puff ensemble activity during the last 5 safe nose-pokes (**A**), lever-presses (**B**) and licks (**C**). Air puff ensemble activity during the first 5 (or 4) nose-pokes (**D**), lever presses (**E**) and licks (**F**).

4.3.6 Instrumental actions and reinforcer ensembles during risk

Next, we compared the levels of activity of instrumental actions and reinforcer ensembles before and after the onset of the risk period of the task. Our hypothesis (§2) was that nose-poke and lever press cells would significantly change their levels of activity during the risk period of the task, given that the outcome of these actions had become associated with a risk of punishment. Additionally, we expected a separate set of cells to start responding to the risky actions. However, we found that nose-poke, lever-press, and also lick cells, had overall decreased levels of activity during the risk period of the task but not significantly across safe and risky trials (Fig. 4.21A, B). We also did not find other cells that significantly responded to the actions during risk. On a trial-by-trial basis, the activity level of individual cells from each instrumental sequence ensemble did not significantly change following a punishment, although there was a greater variance in response magnitude within each group (Fig. 4.22). For this analysis, we z-scored the activity levels using the mean from the last five safe trials (trials -1 to -5 in Fig. 4.22).

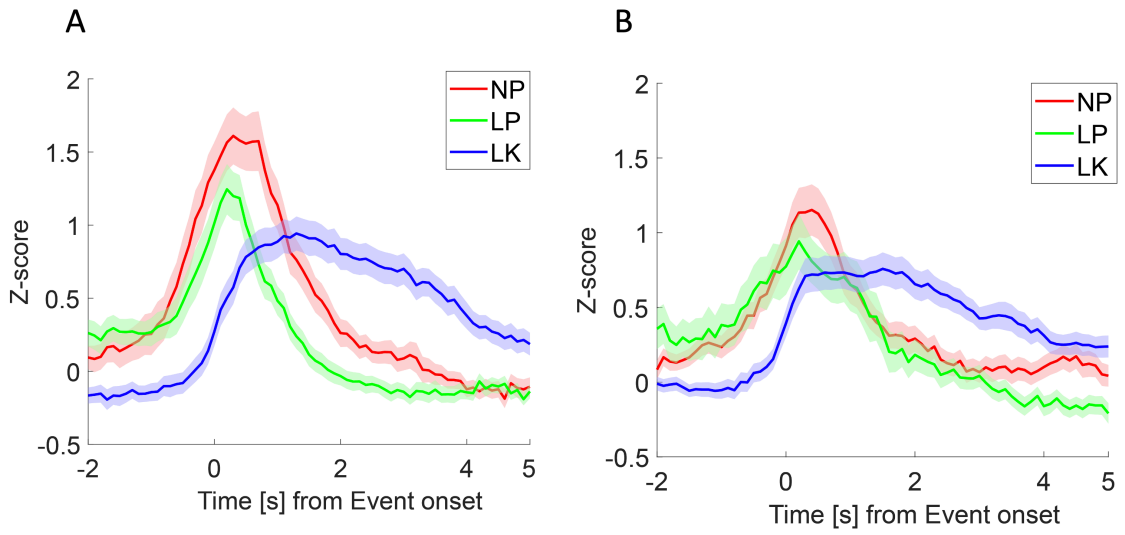

Figure 4.21 BLA ensembles during safe and risk periods. (**A**) Nose-poke, lever press, and lick cells mean response during the safe period of the task. SEM is shaded. (**B**) Nose-poke, lever press, and lick cells mean response during the risk period of the task.

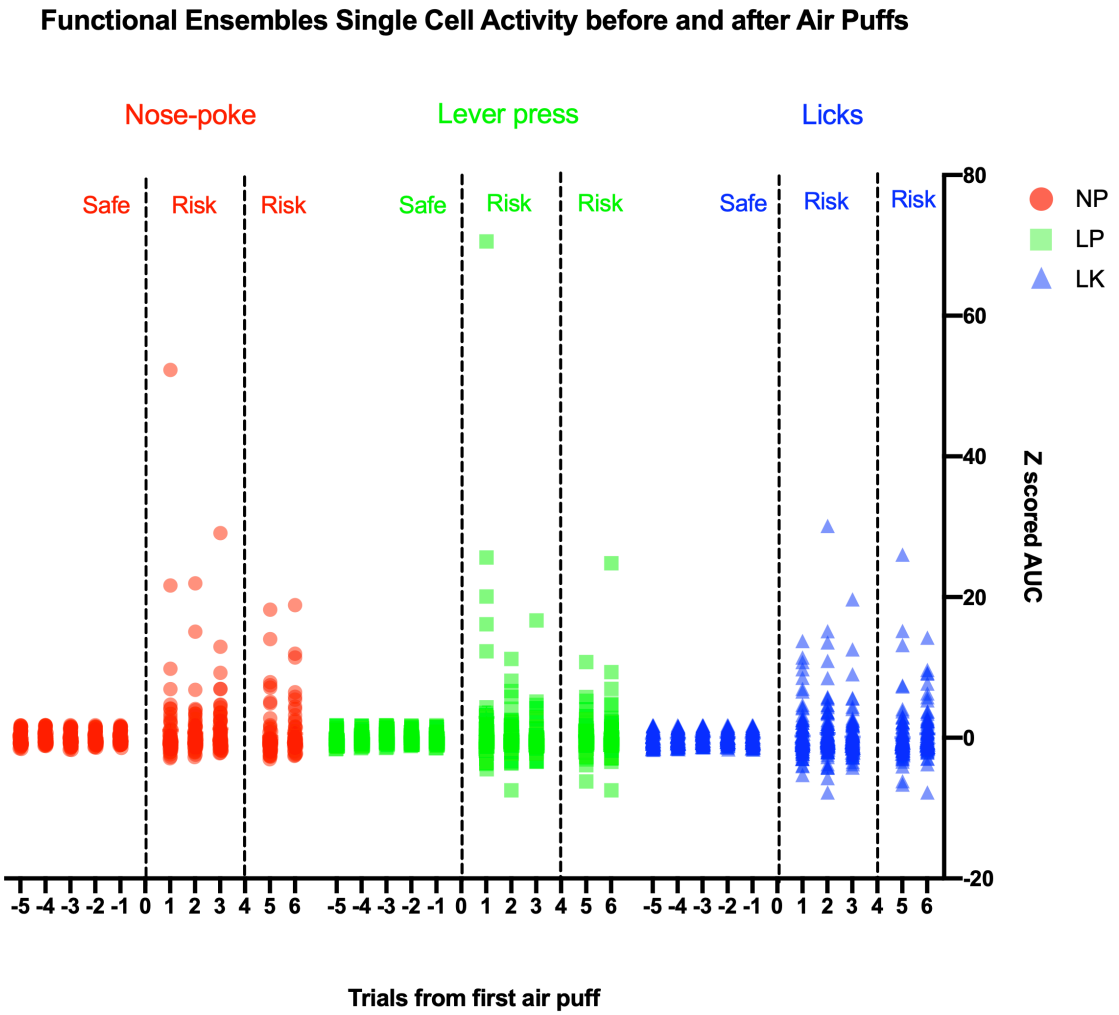

Figure 4.22 BLA Single cell activity by ensemble on a trial-by-trial basis, before and after air puff punishments. Punishments are indicated with black dashed lines. Activity levels were statistically normalized per cell to the mean activity for the last 5 safe trials (trials -1 to -5). For all ensembles, variance increased in risky trials (after a punishment) compared to safe trials.

At the single cell and ensemble activity level as measured by the z-score, we observed changes in the nose-poke and lever press ensembles across risk trials (Fig. 4.23 D, E). In the former activity decreased with the number of unpunished trials and while in latter activity increased. This differences across risk trials was however not statistically significant, nor it was the difference between safe and risk trials.

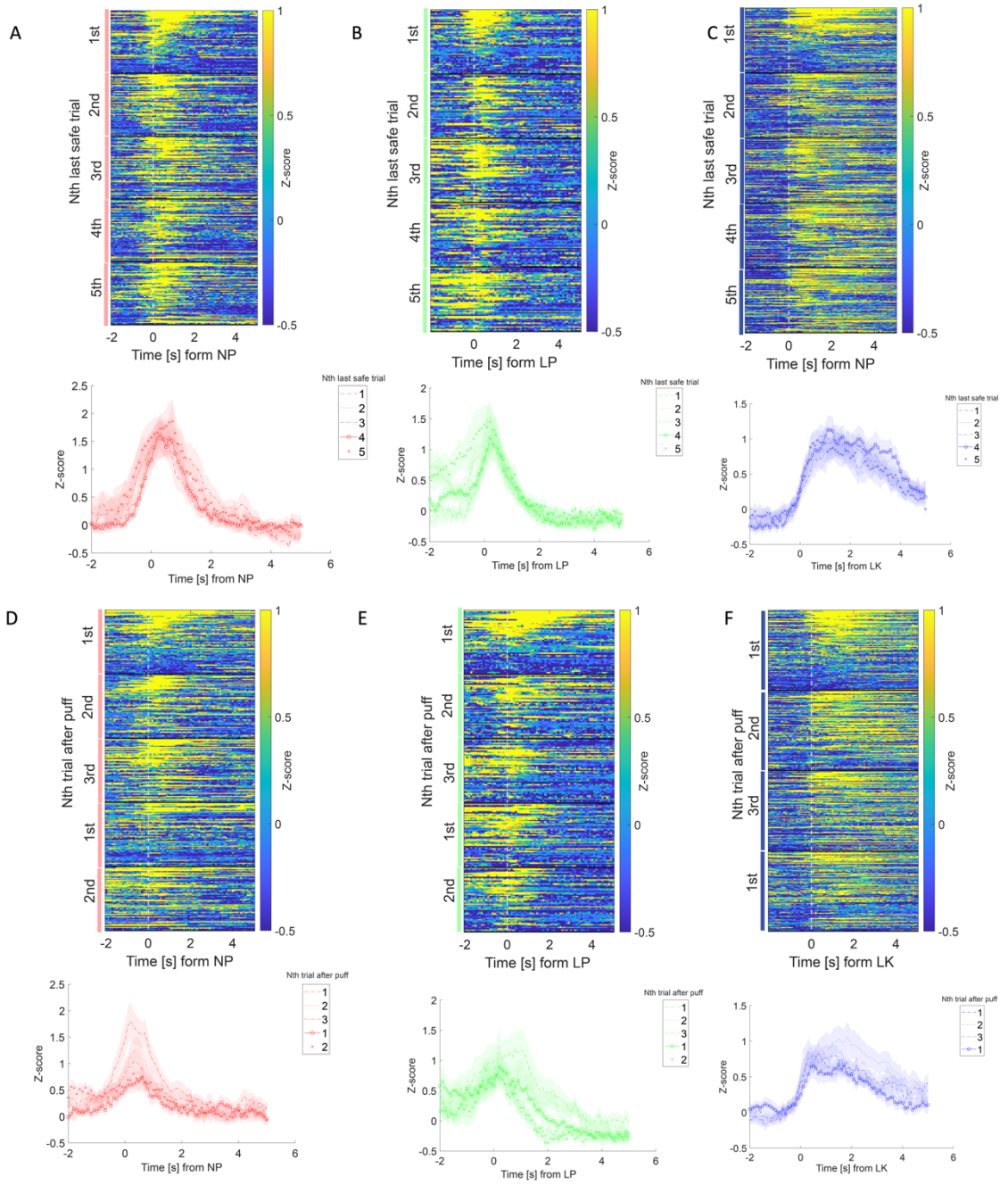

Figure 4.23 BLA instrumental and reinforcer ensembles during safe (A, B, C) and risk (D, E, F) trials. Air puff cells were not active during the risk period for nose-pokes, lever-presses or licks (**A**, **B**, **C**, respectively).

On the other hand, we examined the activity of the air puff ensemble during the risk period of the task. We found that air puff punishment cells were not active during nose-pokes, lever-presses or licks during the risk period of the task (Fig. 4.24A, B, C, respectively).

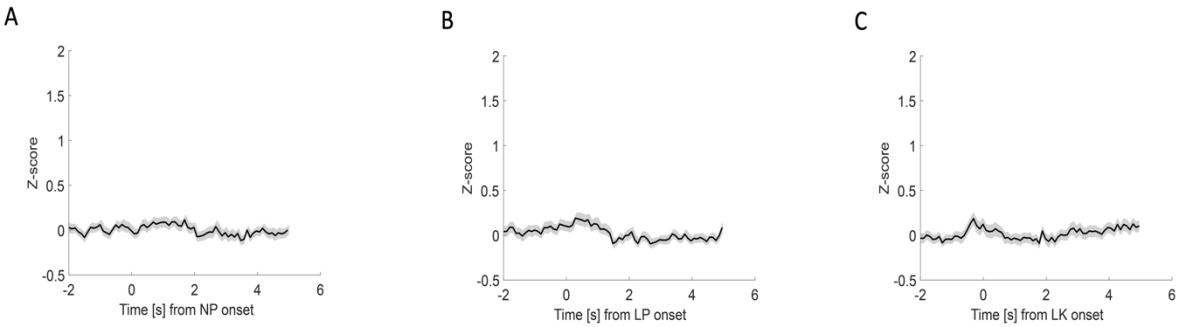

Figure 4.24 Air puff ensemble activity during risk. Air puff cells were not active during the risk period for nose-pokes, lever-presses or licks (**A**, **B**, **C**, respectively).

Additionally, we analyzed the activity changes of cells that showed a significant response to both a task-related action (Fig. 4.25A) and the air puff punishment (Fig. 4.25B), given that these cells are potential candidates to integrate punishment information into the representation of the instrumental actions in the BLA. However, we found that these cells did not exhibit a pattern of activity different to the one of cells from the other ensembles during the risk period (4.25C).

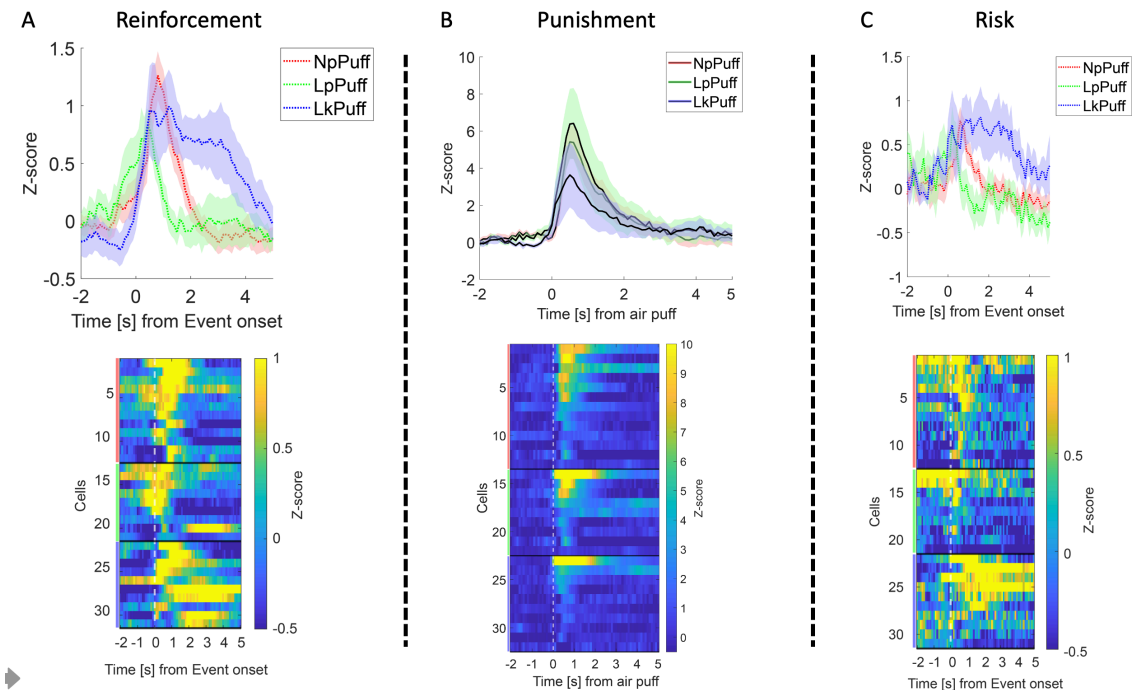

Figure 4.25 Reinforcement, punishment and risk activity for cells significantly active to both air puff punishments and nose-pokes, lever presses or licks. Task (**A**) and air puff punishment (**B**) responding cells did not exhibit a pattern of activity different to other task cells during the risk period (**C**).

5. Discussion

Below we discuss the implications of the results and our interpretations. It is worth noting that in studies with similar behavioral paradigms (Orsini et al., 2017), it has been proposed that 'deliberation' processes occur around the time of the nose-poke, when animals are thought to decide which lever to press. However, based on the premises underlying our experimental design and in our analysis of the behavior, we did not find any reason or evidence to pursue this line of analysis in our paradigm, where an exclusive preference for a certain reward is stable and predictable. Therefore, we do not address the nose-poke as a deliberation time point, but as one of two different actions in an instrumental sequence.

5.1 Decrease in instrumental performance reflects risk taking behavior

An outstanding and prevailing behavioral effect across mice is that punishment and risk of punishment significantly decrease instrumental performance but do not cause a switch in preference between the large-but-now-risky reward and the small-but-safe reward (Fig. 4.5). One interpretation is that the safety of the small reward choice is not made explicit during the risk period of the task, thus, given the reward magnitude to risk ratio, this choice becomes unappealing. However, there is, in most cases, an exploration of the safe but less rewarding choice during the risk period of the task (Fig. 4.5B). This exploration is unpunished but does not transition into a complete switch of choice preference. Moreover, mice do not decrease the amount of time spent in the small reward zone during the risk period, whereas they do so for the large reward zone (Fig. 4.8C, D). Therefore, the lack of a switch of preference is more related to the magnitude of the small reward per se rather than its magnitude when compounded with a risk of punishment. This opens the question of whether the small reward is indeed rewarding, which is addressed in control experiments that show that mice prefer 2% sucrose to water (Fig. 4.1B). As shown in further control experiments, a small reward with a higher

magnitude would have compromised the discriminability between small and high reward choices (Fig. 4.1A). Furthermore, the ability to switch from punished to unpunished choice, given two equally rewarding choices, was confirmed in other control experiments (Fig. 4.2). One last open interpretation is that the punishment-induced decrease in instrumental performance of the task was unspecific and spread across all levels of activity. However, general locomotion did not change between safe and risk periods (Fig. 4.8B). Therefore, we interpreted the decreased but persistent preference for the large-but-risky reward during the risk period of the task as deliberate risk taking.

5.2 Mice rapidly learn to localize the source of the air puff punishment

Given the dramatic behavioral and physiological effect we observed for the air puff punishment across mice, we looked for evidence of learning across punished trials. Although there were no observable changes in escape speed or escape onset, mice did show a directional optimization of their escape trajectories after just three punishments (Fig. 4.9C). This behavioral change suggests mice rapidly learn to locate the source of the air puff punishment.

5.3 Distinct ensembles and changes upon risk onset

Our results suggest the existence of largely distinct BLA ensembles that encode different reinforced instrumental actions, reinforcers and punishers. We did not observe a significant overlap between groups (Fig. 4.15B). An important missing piece of information is how the representation of instrumental actions in the BLA evolves with learning, a question which calls for its own dedicated set of experiments. Nonetheless, the absence of a coordinated ensemble response for the wide range of non-reinforced behaviors in our freely-moving mice suggests that indeed the reinforced instrumental action representation in the BLA emerged from the learning of the action-reward contingency. In this sense, nose-pokes (NP) and lever-presses (LP) responding cells are

positive valence cells because they encode the value of the reward associated to these actions. On the other hand, reward-consumption / lick (LK) cells and puff cells are positive and negative valence cells, defined by the valence of the unconditioned stimulus they represent. Historically, however, BLA function has been studied within the context of associative learning, where it has proposed as an essential structure in the process of assigning a valence to the representation of neutral cue, and in orchestrating the appropriate behavioral response. This ability lies at the core of adaptive behavior, and therefore underlies our understanding of maladaptive behaviors. In this context, BLA positive and negative valence cells have been shown to reliably represent cues that predict stimuli of their respective valence, even when the cue-stimulus contingency is reversed (Paton et al., 2006). Yet, BLA valence cells representing action-outcome contingencies and changes in these contingencies remained unexplored. Here our results present the first characterization of cellular responses to changes in action-outcome contingencies. It is worth noting that, different from cue value reversal experiments, in instrumental action-outcome experiments it is not possible to completely replace an appetitive outcome with an aversive one because the animal will no longer execute the action, and therefore its representation can no longer be investigated. For this reason, instead of a valence reversal, we used a probabilistic risk of punishment. Our results indicate that, differently to what has been reported in cue-stimulus valence reversal experiments, BLA instrumental action ensembles do not significantly change after the risk of punishment is introduced in the action-outcome contingency (Fig. 4.21, 4.22). There is, however, the possibility that a change in representation of the instrumental actions occurs after more action-punishment pairings, given that CS-stimulus reversal studies (Paton et al., 2006) use several (e.g. 20) pairings before and after reversal, and in our analysis, we were only able to include the three trials that were punished across all mice. This hypothesis is also supported by research from our group indicating that, when a fear-conditioned stimulus undergoes extinction, its representation on the first five trials of extinction greatly differs from its representation on the last five trials out of a total 25 extinction trials. To investigate this

further in our paradigm, a milder punishment could be used to allow for more punished trials across all mice, although this strategy could result in the animals developing a tolerance to the punishment. Alternatively, a more frequent punishment schedule could be used, but this may deter animals from performing the instrumental task within a reasonable time. Having these constraints in mind, we pursued our current experimental design and limited the experimental sessions to a maximum duration of 1 hour.

Interestingly, we observed a subset of NP and LP cells that were also responsive to air puff punishments (Fig. 4.24). Although these cells did not significantly change their response during the risk period of the task, their prominent response to the air puff punishment suggests they are potential candidate drivers of the behavior during the risk period of the task, as they would integrate both reward and punishment related inputs into BLA instrumental action cells.

The stability of NP and LP ensembles across trials suggests that these cells are preferentially recruited from the general population. Studies examining the recruitment of competing valence related amygdala networks (Lee, Amir, Haufler, & Pare, 2017) have reported that only 27% of BLA projection neurons remain unresponsive to either an appetitive or aversive conditioned stimulus. However, our results indicate that around 60% of the cells did not respond to any instrumental action, reward or punishment. This difference might stem from the fact that the former results come from electrophysiological recordings where assessing the level of inhibitory responses is possible, while our calcium imaging approach is best suited to image excitatory responses only. A final consideration is that the recruitment of a cell to a valence related ensemble has been proposed to depend on its genetic markers, projection targets and synaptic inputs (Pignatelli & Beyeler, 2019). Given that our results show that nose-poke and lever-press cells do not incorporate the air-puff risk related information after the onset of the risk period of the task, when behavior has already changed, this would imply

that action and punishment cells form part of at least partially segregated circuits with different inputs. Therefore, based on our data, we conclude that the punishment and risk of punishment information is not integrated by the action ensembles to update the value of the action, but instead it is integrated in a separate circuit from which the air puff ensemble is a part of. Nonetheless, the finding of some cells that respond to both actions and punishments suggests the existence of a group of cells capable of integrating both action and punishment inputs. Whether this minority of cells is a major driver of the changes observed in the behavior is a question that remains open for future investigation.

5.4 Rapidly adapting punisher ensemble suggests rapid learning

Over the three air puff punishments analyzed across mice we observed a fast adaptation of the air puff ensemble response magnitude but no change in the escape behavior speed or onset (Fig. 4.9, 4.19). In this sense this adaptation does not reflect desensitization or development of a tolerance to the punishment. On the other hand, we observed a backward shift in the response onset time with regards to the air puff delivery time (Fig. 4.19D). Because the backward shift was never larger than 500 ms (that is, never before the lever-press), we interpreted this shift as learning driven by the association of the air puff delivery to an environmental cue proceeding it, instead of a signal predicting the outcome of the lever press. The absence of the noise of the pump used to deliver the reward or the clicking of the solenoid valve used to control the delivery of the air puff could be among the candidate environmental cues that proceeded the air puff. It is also interesting to note that our results on the spatial clustering of air puff cells (Fig. 4.17) are the first ones to indicate such organization for a functionally defined BLA ensemble. We observed this clustering in both cohorts of mice with different GRIN lens sizes and dorsoventral coordinates. To the best of our knowledge, all other studies have found a salt-and-pepper distribution of functional cell types in the BLA. This may be due to the use of different punishment stimuli, some of

which evoke pain responses (e.g., electric shocks), or to the fact that many previous studies used indirect markers of activity to localize of functional cells *ex vivo*, while we were able to correlate function to calcium activity in spatially defined cells *in vivo*. Together with our data showing that, on a mouse-by-mouse basis, air puff cells represent a larger proportion of the BLA population than action cells (Fig. 4.15C), this result suggests that at the population level there is a bias towards recruitment of BLA cells to ensembles encoding punishment. Finally, we did not observe any gradient distribution of licks and punishment cells, in contrast to a contemporary study which found that cells responding to innate rewards and punishments follow an opposing anterior-posterior concentration gradient (J. Kim et al., 2016). Again, this difference may stem from the fact that different reward and punishment stimuli, as well as different proxies for activity, were used to classify cells.

5.5 Implications and limitations

We demonstrated the existence of largely distinct BLA ensembles that encode a primary (lever press) and secondary (nose-poke) instrumental action, that is, actions that are not part of the natural behavior repertoire but that have been learned through the association of their execution and a rewarding outcome. In this sense we logically concluded that these are positive valence cells, for they learn to respond to previously meaningless actions that become associated to reward delivery. Thus, we focused on investigating the changes in these ensembles after the rewarding outcome became associated to a risk of punishment. Our findings suggest that these ensembles do not incorporate the punishment related information, but instead that this information is relayed by the air puff cells to other at-least-partially-separate circuits. An alternative interpretation, given the existence of a minority of action & air puff responsive cells, is that this fraction of the population is driving the pronounced changes in behavior we observed. Certainly, this is a question worth of further investigation. Finally, it is wort noting that we did not examine local inhibitory interactions, which, based on work of our group and other labs, are known to play an important regulatory role in learning

circuits of the BLA. All in all, our findings suggest that the representations of actions in the BLA do not change when these actions become associated to a risk of punishment, but instead that a separate group of BLA cells responding prominently to the punishment relay the information to other separate circuits for learning. The implications of this claim would be that failure to adapt previously reinforced behavior, given new information about a potential punishment associated to that behavior, is associated to deficits in the circuits responsible for driving the learning based on the punishment information relayed by the BLA, but not necessarily to failure of the BLA circuits that represent the actions to integrate the punishment information. To support this claim, a potential testable hypothesis would be that optogenetic inhibition of air-puff cells during air-puff delivery results in unperturbed instrumental behavior, while optogenetic inhibition of action cells during air-puff delivery has no effect. In fact, temporally precise optogenetic inhibition of the BLA during the delivery of a foot-shock punishment in a decision-making task in rats has been shown to increase risk-taking behavior (Orsini et al., 2017). To this finding, our data adds another layer of specificity by suggesting that this effect is due to the disruption of ensembles encoding and conveying the punishment information to other circuits, but not due to the disruption of ensembles updating the representation of the action.

Bibliography

Akli, S., Caillaud, C., Vigne, E., Stratford-Perricaudet, L. D., Poenaru, L., Perricaudet, M., . . . Peschanski, M. R. (1993). Transfer of a foreign gene into the brain using adenovirus vectors. *Nat Genet, 3*(3), 224-228. doi:10.1038/ng0393-224

Ali, F., & Kwan, A. C. (2019). Interpreting in vivo calcium signals from neuronal cell bodies, axons, and dendrites: a review. *Neurophotonics, 7*(1), 011402. Retrieved from https://doi.org/10.1117/1.NPh.7.1.011402

Applegate, C. D., Kapp, B. S., Underwood, M. D., & McNall, C. L. (1983). Autonomic and somatomotor effects of amygdala central N. stimulation in awake rabbits. *Physiology & Behavior, 31*(3), 353-360. doi:https://doi.org/10.1016/0031-9384(83)90201-9

Armbruster, B., & Roth, B. (2005). Creation of designer biogenic amine receptors via directed molecular evolution. *Neuropsychopharmacology, 30*, S265-S265.

Balleine, B. W., Killcross, A. S., & Dickinson, A. (2003). The effect of lesions of the basolateral amygdala on instrumental conditioning. *J Neurosci, 23*(2), 666-675. Retrieved from https://www.ncbi.nlm.nih.gov/pubmed/12533626

Balleine, B. W., & Killcross, S. (2006). Parallel incentive processing: an integrated view of amygdala function. *Trends Neurosci, 29*(5), 272-279. doi:10.1016/j.tins.2006.03.002

Barretto, R. P. J., Messerschmidt, B., & Schnitzer, M. J. (2009). In vivo fluorescence imaging with high-resolution microlenses. *Nature Methods, 6*(7), 511-512. doi:10.1038/nmeth.1339

Baxter, M. G., & Murray, E. A. (2002). The amygdala and reward. *Nat Rev Neurosci, 3*(7), 563-573. doi:10.1038/nrn875

Belova, M. A., Paton, J. J., Morrison, S. E., & Salzman, C. D. (2007). Expectation modulates neural responses to pleasant and aversive stimuli in primate amygdala. *Neuron, 55*(6), 970-984. doi:10.1016/j.neuron.2007.08.004

Betley, J. N., Xu, S., Cao, Z. F. H., Gong, R., Magnus, C. J., Yu, Y., & Sternson, S. M. (2015). Neurons for hunger and thirst transmit a negative-valence teaching signal. *Nature, 521*(7551), 180-185. doi:10.1038/nature14416

Beyeler, A., Chang, C.-J., Silvestre, M., Lévêque, C., Namburi, P., Wildes, C. P., & Tye, K. M. (2018). Organization of Valence-Encoding and Projection-Defined Neurons in

the Basolateral Amygdala. *Cell Reports, 22*(4), 905-918. doi:https://doi.org/10.1016/j.celrep.2017.12.097

Beyeler, A., & Dabrowska, J. (2020). Neuronal diversity of the amygdala and the bed nucleus of the stria terminalis. *Handb Behav Neurosci, 26*, 63-100. doi:10.1016/b978-0-12-815134-1.00003-9

Beyeler, A., Namburi, P., Glober, G. F., Simonnet, C., Calhoon, G. G., Conyers, G. F., . . . Tye, K. M. (2016). Divergent Routing of Positive and Negative Information from the Amygdala during Memory Retrieval. *Neuron, 90*(2), 348-361. doi:10.1016/j.neuron.2016.03.004

Blanchard, D. C., & Blanchard, R. J. (1972). Innate and conditioned reactions to threat in rats with amygdaloid lesions. *Journal of Comparative and Physiological Psychology, 81*(2), 281-290. doi:10.1037/h0033521

Blanchard, D. C., & Blanchard, R. J. (1988). Ethoexperimental approaches to the biology of emotion. *Annu Rev Psychol, 39*, 43-68. doi:10.1146/annurev.ps.39.020188.000355

Blanchard, R. J., & Blanchard, D. C. (1969). Crouching as an index of fear. *Journal of Comparative and Physiological Psychology, 67*(3), 370-375. doi:10.1037/h0026779

Blanchard, R. J., Dielman, T. E., & Blanchard, D. C. (1968). Postshock crouching: Familiarity with the shock situation. *Psychonomic Science, 10*(11), 371-372. doi:10.3758/BF03331566

Boyden, E. S., Zhang, F., Bamberg, E., Nagel, G., & Deisseroth, K. (2005). Millisecond-timescale, genetically targeted optical control of neural activity. doi:10.1038/nn1525

Britt, J. P., Benaliouad, F., McDevitt, R. A., Stuber, G. D., Wise, R. A., & Bonci, A. (2012). Synaptic and behavioral profile of multiple glutamatergic inputs to the nucleus accumbens. *Neuron, 76*(4), 790-803. doi:10.1016/j.neuron.2012.09.040

Brown, S., & Schäfer, E. (1888). An investigation into the functions of the occipital and temporal lobes of the monkey's brain. *Philos Trans R Soc Lond, 179B*, 303-327.

Burgos-Robles, A., Kimchi, E. Y., Izadmehr, E. M., Porzenheim, M. J., Ramos-Guasp, W. A., Nieh, E. H., . . . Tye, K. M. (2017). Amygdala inputs to prefrontal cortex guide behavior amid conflicting cues of reward and punishment. *Nat Neurosci, 20*(6), 824-835. doi:10.1038/nn.4553

Cador, M., Robbins, T. W., & Everitt, B. J. (1989). Involvement of the amygdala in stimulus-reward associations: interaction with the ventral striatum. *Neuroscience, 30*(1), 77-86. doi:10.1016/0306-4522(89)90354-0

Campeau, S., & Davis, M. (1995). Involvement of subcortical and cortical afferents to the lateral nucleus of the amygdala in fear conditioning measured with fear-potentiated startle in rats trained concurrently with auditory and visual conditioned stimuli. *J Neurosci, 15*(3 Pt 2), 2312-2327. doi:10.1523/jneurosci.15-03-02312.1995

Campos, P., Walker, J. J., & Mollard, P. (2020). Diving into the brain: deep-brain imaging techniques in conscious animals. *Journal of Endocrinology, 246*(2), R33. doi:10.1530/joe-20-0028

Cardinal, R. N., & Howes, N. J. (2005). Effects of lesions of the nucleus accumbens core on choice between small certain rewards and large uncertain rewards in rats. *BMC Neuroscience, 6*(1), 37. doi:10.1186/1471-2202-6-37

Chen, T.-W., Wardill, T. J., Sun, Y., Pulver, S. R., Renninger, S. L., Baohan, A., . . . Kim, D. S. (2013). Ultrasensitive fluorescent proteins for imaging neuronal activity. *Nature, 499*(7458), 295-300. doi:10.1038/nature12354

Choi, V. W., McCarty, D. M., & Samulski, R. J. (2005). AAV hybrid serotypes: improved vectors for gene delivery. *Curr Gene Ther, 5*(3), 299-310. doi:10.2174/1566523054064968

Churchwell, J. C., Morris, A. M., Heurtelou, N. M., & Kesner, R. P. (2009). Interactions between the prefrontal cortex and amygdala during delay discounting and reversal. *Behav Neurosci, 123*(6), 1185-1196. doi:10.1037/a0017734

Ciocchi, S., Herry, C., Grenier, F., Wolff, S. B., Letzkus, J. J., Vlachos, I., . . . Luthi, A. (2010). Encoding of conditioned fear in central amygdala inhibitory circuits. *Nature, 468*(7321), 277-282. doi:10.1038/nature09559

Colwill, R. M., & Motzkin, D. K. (1994). Encoding of the unconditioned stimulus in Pavlovian conditioning. *Animal Learning & Behavior, 22*(4), 384-394. doi:10.3758/BF03209158

Colwill, R. M., & Rescorla, R. A. (1988). Associations between the discriminative stimulus and the reinforcer in instrumental learning. *Journal of Experimental Psychology: Animal Behavior Processes, 14*(2), 155-164. doi:10.1037/0097-7403.14.2.155

Corbit, L. H., & Balleine, B. W. (2005). Double dissociation of basolateral and central amygdala lesions on the general and outcome-specific forms of pavlovian-

instrumental transfer. *J Neurosci, 25*(4), 962-970. doi:10.1523/JNEUROSCI.4507-04.2005

Darwin, C. (1872). *The Expression of the Emotions in Man and Animals*: John Murray.

Davis, E. R., & Platt, J. R. (1983). Contiguity and contingency in the acquisition and maintenance of an operant. *Learning and Motivation, 14*(4), 487-512. doi:10.1016/0023-9690(83)90029-2

Delgado, J. M. R., Roberts, W. W., & Miller, N. E. (1954). Learning Motivated by Electrical Stimulation of the Brain. *American Journal of Physiology-Legacy Content, 179*(3), 587-593. doi:10.1152/ajplegacy.1954.179.3.587

Delgado, J. M. R., Rosvold, H. E., & Looney, E. (1956). Evoking conditioned fear by electrical stimulation of subcortical structures in the monkey brain. *Journal of Comparative and Physiological Psychology, 49*(4), 373-380. doi:10.1037/h0088005

Di Ciano, P., & Everitt, B. J. (2004). Direct interactions between the basolateral amygdala and nucleus accumbens core underlie cocaine-seeking behavior by rats. *J Neurosci, 24*(32), 7167-7173. doi:10.1523/jneurosci.1581-04.2004

Diagnostic, A. (2013). statistical Manual of mental disorders–Fifth edition (DSM-5). *Edisi ke-5. Washington DC: American Psychiatric Association*.

Ellenbroek, B., & Youn, J. (2016). Rodent models in neuroscience research: is it a rat race? *Dis Model Mech, 9*(10), 1079-1087. doi:10.1242/dmm.026120

Erö, C., Gewaltig, M.-O., Keller, D., & Markram, H. (2018). A cell atlas for the mouse brain. *Frontiers in neuroinformatics, 12*, 84.

Faber, E. S., & Sah, P. (2002). Physiological role of calcium-activated potassium currents in the rat lateral amygdala. *J Neurosci, 22*(5), 1618-1628. Retrieved from https://www.ncbi.nlm.nih.gov/pubmed/11880492

Fadok, J. P., Krabbe, S., Markovic, M., Courtin, J., Xu, C., Massi, L., . . . Luthi, A. (2017). A competitive inhibitory circuit for selection of active and passive fear responses. *Nature, 542*(7639), 96-100. doi:10.1038/nature21047

Fanselow, M. S. (1994). Neural organization of the defensive behavior system responsible for fear. *Psychonomic bulletin & review, 1*(4), 429-438. doi:10.3758/bf03210947

Fanselow, M. S., & Lester, L. S. (1988). A functional behavioristic approach to aversively motivated behavior: Predatory imminence as a determinant of the topography

of defensive behavior. In *Evolution and learning.* (pp. 185-212). Hillsdale, NJ, US: Lawrence Erlbaum Associates, Inc.

Feindel, W., & Penfield, W. (1954). Localization Of Discharge In Temporal Lobe Automatism. *A.M.A. Archives of Neurology & Psychiatry, 72*(5), 605-630. doi:10.1001/archneurpsyc.1954.02330050075012

Flusberg, B. A., Nimmerjahn, A., Cocker, E. D., Mukamel, E. A., Barretto, R. P., Ko, T. H., . . . Schnitzer, M. J. (2008). High-speed, miniaturized fluorescence microscopy in freely moving mice. *Nat Methods, 5*(11), 935-938. doi:10.1038/nmeth.1256

Forli, A., Vecchia, D., Binini, N., Succol, F., Bovetti, S., Moretti, C., . . . Fellin, T. (2018). Two-Photon Bidirectional Control and Imaging of Neuronal Excitability with High Spatial Resolution In Vivo. *Cell Rep, 22*(11), 3087-3098. doi:10.1016/j.celrep.2018.02.063

Fuchs, R. A., Weber, S. M., Rice, H. J., & Neisewander, J. L. (2002). Effects of excitotoxic lesions of the basolateral amygdala on cocaine-seeking behavior and cocaine conditioned place preference in rats. *Brain Res, 929*(1), 15-25. doi:10.1016/s0006-8993(01)03366-2

Fuster, J. M., & Uyeda, A. A. (1971). Reactivity of limbic neurons of the monkey to appetitive and aversive signals. *Electroencephalogr Clin Neurophysiol, 30*(4), 281-293. doi:10.1016/0013-4694(71)90111-8

Gale, H. G. (1907). Physical Optics, by Robert W. Wood. *The Astrophysical Journal, 25*, 290. doi:10.1086/141453

García-Amado, M., & Prensa, L. (2012). Stereological analysis of neuron, glial and endothelial cell numbers in the human amygdaloid complex. *PLoS One, 7*(6), e38692. doi:10.1371/journal.pone.0038692

Gaston, M. G., & Freed, L. (1969). Effect of amygdaloid lesions in a fear conditioning situation not involving instrumental learning. *Psychonomic Science, 16*(1), 55-56. doi:10.3758/BF03331913

Ghods-Sharifi, S., St Onge, J. R., & Floresco, S. B. (2009). Fundamental contribution by the basolateral amygdala to different forms of decision making. *J Neurosci, 29*(16), 5251-5259. doi:10.1523/jneurosci.0315-09.2009

Ghosh, K. K., Burns, L. D., Cocker, E. D., Nimmerjahn, A., Ziv, Y., Gamal, A. E., & Schnitzer, M. J. (2011). Miniaturized integration of a fluorescence microscope. *Nature Methods, 8*(10), 871-878. doi:10.1038/nmeth.1694

Bibliography

Gloor, P. (1955). Electrophysiological studies on the connections of the amygdaloid nucleus in the cat. Part II: The electrophysiological properties of the amygdaloid projection system. *Electroencephalography & Clinical Neurophysiology, 7*, 243-264. doi:10.1016/0013-4694(55)90038-9

Hagiwara , S., Chichibu , S., & Naka , K.-i. (1964). The Effects of Various Ions on Resting and Spike Potentials of Barnacle Muscle Fibers. *Journal of General Physiology, 48*(1), 163-179. doi:10.1085/jgp.48.1.163

Hara-Kuge, S., Nishihara, T., Matsuda, T., Kitazono, T., Teramoto, T., Nagai, T., & Ishihara, T. (2018). An improved inverse-type Ca2+ indicator can detect putative neuronal inhibition in Caenorhabditis elegans by increasing signal intensity upon Ca2+ decrease. *PLoS One, 13*(4), e0194707. doi:10.1371/journal.pone.0194707

Haubensak, W., Kunwar, P. S., Cai, H., Ciocchi, S., Wall, N. R., Ponnusamy, R., . . . Anderson, D. J. (2010). Genetic dissection of an amygdala microcircuit that gates conditioned fear. *Nature, 468*(7321), 270-276. doi:10.1038/nature09553

Haw, J. (2008). Random-ratio schedules of reinforcement: The role of early wins and unreinforced trials. *Journal of Gambling Issues, 21*, 56-67. doi:10.4309/jgi.2008.21.6

Helmchen, F., Fee, M. S., Tank, D. W., & Denk, W. (2001). A Miniature Head-Mounted Two-Photon Microscope: High-Resolution Brain Imaging in Freely Moving Animals. *Neuron, 31*(6), 903-912. doi:https://doi.org/10.1016/S0896-6273(01)00421-4

Henke, P. G. (1983). Unit-activity in the central amygdalar nucleus of rats in response to immobilization—stress. *Brain Research Bulletin, 10*(6), 833-837. doi:https://doi.org/10.1016/0361-9230(83)90216-2

Hildinger, M., Auricchio, A., Gao, G., Wang, L., Chirmule, N., & Wilson, J. M. (2001). Hybrid Vectors Based on Adeno-Associated Virus Serotypes 2 and 5 for Muscle-Directed Gene Transfer. *Journal of Virology, 75*(13), 6199-6203. doi:10.1128/jvi.75.13.6199-6203.2001

Holland, P. C., & Petrovich, G. D. (2005). A neural systems analysis of the potentiation of feeding by conditioned stimuli. *Physiol Behav, 86*(5), 747-761. doi:10.1016/j.physbeh.2005.08.062

Holland, P. C., Petrovich, G. D., & Gallagher, M. (2002). The effects of amygdala lesions on conditioned stimulus-potentiated eating in rats. *Physiol Behav, 76*(1), 117-129. doi:10.1016/s0031-9384(02)00688-1

Holmes, N. M., Marchand, A. R., & Coutureau, E. (2010). Pavlovian to instrumental transfer: A neurobehavioural perspective. *Neuroscience & Biobehavioral Reviews, 34*(8), 1277-1295. doi:https://doi.org/10.1016/j.neubiorev.2010.03.007

Hu, Y., Salmeron, B. J., Krasnova, I. N., Gu, H., Lu, H., Bonci, A., . . . Yang, Y. (2019). Compulsive drug use is associated with imbalance of orbitofrontal- and prelimbic-striatal circuits in punishment-resistant individuals. *Proceedings of the National Academy of Sciences, 116*(18), 9066-9071. doi:10.1073/pnas.1819978116

Inoue, M., Takeuchi, A., Manita, S., Horigane, S.-i., Sakamoto, M., Kawakami, R., . . . Bito, H. (2019). Rational Engineering of XCaMPs, a Multicolor GECI Suite for In Vivo Imaging of Complex Brain Circuit Dynamics. *Cell, 177*(5), 1346-1360.e1324. doi:https://doi.org/10.1016/j.cell.2019.04.007

Jackson, J. H., & Stewart, P. (1899). Epileptic Attacks With A Warning Of A Crude Sensation Of Smell And With The Intellectual Aura (Dreamy State) In A Patient Who Had Symptoms Pointing To Gross Organic Disease Of The Right Temporo-Sphenoidal Lobe. *Brain, 22*(4), 534-549. doi:10.1093/brain/22.4.534

Janak, P. H., & Tye, K. M. (2015). From circuits to behaviour in the amygdala. *Nature, 517*(7534), 284-292. doi:10.1038/nature14188

Jean-Richard-Dit-Bressel, P., & McNally, G. P. (2015). The role of the basolateral amygdala in punishment. *Learn Mem, 22*(2), 128-137. doi:10.1101/lm.035907.114

Johnston, J. B. (1923). Further contributions to the study of the evolution of the forebrain. *Journal of Comparative Neurology, 35*(5), 337-481. doi:10.1002/cne.900350502

Kaplitt, M. G., Leone, P., Samulski, R. J., Xiao, X., Pfaff, D. W., O'Malley, K. L., & During, M. J. (1994). Long-term gene expression and phenotypic correction using adeno-associated virus vectors in the mammalian brain. *Nat Genet, 8*(2), 148-154. doi:10.1038/ng1094-148

Kapp, B. S., Frysinger, R. C., Gallagher, M., & Haselton, J. R. (1979). Amygdala central nucleus lesions: Effect on heart rate conditioning in the rabbit. - *23*(- 6), - 1117.

Kim, J., & Fanselow, M. (1992). Modality-specific retrograde amnesia of fear. *Science, 256*(5057), 675-677. doi:10.1126/science.1585183

Kim, J., Pignatelli, M., Xu, S., Itohara, S., & Tonegawa, S. (2016). Antagonistic negative and positive neurons of the basolateral amygdala. *Nat Neurosci, 19*(12), 1636-1646. doi:10.1038/nn.4414

Kim, J., Zhang, X., Muralidhar, S., LeBlanc, S. A., & Tonegawa, S. (2017). Basolateral to Central Amygdala Neural Circuits for Appetitive Behaviors. *Neuron, 93*(6), 1464-1479 e1465. doi:10.1016/j.neuron.2017.02.034

Klüver, H., & Bucy, P. C. (1937). "Psychic blindness" and other symptoms following bilateral temporal lobectomy in Rhesus monkeys. *American Journal of Physiology, 119*, 352-353.

Klüver, H., & Bucy, P. C. (1939). Preliminary Analysis of Functions of the Temporal lobes in Monkeys. *Archives of Neurology & Psychiatry, 42*(6), 979-1000. doi:10.1001/archneurpsyc.1939.02270240017001 %J Archives of Neurology & Psychiatry

Krabbe, S., Paradiso, E., d'Aquin, S., Bitterman, Y., Courtin, J., Xu, C., . . . Luthi, A. (2019). Adaptive disinhibitory gating by VIP interneurons permits associative learning. *Nat Neurosci, 22*(11), 1834-1843. doi:10.1038/s41593-019-0508-y

Kruse, J. M., Overmier, J. B., Konz, W. A., & Rokke, E. (1983). Pavlovian conditioned stimulus effects upon instrumental choice behavior are reinforcer specific. *Learning and Motivation, 14*(2), 165-181. doi:https://doi.org/10.1016/0023-9690(83)90004-8

Kuhn, R., Schwenk, F., Aguet, M., & Rajewsky, K. (1995). Inducible gene targeting in mice. *Science, 269*(5229), 1427-1429. doi:10.1126/science.7660125

LeDoux, J., Cicchetti, P., Xagoraris, A., & Romanski, L. (1990). The lateral amygdaloid nucleus: sensory interface of the amygdala in fear conditioning. *The Journal of Neuroscience, 10*(4), 1062-1069. doi:10.1523/jneurosci.10-04-01062.1990

LeDoux, J., Iwata, J., Cicchetti, P., & Reis, D. (1988). Different projections of the central amygdaloid nucleus mediate autonomic and behavioral correlates of conditioned fear. *The Journal of Neuroscience, 8*(7), 2517-2529. doi:10.1523/jneurosci.08-07-02517.1988

Lee, S. C., Amir, A., Haufler, D., & Pare, D. (2017). Differential Recruitment of Competing Valence-Related Amygdala Networks during Anxiety. *Neuron, 96*(1), 81-88 e85. doi:10.1016/j.neuron.2017.09.002

Lesscher, H. M., & Vanderschuren, L. J. (2012). Compulsive drug use and its neural substrates. *Rev Neurosci, 23*(5-6), 731-745. doi:10.1515/revneuro-2012-0066

Letzkus, J. J., Wolff, S. B., Meyer, E. M., Tovote, P., Courtin, J., Herry, C., & Luthi, A. (2011). A disinhibitory microcircuit for associative fear learning in the auditory cortex. *Nature, 480*(7377), 331-335. doi:10.1038/nature10674

Lin, M. Z., & Schnitzer, M. J. (2016). Genetically encoded indicators of neuronal activity. *Nature Neuroscience, 19*(9), 1142-1153. doi:10.1038/nn.4359

MacLean, P. D. (1986). Ictal symptoms relating to the nature of affects and their cerebral substrate. In *Biological foundations of emotion* (pp. 61-90): Elsevier.

MacLean, P. D., & Delgado, J. R. (1953). Electrical and chemical stimulation of frontotemporal portion of limbic system in the waking animal. *Electroencephalography and Clinical Neurophysiology, 5*(1), 91-100. doi:https://doi.org/10.1016/0013-4694(53)90056-X

McDonald, A. J. (1982). Neurons of the lateral and basolateral amygdaloid nuclei: A golgi study in the rat. *Journal of Comparative Neurology, 212*(3), 293-312. doi:10.1002/cne.902120307

McDonald, A. J., Muller, J. F., & Mascagni, F. (2002). GABAergic innervation of alpha type II calcium/calmodulin-dependent protein kinase immunoreactive pyramidal neurons in the rat basolateral amygdala. *J Comp Neurol, 446*(3), 199-218. doi:10.1002/cne.10204

Meil, W. M., & See, R. E. (1997). Lesions of the basolateral amygdala abolish the ability of drug associated cues to reinstate responding during withdrawal from self-administered cocaine. *Behav Brain Res, 87*(2), 139-148. doi:10.1016/s0166-4328(96)02270-x

Meynert, T. (1868). *Der Bau der Gross-Hirnrinde: und seine örtlichen Verschiedenheiten, nebst einem pathologisch-anatomischen Corollarium*: Heuser.

Miller, N. E. (1948). Studies of fear as an acquirable drive: I. Fear as motivation and fear-reduction as reinforcement in the learning of new responses. *Journal of Experimental Psychology, 38*(1), 89-101. doi:10.1037/h0058455

Miltenberger, R. G. (2008). Behavior modification. In *Handbook of clinical psychology, vol 2: Children and adolescents.* (pp. 626-652). Hoboken, NJ, US: John Wiley & Sons, Inc.

Morrison, S. E., Saez, A., Lau, B., & Salzman, C. D. (2011). Different time courses for learning-related changes in amygdala and orbitofrontal cortex. *Neuron, 71*(6), 1127-1140. doi:10.1016/j.neuron.2011.07.016

Murray, E. A. (2007). The amygdala, reward and emotion. *Trends Cogn Sci, 11*(11), 489-497. doi:10.1016/j.tics.2007.08.013

Nahm, F. K., & Pribram, K. H. (1998). Heinrich Klüver: Biographical Memoir. In: Washington, DC: National Academies Press.

Nakai, J., Ohkura, M., & Imoto, K. (2001). A high signal-to-noise Ca2+ probe composed of a single green fluorescent protein. *Nature Biotechnology, 19*(2), 137-141. doi:10.1038/84397

Namburi, P., Beyeler, A., Yorozu, S., Calhoon, G. G., Halbert, S. A., Wichmann, R., . . . Tye, K. M. (2015). A circuit mechanism for differentiating positive and negative associations. *Nature, 520*(7549), 675-678. doi:10.1038/nature14366

Orsini, C. A., Hernandez, C. M., Singhal, S., Kelly, K. B., Frazier, C. J., Bizon, J. L., & Setlow, B. (2017). Optogenetic Inhibition Reveals Distinct Roles for Basolateral Amygdala Activity at Discrete Time Points during Risky Decision Making. *J Neurosci, 37*(48), 11537-11548. doi:10.1523/jneurosci.2344-17.2017

Orsini, C. A., Trotta, R. T., Bizon, J. L., & Setlow, B. (2015). Dissociable roles for the basolateral amygdala and orbitofrontal cortex in decision-making under risk of punishment. *J Neurosci, 35*(4), 1368-1379. doi:10.1523/jneurosci.3586-14.2015

Ostlund, S. B., & Balleine, B. W. (2008). Differential involvement of the basolateral amygdala and mediodorsal thalamus in instrumental action selection. *J Neurosci, 28*(17), 4398-4405. doi:10.1523/JNEUROSCI.5472-07.2008

Ostlund, S. B., & Balline, B. W. (2007). Selective reinstatement of instrumental performance depends on the discriminative stimulus properties of the mediating outcome. *Learn Behav, 35*(1), 43-52. doi:10.3758/bf03196073

Otis, J. M., Namboodiri, V. M., Matan, A. M., Voets, E. S., Mohorn, E. P., Kosyk, O., . . . Stuber, G. D. (2017). Prefrontal cortex output circuits guide reward seeking through divergent cue encoding. *Nature, 543*(7643), 103-107. doi:10.1038/nature21376

Paton, J. J., Belova, M. A., Morrison, S. E., & Salzman, C. D. (2006). The primate amygdala represents the positive and negative value of visual stimuli during learning. *Nature, 439*(7078), 865-870. doi:10.1038/nature04490

Pavlov, I. P. (1927). *Conditioned reflexes: an investigation of the physiological activity of the cerebral cortex*. Oxford, England: Oxford Univ. Press.

Pignatelli, M., & Beyeler, A. (2019). Valence coding in amygdala circuits. *Current opinion in behavioral sciences, 26*, 97-106. doi:10.1016/j.cobeha.2018.10.010

Pitkänen, A. (2000). The amygdala: a functional analysis. *Connectivity of the rat amygdaloid complex. Oxford University Press, Oxford*, 31-115.

Price, J., Russchen, R., & Amaral, D. (1987). Handbook of chemical neuroanatomy, Vol 5, Integrated systems of the CNS, Part I, Hypothalamus, hippocampus, amygdala, retina.

Rainnie, D. G., Asprodini, E. K., & Shinnick-Gallagher, P. (1993). Intracellular recordings from morphologically identified neurons of the basolateral amygdala. *Journal of Neurophysiology, 69*(4), 1350-1362. doi:10.1152/jn.1993.69.4.1350

Rescorla, R. A., & Solomon, R. L. (1967). Two-process learning theory: Relationships between Pavlovian conditioning and instrumental learning. *Psychol Rev, 74*(3), 151-182. doi:10.1037/h0024475

Rubinow, M. J., Mahajan, G., May, W., Overholser, J. C., Jurjus, G. J., Dieter, L., . . . Stockmeier, C. A. (2016). Basolateral amygdala volume and cell numbers in major depressive disorder: a postmortem stereological study. *Brain structure & function, 221*(1), 171-184. doi:10.1007/s00429-014-0900-z

Sah, P., Faber, E. S. L., Armentia, M. L. D., & Power, J. (2003). The Amygdaloid Complex: Anatomy and Physiology. *Physiological Reviews, 83*(3), 803-834. doi:10.1152/physrev.00002.2003

Savander, V., Go, C.-G., Ledoux, J. E., & Pitkänen, A. (1995). Intrinsic connections of the rat amygdaloid complex: Projections originating in the basal nucleus. *Journal of Comparative Neurology, 361*(2), 345-368. doi:10.1002/cne.903610211

Schoenbaum, G., Chiba, A. A., & Gallagher, M. (1999). Neural encoding in orbitofrontal cortex and basolateral amygdala during olfactory discrimination learning. *J Neurosci, 19*(5), 1876-1884. doi:10.1523/jneurosci.19-05-01876.1999

Schoenbaum, G., Setlow, B., Nugent, S. L., Saddoris, M. P., & Gallagher, M. (2003). Lesions of orbitofrontal cortex and basolateral amygdala complex disrupt acquisition of odor-guided discriminations and reversals. *Learn Mem, 10*(2), 129-140. doi:10.1101/lm.55203

Schwartzbaum, J. S. (1960). Changes in reinforcing properties of stimuli following ablation of the amygdaloid complex in monkeys. *J Comp Physiol Psychol, 53*, 388-395. doi:10.1037/h0049187

Senn, V., Wolff, S. B., Herry, C., Grenier, F., Ehrlich, I., Grundemann, J., . . . Luthi, A. (2014). Long-range connectivity defines behavioral specificity of amygdala neurons. *Neuron, 81*(2), 428-437. doi:10.1016/j.neuron.2013.11.006

Shabel, S. J., & Janak, P. H. (2009). Substantial similarity in amygdala neuronal activity during conditioned appetitive and aversive emotional arousal. *Proc Natl Acad Sci U S A, 106*(35), 15031-15036. doi:10.1073/pnas.0905580106

Skinner, B. F. (1938). *The behavior of organisms: an experimental analysis*. Oxford, England: Appleton-Century.

St Onge, J. R., & Floresco, S. B. (2009). Dopaminergic modulation of risk-based decision making. *Neuropsychopharmacology, 34*(3), 681-697. doi:10.1038/npp.2008.121

Stuber, G. D., Sparta, D. R., Stamatakis, A. M., van Leeuwen, W. A., Hardjoprajitno, J. E., Cho, S., . . . Bonci, A. (2011). Excitatory transmission from the amygdala to nucleus accumbens facilitates reward seeking. *Nature, 475*(7356), 377-380. doi:10.1038/nature10194

Susaki, E. A., Tainaka, K., Perrin, D., Kishino, F., Tawara, T., Watanabe, T. M., . . . Ueda, H. R. (2014). Whole-brain imaging with single-cell resolution using chemical cocktails and computational analysis. *Cell, 157*(3), 726-739. doi:10.1016/j.cell.2014.03.042

Thomas, G. (1981). Contiguity, Reinforcement Rate and the law of Effect. *The Quarterly Journal of Experimental Psychology Section B, 33*(1b), 33-43. doi:10.1080/14640748108400827

Thorndike, E. L., & Woodworth, R. S. (1901). The influence of improvement in one mental function upon the efficiency of other functions. II. The estimation of magnitudes. *Psychological Review, 8*(4), 384-395. doi:10.1037/h0071280

Tian, L., Hires, S. A., Mao, T., Huber, D., Chiappe, M. E., Chalasani, S. H., . . . Looger, L. L. (2009). Imaging neural activity in worms, flies and mice with improved GCaMP calcium indicators. *Nature Methods, 6*(12), 875-881. doi:10.1038/nmeth.1398

Tovote, P., Esposito, M. S., Botta, P., Chaudun, F., Fadok, J. P., Markovic, M., . . . Luthi, A. (2016). Midbrain circuits for defensive behaviour. *Nature, 534*(7606), 206-212. doi:10.1038/nature17996

Tovote, P., Fadok, J. P., & Luthi, A. (2015). Neuronal circuits for fear and anxiety. *Nature reviews. Neuroscience, 16*(6), 317-331. doi:10.1038/nrn3945

Tremblay, M., Cocker, P. J., Hosking, J. G., Zeeb, F. D., Rogers, R. D., & Winstanley, C. A. (2014). Dissociable effects of basolateral amygdala lesions on decision making biases in rats when loss or gain is emphasized. *Cogn Affect Behav Neurosci, 14*(4), 1184-1195. doi:10.3758/s13415-014-0271-1

Tsien, R. W., Lipscombe, D., Madison, D. V., Bley, K. R., & Fox, A. P. (1988). Multiple types of neuronal calcium channels and their selective modulation. *Trends in Neurosciences, 11*(10), 431-438. doi:https://doi.org/10.1016/0166-2236(88)90194-4

Vanderschuren, L. J., & Ahmed, S. H. (2013). Animal studies of addictive behavior. *Cold Spring Harbor Perspectives in Medicine, 3*(4), a011932.

Vanderschuren, L. J. M. J., Minnaard, A. M., Smeets, J. A. S., & Lesscher, H. M. B. (2017). Punishment models of addictive behavior. *Current Opinion in Behavioral Sciences, 13*, 77-84. doi:https://doi.org/10.1016/j.cobeha.2016.10.007

Wall, N. R., Wickersham, I. R., Cetin, A., De La Parra, M., & Callaway, E. M. (2010). Monosynaptic circuit tracing in vivo through Cre-dependent targeting and complementation of modified rabies virus. *Proceedings of the National Academy of Sciences, 107*(50), 21848-21853. doi:10.1073/pnas.1011756107

Wassum, K. M., Cely, I. C., Balleine, B. W., & Maidment, N. T. (2011). Micro-opioid receptor activation in the basolateral amygdala mediates the learning of increases but not decreases in the incentive value of a food reward. *J Neurosci, 31*(5), 1591-1599. doi:10.1523/JNEUROSCI.3102-10.2011

Wassum, K. M., & Izquierdo, A. (2015). The basolateral amygdala in reward learning and addiction. *Neuroscience and biobehavioral reviews, 57*, 271-283. doi:10.1016/j.neubiorev.2015.08.017

Wassum, K. M., Ostlund, S. B., Maidment, N. T., & Balleine, B. W. (2009). Distinct opioid circuits determine the palatability and the desirability of rewarding events. *Proc Natl Acad Sci U S A, 106*(30), 12512-12517. doi:10.1073/pnas.0905874106

Wei, Z., Lin, B.-J., Chen, T.-W., Daie, K., Svoboda, K., & Druckmann, S. (2020). A comparison of neuronal population dynamics measured with calcium imaging and electrophysiology. *PLOS Computational Biology, 16*(9), e1008198. doi:10.1371/journal.pcbi.1008198

Weiskrantz, L. (1956). Behavioral changes associated with ablation of the amygdaloid complex in monkeys. *J Comp Physiol Psychol, 49*(4), 381-391. doi:10.1037/h0088009

Wilensky, A. E., Schafe, G. E., Kristensen, M. P., & LeDoux, J. E. (2006). Rethinking the fear circuit: the central nucleus of the amygdala is required for the acquisition, consolidation, and expression of Pavlovian fear conditioning. *J Neurosci, 26*(48), 12387-12396. doi:10.1523/JNEUROSCI.4316-06.2006

Wolff, S. B., Grundemann, J., Tovote, P., Krabbe, S., Jacobson, G. A., Muller, C., . . . Luthi, A. (2014). Amygdala interneuron subtypes control fear learning through disinhibition. *Nature, 509*(7501), 453-458. doi:10.1038/nature13258

Xu, C., Krabbe, S., Grundemann, J., Botta, P., Fadok, J. P., Osakada, F., . . . Luthi, A. (2016). Distinct Hippocampal Pathways Mediate Dissociable Roles of Context in Memory Retrieval. *Cell, 167*(4), 961-972 e916. doi:10.1016/j.cell.2016.09.051

Zeeb, F. D., & Winstanley, C. A. (2011). Lesions of the basolateral amygdala and orbitofrontal cortex differentially affect acquisition and performance of a rodent gambling task. *J Neurosci, 31*(6), 2197-2204. doi:10.1523/jneurosci.5597-10.2011

Zhou, P., Resendez, S. L., Rodriguez-Romaguera, J., Jimenez, J. C., Neufeld, S. Q., Giovannucci, A., . . . Paninski, L. (2018). Efficient and accurate extraction of in vivo calcium signals from microendoscopic video data. *Elife, 7*. doi:10.7554/eLife.28728

Zimmerman, J. M., & Maren, S. (2010). NMDA receptor antagonism in the basolateral but not central amygdala blocks the extinction of Pavlovian fear conditioning in rats. *Eur J Neurosci, 31*(9), 1664-1670. doi:10.1111/j.1460-9568.2010.07223.x

Alejandro Tsai

I crossed the planet from Colombia to Mexico to Japan to Switzerland to pursue my dream of becoming a biomedical scientist.

Work Experience

2016/01 – 2021/03 **Novartis - Friedrich Miescher Institute for Biomedical Research** – *PhD in Neurobiology*

- Calcium imaging of basolateral amygdala cells in freely-moving mice during reinforcement, punishment and risk.

2015/08 – 2015/12 **Psychiatric University Clinic Zurich (PUK)** – *Research Associate in Neuroscience*

- Optogenetic manipulation of hippocampal cells in freely-moving mice during exploration.

Education

2016/01– 2021/03 **University of Basel - Friedrich Miescher Institute for Biomedical Research**
International PhD program in Neurobiology.

2013/09– 2015/08 **ETH Zurich**
Master of Science in Neuroscience.

2013/04– 2013/08 **The University of Tokyo** – *Left in order to go to Switzerland.*
Master of Science in Medical Science.

2009/04– 2013/03 **Tokyo Institute of Technology**
Bachelor of Engineering in Biotechnology.

2008/04– 2009/03 **Osaka University** (nongraded)
Intensive program for Japanese language.

2006/08– 2007/12 **Monterrey Institute of Technology (ITESM)** – *Left to Japan to pursue a career in Biotech*.
Bachelor of Engineering in Mechatronics.

2003/08– 2006/06 **Jefferson High School Colombia**
Spanish/English bilingual high school diploma.

Publications

Tsai Cabal et al., 2017. Selective amotivation deficits following chronic psychosocial stress in mice. Behav. Brain Res. 2017 Jan 15; 317:424-433. doi: 10.1016/j.bbr.2016.09.055. Epub 2016 Sep 28.

Tsai Cabal et al., 2017. Suitability of the new frontier task across mouse housing population sizes. Matters. doi: 10.19185/matters.201611000019. Epub 2016 Dec 8.

Languages

Spanish (native), **English** (fluent), **Japanese** (fluent), **German** (intermediate).

Scholarships & Awards

2018 Japanese Society for Neuroscience Travel Award for an Excellent Presentation.

2014 ETH Zurich Birkigt Scholarship.

2013 Japanese Government (MEXT) Graduate Scholarship for Academic Achievement.

2011 MIT Synthetic Biology Competition Best Team (iGEMer's Prize).

2011 Hong Kong University (HKUST) iGEM Best Biological Model Prize.

2008 Japanese Government (MEXT) Undergraduate Scholarship for Academic Achievement.

2007 ITESM Academic Excellence Award (3 times).

2006 Best 100 Latin American students' Scholarship for Academic Achievement at ITESM.